U.PORTO

FEUP FACULDADE DE ENGENHARIA
UNIVERSIDADE DO PORTO

Power Loss in Cylindrical Roller Thrust Bearings Lubricated with Automotive Gear Oils

António João Monteiro Paiva Coimbra

Porto, July 2015

Faculdade Engenharia da Universidade do Porto
Departamento de Engenharia Mecânica e Gestão Industrial

Power Loss in Cylindrical Roller Thrust Bearings Lubricated with Automotive Gear Oils

António João Monteiro Paiva Coimbra

Master's Degree Dissertation presented to Faculdade de Engenharia da Universidade do Porto

Dissertation supervised by

Doctor Ramiro C. Martins
Senior researcher of INEGI

Doctor Jorge H. O. Seabra
Full Professor of FEUP

Porto, July 2015

LaTeX

Power Loss in Cylindrical Roller Thrust Bearings Lubricated with Automotive Gear Oils

A. J. Coimbra

2015

FEUP-U.PORTO

To my family

Acknowledgements

Firstly I would like to address Faculdade de Engenharia da Universidade do Porto (FEUP) for all the resources provided in helping me obtain the Master's Degree in Mechanical Engineering.

I would like to express my gratitude to my supervisors Doctor Jorge Seabra, Doctor Ramiro Martins and Doctor Carlos Fernandes for the opportunity given and all their guidance and support during the elaboration of this work.

I would also like to thank the staff of CETRIB (André Gama, Armando Campos, Beatriz Graça, David Gonçalves, Jorge Castro, José Brandão, Maroua Hammami, Pedro Marques) and my fellow Master Degree colleagues (André Lourenço, Cláudio Pinto, David Costa, José Sarilho, Pedro Aires) for all the help provided when I needed and the great working environment that made everything more enjoyable.

To my great friend Francisco Pereira, my friends in FEUP and in Maiorff Escola de Música, I would like to express my eternal gratitude for always being there no matter what and for making part of my journey in these last 5 years.

Finally to my family, for all the encouragement, help and advise, not only during these past 5 years, but my entire life.

Abstract

Nowadays, efforts are being made to produce not only increasingly energy efficient machines, but also environmentally friendly equipments that provide lower CO_2 emissions. Furthermore, friction, lubrication and wear have a major role in the efficiency and lifetime of various machinery components.

Knowing that a big part of global energy consumption is used by transportation, and that a part of that energy is used to overcome friction, it is important to develop new technology that reduces costs, fuel consumption and CO_2 emissions.

Taking into account automotive vehicles, there are several parts that can be improved to maximize the vehicle's energy efficiency. The differential, which is one of the automotive transmission components with lower efficiency, is also submitted to study in order to minimize energy losses, as a small increase in efficiency, when applied globally can lead to significant energy savings.

The primary aim of this work is to analyse the power loss in cylindrical roller thrust bearings when lubricated with automotive axle gear oils.

In the first phase of this work, three automotive gear oils were analysed in order to obtain the physical and rheological properties. Secondly, friction torque measurements in the cylindrical roller thrust bearings were made using the three oils at different temperatures and axial loads. With the results obtained it was possible to calibrate a rolling bearing friction torque model for each oil and compare the behaviour of these oils in different operating conditions.

Resumo

Nos dias de hoje, para além de se produzir máquinas energeticamente cada vez mais eficientes, um requisito fundamental é os equipamentos produzirem baixas emissões de CO_2, e os fenómenos de atrito, lubrificação e desgaste têm uma grande influência na eficiencia e duração dos mais diversos componentes de máquinas.

Sabendo que uma grande parte do consumo global de energia é utilizado em meios de transporte, e que parte dessa energia é utilizada para vencer os fenómenos de atrito, é importante o desenvolvimento tecnológico que permite reduzir custos, o consumo de combustível e as emissões de CO_2.

Se se tomar em atenção os veiculos automóveis, existem diversos componentes que poderão ser melhorados de modo a maximizar a eficiência energética dos veículos. O diferencial, que é um dos componentes da transmissão com menor eficiência, também é sujeito a análise de modo a minimizar perdas energéticas, já que um aumento de eficiência por mais pequeno que seja, a nivel global pode se traduzir em grandes poupanças de energia.

O objectivo principal deste trabalho é a análise das perdas de potência em rolamentos axiais de rolos lubrificados com óleos para engrenagens de diferenciais.

Na primeira fase do trabalho, três óleos para diferenciais foram analisados de modo a obter as suas propriedades físicas e reológicas. De seguida, foram efectuadas medições do binário de atrito nos rolamentos axiais de rolos usando os três óleos em estudo, com diferentes temperaturas de funcionamento e cargas axiais aplicadas. Com os resultados obtidos foi possível calibrar um modelo para as perdas de potência nos rolamentos para cada óleo, e comparar o comportamento destes óleos nas diferentes condições de funcionamento.

Keywords

Drivetrain

Differential

Axle Gear Oil

Cylindrical Roller Thrust Bearing

Friction Torque

Coefficient of Friction

Film Thickness

Palavras-Chave

Transmissão

Diferencial

Óleo para Engrenagem Hipóide

Rolamento Axial de Rolos Cilíndricos

Binário de Atrito

Coeficiente de Atrito

Espessura de Filme

List of Symbols

Parameter	Unit	Description
a	[m]	Hertz's semi-width
$CPUC$	[/]	concentration of wear particles index
D_L	[/]	ferrometric index for the amount of large particles
D_S	[/]	ferrometric index for the amount of small particles
D	[/]	bearing's external diameter
d	[/]	bearing's internal diameter
d_m	[mm]	bearing's mean diameter
E^*	[Pa]	equivalent Young modulus
F_n	[N]	axial load
G	[/]	material parameter in the Dowson and Higginson model
G_{rr}	[/]	rolling torque calculation constant
G_{sl}	[/]	sliding torque calculation constant
h_0	[m]	center film thickness
h_{0C}	[m]	corrected film thickness
h_m	[m]	minimum film thickness
$ISUC$	[/]	severity of wear particles index
k	[/]	viscosity ratio
k_L	[W/m °K]	lubricant thermal conductivity
k_1, k_2, k_3	[/]	constants to convert ° Engler to cSt
K_{rs}	[/]	starvation constant
K_z	[/]	bearing type constant
l	[m]	length of a contact
LP	[s]	lubricant parameter
m, n	[/]	ASTM D341 constants
M	[Nmm]	total friction torque
M_{exp}	[Nmm]	experimentally measured friction torque
M_{rr}	[Nmm]	rolling friction torque

M_{sl}	[Nmm]	sliding friction torque
M_{seal}	[Nmm]	seals friction torque
M_{drag}	[Nmm]	drag losses
n	[rpm]	rotational speed
P_{VL}	[W]	bearing power loss
p_0	[Pa]	Hertz's maximum pressure
R^*	[m]	equivalent curvature radius in elliptical contacts
R_x	[m]	equivalent curvature radius in linear contacts
S	[/]	slide-to-roll ratio
SRR	[%]	slide-to-roll ratio
S_p	[/]	modified Stribeck parameter
s, t	[/]	Gold's constants for each oil base
T	[K]	working temperature
U	[/]	velocity parameter in the Dowson and Higginson model
U_S	[m/s]	linear speed in the modified Hersey Parameter
U_e	[m/s]	cylindrical roller peripherical speed
U_g	[m/s]	cylindrical roller center speed
U_i	[m/s]	cylindrical roller interior speed
U_{disc}	[m/s]	disc speed
U_{ball}	[m/s]	ball speed
V_e	[/]	sliding velocity
VI	[/]	viscosity index
W	[/]	load parameter in the Dowson and Higginson model
α	[Pa^{-1}]	piezoviscosity coefficient
β_L	[K^{-1}]	thermoviscosity coefficient
η	[mPa·s]	dynamic viscosity
$\eta_{‰}$	[mPa·s]	factor to calculate dynamic viscosity
λ	[/]	specific film thickness
ϕ_A	[/]	feeding conditions correction factor
ϕ_{bl}	[/]	weighting factor for the sliding friction coefficient
ϕ_{ish}	[/]	inlet shear heating reduction factor
ϕ_R	[/]	roughness correction factor
ϕ_{rs}	[/]	kynematic replenishment reduction factor
ϕ_T	[/]	heating correction factor

ρ	[kg/m^3]	density
σ	[m]	composite roughness
τ	[mPa]	shear stress
$\tau‰$	[mPa]	factor to calculate shear stress
μ_{bl}	[/]	boundary friction coefficient
μ_{EHL}	[/]	friction coefficient due to lubricant shearing
μ_{sl}	[/]	sliding friction coefficient
ν	[cSt]	kynematic viscosity

Contents

List of Figures

List of Tables

1. Introduction

1.1. Background and Purpose

Automotive vehicles represent the largest division in energy consumption when taking into account the energy used by the transportation sector. According to Holmberg *et al.*[1], in passenger cars 1/3 of the energy is used to overcome friction, as represented in Figure 1.1 which corresponds in average to 340 liters of fuel consumed per year and vehicle for this purpose alone. If advanced friction control techniques were to be applied, the impact in the next 5 to 10 years would be:

- Energy losses in engines reduced by 18 %
- 117000 million liters of fuel saved globally per year
- Economic savings of 174000 million euros globally
- Reduction of CO_2 emissions in 290 million tons globally per year

The car's driveline is already considered an efficient system and usually when improving a vehicle's efficiency greater importance is given to the engine and the car's weight. However, small changes in the efficiency of the driveline can lead to global savings of an high order, therefore the importance of studying improvements to be made in this component. Optimal performance of the driveline can be achieved optimizing gears, rolling bearings and seals, optimizing lubrication systems and using multigrade oils with lower viscosity and lower shear rate, as suggested by Joachim *et al.* in Figure 1.2 [2].

Taking into account the goal of achieving greater efficiency, the object of this work is to study power losses in cylindrical roller thrust bearings when lubricated with automotive axle gear oils. For that purpose the friction torque will be measured experimentally in those bearings when lubricated with three different multigrade oils that are used in automotive differentials. The experimental tests will be performed at different operating speeds, temperatures and loads. With the results obtained it is possible to observe the behaviour of each oil at each operating condition and calibrate a power loss model to accurately predict the experimental results.

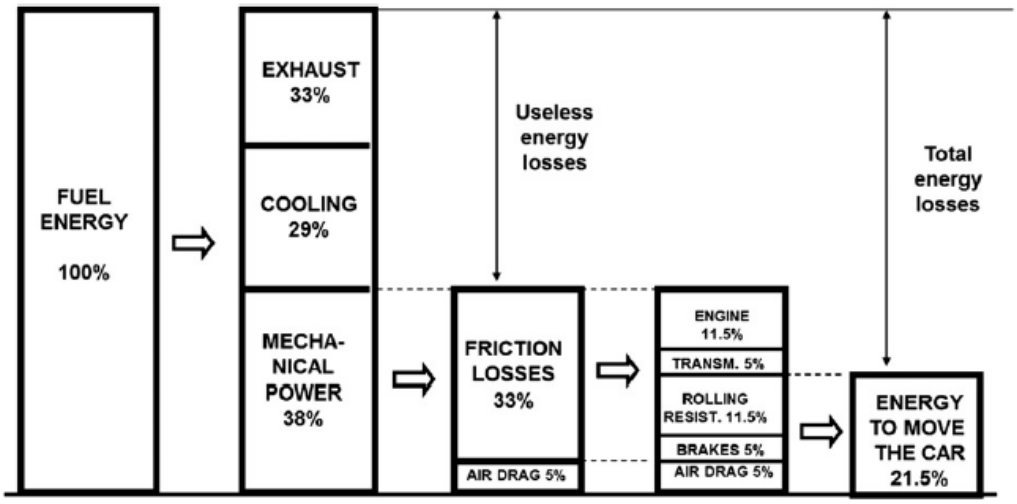

Figure 1.1.: Car energy consumption [1]

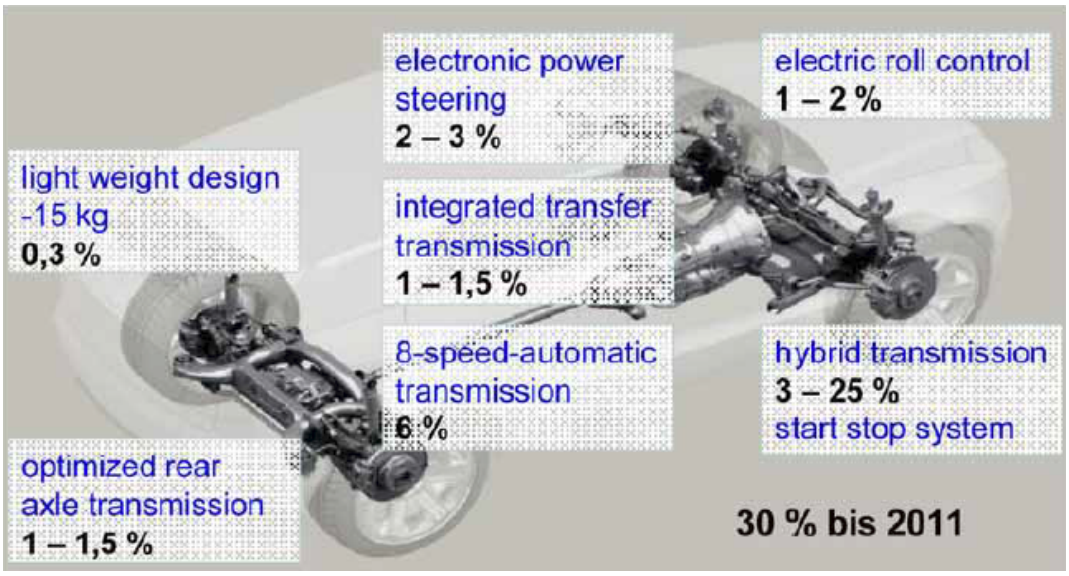

Figure 1.2.: Driveline potential improvements [2]

1.2. Thesis Outline

- **Chapter 2 - Automotive Transmissions** gives an overview of the different types of automotive transmission systems and how they work, types of differentials and differential gears and bearings. Lubricant types and requirements for this application are also described, as well as studies on the type of oils used in these systems.

- **Chapter 3 - Lubricants Selection and Characterization** describes the first phase of experimental work that consists on the measurements of the oil's physical and rheological properties. Experimental procedures and results are exposed.

- **Chapter 4 - Film Thickness and Traction Curves of Axle Gear Oils** describes film thickness and traction coefficient measurements made on a ball on disc contact with axle gear oils. The analysis of the results will provide the comparison of the experimental with the predicted film thickness in the contact. The traction coefficient results when observed on stribeck curves provide information on the lubrication regime in a contact.

- **Chapter 5 - Elastohydrodynamic Lubrication** reviews the theory behind the calculation of the film thickness in roller bearings and introduces the concept of the Stribeck curve as a way to evaluate the lubrication regime.

- **Chapter 6 - Friction Torque/Power Loss in Cylindrical Roller Thrust Bearings** gives a description of the model used by SKF to calculate the coefficient of friction and describes the process to calibrate this model according to the experimental results obtained. A brief description of the tested bearings is also included.

- **Chapter 7 - Roller Bearings Experimental Results** shows the friction torque measurement procedure and the tested operating conditions. Then, it is presented the measurements of friction torque made for the bearings with the tested oils at diverse operating conditions, and the analysis of the results obtained from those measurements.

- **Chapter 8 - Conclusions and Future Work** shows the main conclusions that can be obtained from the experimental work and consequent analysis present in this thesis, as well as work that can be developed in the future.

Part I.

Bibliographical Revision and Lubricant Characterization

2. Automotive Transmissions

In an automotive vehicle, the goal of the transmission system is to transfer the power and torque produced by the engine to the wheels so the vehicle can be manouvered.

In the process of the design of an automotive transmission, the main purpose is to optimally convert the traction provided by the engine into the traction force of the vehicles over a great variety of speeds. In the end, a compromise must be achieved between the number of speeds, the vehicle's performance and acceleration and fuel consumption, while taking into account the required service lifetime, environmental impact and social issues. The information of this chapter is based on literature regarding the subject [3] [4] [5] [6].

2.1. Types of Transmission Systems

According to the type of vehicle, there are three possible configurations for the transmission system: front-wheel drive, rear-wheel drive and all-wheel drive. In these three cases, the engine is generally located in the front of the vehicle, and the difference between the three is which pair of wheels is driven by engine power, in other words, the location of the axle with the differential.

2.1.1. Front-Wheel Drive

Front-Wheel driving systems, represented in Figure 2.1a, are the most commonly found in passenger cars, with the engine being in front of the axle that drives the front wheels. This configuration has the advantage of being compact since it is located in the front of the vehicle, which transmits benefits in terms of adherence in slippery grounds (snow, mud,...). Since there is no need for a driveshaft crossing the vehicle (assuming the engine is located in the front), this system has lower weight when compared with rear-wheel or all-wheel drives, which can translate in a better fuel efficiency.

The biggest disadvantages of this system are the lower capability of acceleration, since the weight of the vehicle shifts to the back in sudden acceleration, thus improving traction in the rear wheels, the tendency to understeer due to the most weight being located in the front of the vehicle, the reduced traction while driving uphill in slippery conditions and the lower traction in the rear wheels when braking under extreme conditions.

2.1.2. Rear-Wheel Drive

Rear-Wheel driving systems, represented in Figure 2.1b were the most commonly used in vehicles up to the 1980s. In this layout, the engine is generally mounted in the front of the vehicle, although engine in the rear or in the middle are also possible, and the driven wheels are the rear wheels, that are driven by the differential that connects to the engine by means of a driveshaft. This configuration is usually applied in sports cars due to the better handling provided and the increased grip on the rear wheels in the acceleration process. Also, since the transmission system is mounted over the length of the car, the front can accomodate more powerful engines. Other advantages include a more even weight distribution and better braking response than front-wheel vehicles.

This system however, also has some disadvantages. In opposition of the front-wheel vehicles, this system may cause oversteering due to the lack of weight in the rear wheels, there is lack of traction in the rear wheels in slippery conditions, less space and more weight in the vehicle due to the size of the transmission system, higher cost and lower efficiency.

2.1.3. All-Wheel Drive / Four-Wheel Drive

In all-wheel driving systems, both wheels can be provided with power by the vehicle's engine. In these systems, both front and rear axles can be driven simultaneously by the engine (full-time all-wheel drive), or only one of the axles can be driven and the other only driven when necessary (part-time all-wheel drive). When talking about all-wheel driven systems, it is important to distinguish the terms four wheel-drive and all-wheel drive since they are referring to two different systems.

In all-wheel driven vehicles, represented in Figure 2.1c, not only both front and rear axles contain a differential, but there is also a differential in the center of the vehicle which balances the rotational speed between the front and the rear wheels (assuming a traditional mechanical system, as there are also electronically all-wheel driven systems) while providing an even distribution of torque to all four wheels. New car designs are made using this transmission system as it improves the car's performance and allows better handling in a broad range of surface conditions. The main setbacks of this system is the increased weight and lower fuel economy.

In four-wheel driven vehicles, represented in Figure 2.1d (typically known as 4x4), power transmission is made by means of a transfer case (gearbox) located between the front and rear axles connecting them. Since there is no mechanism (differential) that provides different rotational speeds in each wheel, the vehicle will only turn if the surface is slippery enough to make the tyres slip and allow the vehicle to make the curve (the locking only happens at low speeds in not slippery grounds). Off-Road vehicles typically have this transmission incorporated to improve traction, and in situations with no slip this system can be deactivated to become a two-wheel driven vehicle.

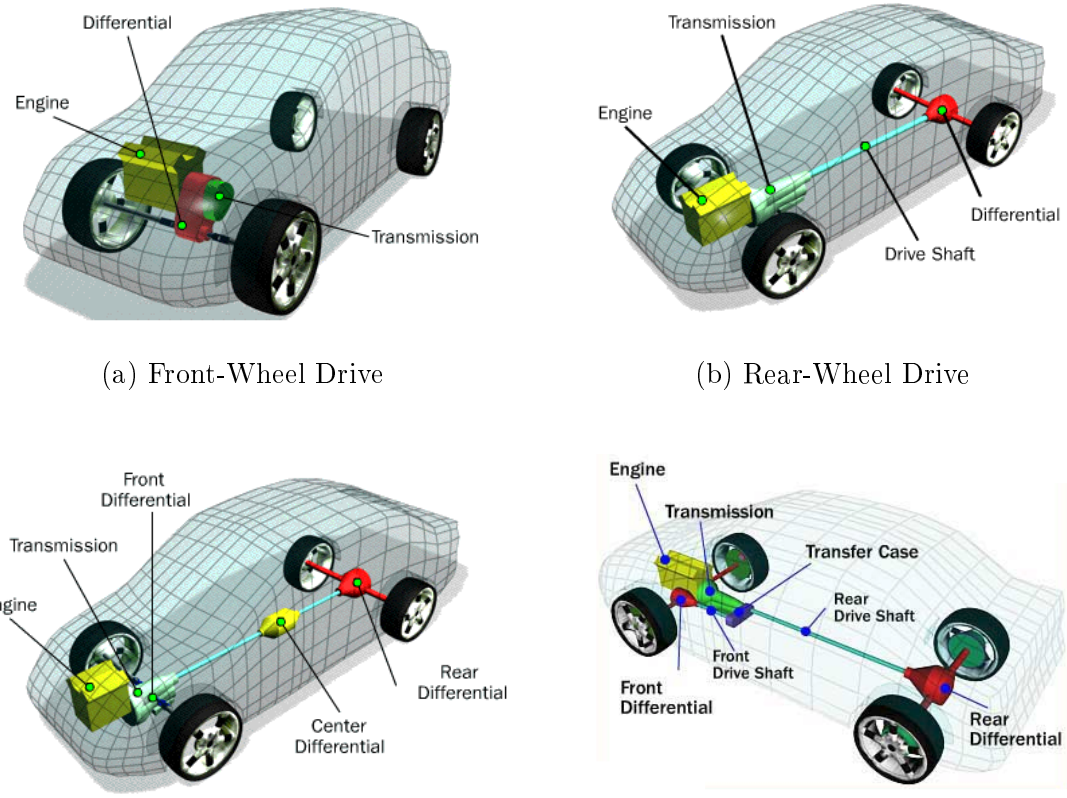

(a) Front-Wheel Drive

(b) Rear-Wheel Drive

(c) All-Wheel Drive

(d) Four-Wheel Drive

Figure 2.1.: Different wheel driving systems

2.2. Types of Differentials

The axle differential is the vehicle's transmission component that transmits power to the wheels, acts as the final gear reduction in the vehicle and allows the wheels to rotate at different speeds when making a curve. The input speed of the shaft is equal to the average rotational speed of the driven wheels, so when one wheel has an increase in speed, the other has a decrease.

As mentioned before, the location of the differential (front axle, rear axle or both) allows the distinction between the different types of transmition systems. For front-wheel and rear-wheel drive mechanisms, the differential is located in the respective driven wheel axle. If the vehicle is all-wheel driven, not only does it have a differential in both wheel axles, it also has (in most cases) a differential between front and rear wheels to balance the rotational speed between front and rear wheels.

In the following section, four types of differentials are described: open differentials, limited-slip differentials, locking differentials and TORSEN differentials.

2.2.1. Open Differential

Open differentials, represented in Figure 2.2a, are the most commonly used type of differentials. In this configuration, the driveshaft of the transmission rotates causing the rotation of the pinion gear of the differential, which in turn causes the rotation of the ring gear that is connected to the wheels by two shafts, allowing the movement of the vehicle. When driving in a straight line, the shafts connected to the ring gear rotate at the same speed, but when making a curve they are forced to rotate at different speeds, allowing the vehicle to turn.

Vehicles with this type of differentials may have trouble when a pair of wheels is in contact with two surfaces with different degrees of friction, because all engine power is directed to the axle's shaft connected to the wheel with least resistance, therefore the other wheel won't rotate.

2.2.2. Limited-Slip Differential

Limited-Slip differentials, represented in Figure 2.2b, are designed to prevent the setback described in open differentials. The design is basically the same of the open differential, but it also includes two springs and pressure plates in the housing located between the shafts that connect to the wheels. When taking a turn, the spring-plate system is compressed and the system will try to behave as if the vehicle was driving in a straight line. However, when making a curve, the shafts of the wheels slip against the plates and start to rotate at different speeds, allowing the vehicle to make the turn.

Taking into account the situation of the driven wheels in two different surfaces, with this type of differential the power will be distributed by the two driven wheels instead of the wheel with least resistance due to the higher compression of the spring-plate system that allows the same amount of rotation on both wheels.

2.2.3. Locking Differential

Locking differentials, represented in Figure 2.2c, are widely used in off-road vehicles, since they can lock the wheels of an axle, making them function as a solid unit. This is benefitial in off-road vehicles when the wheels may be subjected to rotation in different surfaces or even if a wheel of an axle is in the air. Locking differentials use a pneumatic or hydraulic system that lock the wheels of an axle together.

Locking differentials can be described as automatic if they are locked and unlocked with no influence of the driver of the vehicle, or selectable if the driver can lock or unlock the function from the driver's seat. Automatic locking allows a continuous riding since the driver doesn't have to change the function, but on the other hand it increases tire wear and when making a curve, the car shifts from an understeer situation to oversteer in a short amount of time.

2.2.4. TORSEN Differential

The TORSEN (Torque Sensing) differential, represented in Figure 2.2d, is a variation of the limited-slip differential which can be used in the front and rear axle, and in the shaft that connects both axles.

If the torque in the outputs of the differential is the same, the TORSEN differential acts like an open differential. However, if the torque becomes different in a pair of wheels (one wheel looses traction), the gearing mechanism of the TORSEN mechanism prevents the loose wheel to rotate and concentrates the torque output in the wheel with traction. A particular feature of the TORSEN differential is the "Torque Bias Ratio". This ratio indicates the torque distribution in each wheel or axle, and it is constant even if the degree of difference in traction in both wheels or axles is considerably high.

The situation where the TORSEN differential doesn't work is if a wheel or set of wheels completely loses traction. In that case no torque is transferred to the wheels with or without traction.

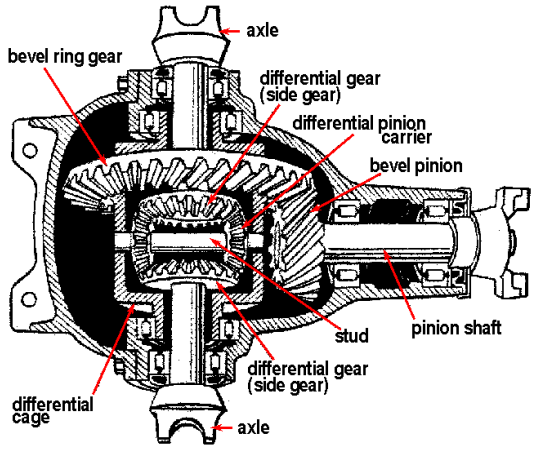

(a) Open Differential

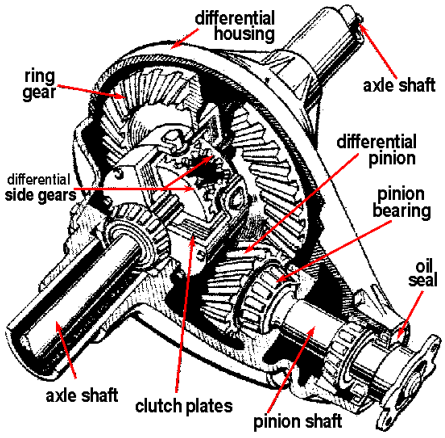

(b) Limited-Slip Differential

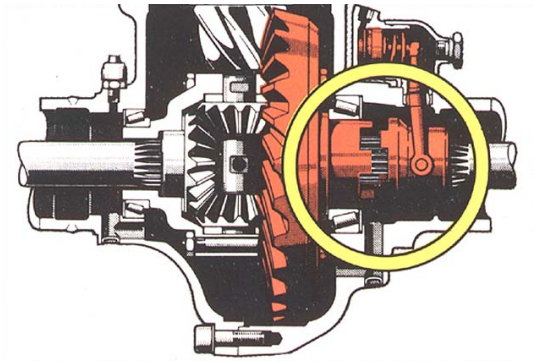

(c) Locking Differential

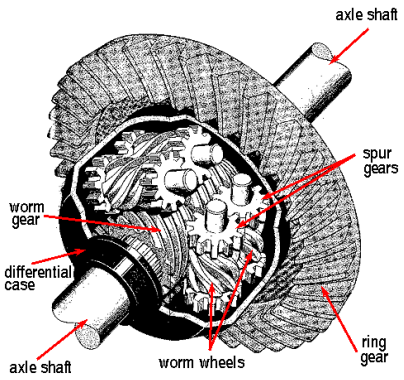

(d) TORSEN Differential

Figure 2.2.: Different types of differentials

2.3. Differential Components

2.3.1. Gears

Differential gears can be divided in two major groups, the gears of an interaxle differential (transfer gearbox), or the gears of an interwheel differential (differential gear unit). The interaxle differential transmits the power from the engine to the two driven axles of the vehicle (all-wheel drive), while the interwheel differential transmits the power to the driven wheels of a vehicle (any kind of drive).

The most common gear arrangements found in differentials (Figure 2.3) are bevel gears (these gears can be helical or hypoid and are generally used in interwheel differentials), spur gears (typically used in interaxle differentials) and worm gears (used in the TORSEN differential which can be an interaxle or an interwheel differential).

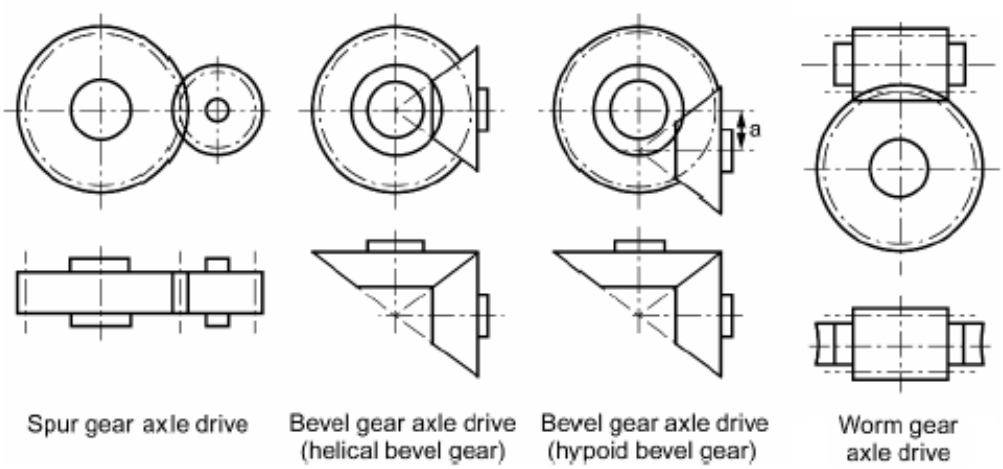

Figure 2.3.: Schematic representation of the gear arrangements used in differentials [4]

2.3.2. Bearings

In an interwheel differential, the type of bearing that is commonly used is the tapered-roller bearing. In the differential unit (Figure 2.4), at least four bearings of this type are used: two that support the differential case and two to support the drive pinion shaft. The bearings that support the differential case are capable of absorbing the forces that are put on it, and are installed with a preload so the pinion and ring gears don't move out of their place. The drive pinion also needs to be accurately mounted with two bearings, because when it rotates, it tries to screw itself out of the ring gear.

An increased efficiency has been proved when replacing the tapered-roller bearings with angular contact ball bearings [7]. The tapered-roller bearings have the tendency

to lose preload overtime due to significant wear and friction in the rollers caused by insufficient lubrication and cooling. Angular contact ball bearings can support the same type of loads (radial and axial) that tapered-roller bearings support, and since the contact area is smaller, it has reduced friction and it is easier to lubricate.

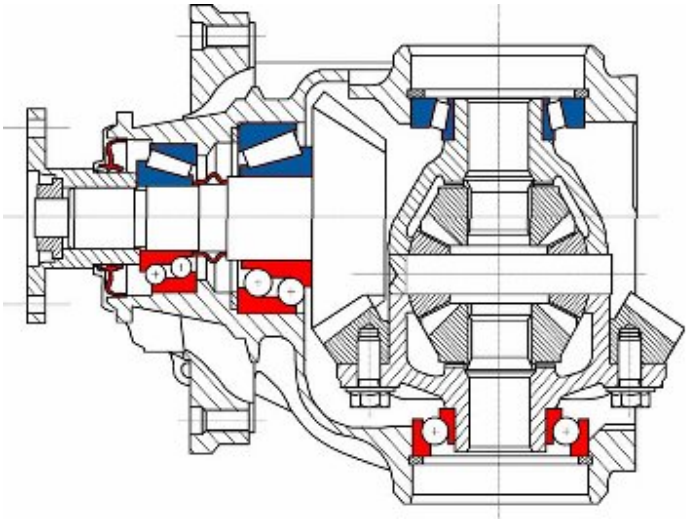

Figure 2.4.: Schematic comparison of tapered-roller bearings (blue) and angular contact ball bearings (red) when mounted on a differential [7]

2.4. Axle Gear Lubrication

To improve the axle's efficiency, a correct choice of lubricant is required in order to reduce the wear, corrosion and oxidation in gears and improve the durability of both gears and bearings [8].

Multigrade oils are being increasingly used in this type of applications, since they typically have an high Viscosity Index, which means that if the oil's viscosity is high enough, a lubricant film can be formed over a broad range of temperatures. However, for the oils to have these properties a significant amount of polymers must be added, and since they are prone to shear degradation in service conditions, this phenom may lead to a sudden drop in viscosity, reduced film thickness and possible equipment failure. Therefore, tests are performed (Figure 2.5) to ensure that the oil maintains its viscosity between certain limits under shear conditions over a large period of time (20 hours) [9].

The base oil for axle gear oils can be mineral or fully synthetic. A fully synthetic base can provide unique properties to the oil, but it also makes it more expensive. Other components of the oil include viscosity modifiers (polymers that increase viscosity at higher temperatures), pour point depressants (polymers that prevent wax crystal formation and growth at low temperatures), anti-wear and extreme pressure additives and corrosion, oxidation and foam inhibitors.

Test	Description	Characteristics measured
ASTM L-33	Gear test using differential assembly	Resistance to corrosion in presence of moisture
ASTM D 6121	Gear test using complete axle assembly	Resistance to gear distress under low-speed, high-torque conditions
ASTM L-42	Gear test using complete axle assembly	Resistance to gear distress (scoring) under high-speed, shock-load conditions
ASTM L-60	Bench test using spur gears	Oxidative stability
ASTM D 5704	Bench test using spur gears	Thermal and oxidative stability and deposits
ASTM D 5662	Bench test	Seal compatibility
ASTM D 5579	Gear test	Transmission cyclic durability (waived for approved lubricants)
ASTM D 5182	Gear test	Spur gear wear
ASTM D 130	Bench test	Stability in the presence of copper and copper alloys
ASTM D 892	Bench test	Foaming tendencies

Figure 2.5.: Automotive gear oil tests [9]

2.5. Lubricant Oils Specifications

Nowadays, there are two kinds of specifications for lubricant oils: viscosity specifications (characterize an oil according to its viscosity) and service specifications (characterize an oil according to its application).

2.5.1. Viscosity Specifications

There are several professional entities that classify oils in a wide range of viscosities. The most currently used are SAE (Society of Automotive Engineers), ISO (International Standards Organization), AGMA (American Gear Manufacturers Association) and ASTM (American Society for Testing and Materials). The most widely used of this classifications in the automotive industry is SAE which is purely based on the viscosity of the oil. As this thesis will focus on oils used in differentials, the corresponding classification (SAE J306) is presented in Figure 2.6.

2.5.2. Service Specifications

The most used classifications according to service are API (American Petroleum Institute) and ACEA (Association des Constructeurs Européens d'Automobiles). The classification that is presented in Figure 2.7 is the API classification for automotive transmissions.

SAE J306
Transmission Oil Viscosity Classification Chart

J306 Viscosity Classification for Automotive Gear Oils			
Efective January 1, 2005			
SAE Viscosity Grade	Maximum Temperature for a viscosity of 150,000 cP (°C)	Minimum Viscosity at (cSt) a 100°C	Maximum Viscosity at (cSt) a 100°C
	ASTM D 2983	ASTM D 445	ASTM D 445
70W	-55	4.1	--
75W	-40	4.1	--
80W	-26	7.0	--
85W	-12	11.0	--
80	--	7.0	<11.0
85	--	11.0	<13.5
90	--	13.5	<18.5
110	--	18.5	<24.0
140	--	24.0	<32.5
190	--	32.5	<41.0
250	--	41.0	--
		Must maintain its viscosity after 20 hours in the CEC L-45-A-99 test.	

Figure 2.6.: SAE classification for gearbox and differential oils - SAE J306

API service designation (performance level)	Application and short characterisation
GL-1	Manual transmissions operating under such mild conditions that straight petroleum or refined petroleum oil may be used satisfactorily. Not satisfactory for many passenger car manual transmissions. GL-1 oils may contain oxidation and rust inhibitors, defoamers, and pour depressants. Friction modifiers (FM) and extreme pressure (EP) additives shall not be used.
GL-4	Axles with spiral bevel gears operating under moderate to severe conditions of speed and load or axles with hypoid gears operating under moderate speeds and loads. GL-4 oils may be used in selected manual transmission and transaxle applications where MT-1 lubricants are unsuitable. GL-4 oils contain up to 4% of extreme pressure (EP) additives.
GL-5	Gears, particularly hypoid gears, in axles operating under various combinations of high-speed/shock load and low-speed/high-torque conditions. GL-5 oils contain up to 6.5% of extreme pressure (EP) additives.
MT-1	Nonsynchronised manual transmissions used in buses and heavy-duty trucks. API MT-1 does not address the performance requirements of synchronized transmissions and transaxles in passenger cars and heavy-duty applications. API MT-1 oils provide protection against the combination of thermal degradation, component wear, and oil-seal deterioration, which is not provided by lubricants in current use meeting only the requirements of API GL-1, 4, or 5.

Figure 2.7.: API classification for gear oils in current use

2.6. Previous Studies on Lubricant's Effect on Rear Axle Efficiency

As mentioned before, friction losses in rear axles can be reduced optimizing gear design, utilizing bearings that provide lower friction and using lubricants with lower viscosity. Regarding lubricants, the trend has been the development of fuel-efficient multigrade gear lubricants with low values of viscosity.

To analyse the efficiency of this type of lubricants, numerous studies have been made over the years. O'Connor et al. [10] verified that applying different synthetic bases cause little changes in the efficiency of an axle, but significant changes are verified when comparing fully synthetic oils with partially synthetic oils. Law [11] showed that synthetic lubricants increase the efficiency of hypoid gears. Watts and Willette [12] compared the efficiency of different viscosity grade lubricants (SAE 75W90, SAE 75W140 and SAE 90) and showed that the multigrade oils provide higher axle efficiency. Willermet and Dixon [8] analysed the effect of viscosity on axle efficiency and adjusted the low and high temperature viscosities to obtain an improvement of 1% in fuel economy. Bala et al. [13] showed that the lubricant's viscosity and viscosity index (VI) affect the axle's efficiency and that oils with higher VI improve an axle's efficiency. Devlin et al. [14] showed that higher viscosity oils are preferred in higher torque and lower speed conditions (higher film thickness), while lower viscosity oils are preferred in lower torque and higher speed conditions (lower shear rate).

For further information regarding lubricant characterization (types of lubricants and additives) and their physical properties (calculation of viscosity, density and viscosity variations with temperature, pressure and shear rate), Appendix A and Appendix B should be consulted.

3. Lubricants Selection and Characterization

To perform the experimental work that will be further explained in this thesis, three multigrade oils with the classification of "fuel-efficiency", which are applied in gearboxes and differentials were selected. Two fully synthetic oils (TOTAL SYN FE 75W90 and TRANSELF SYN FE 75W140) and a semi-synthetic oil (TOTAL RS FE 80W90). In Table 3.1 are displayed the properties of the three oils gathered from the data sheets provided by the manufacturers, which are presented in Appendix C. The three oils are described by the manufacturers as:

- having extreme pressure and anti-wear properties
- having very low loss in viscosity due to shear
- having excellent anti-foam, anti-rust and anti-corrosion behaviour
- having excellent thermal and service stability.

Table 3.1.: Oil properties provided by the manufacturers

Parameter	Unit	Standard	75W90 (PAO)	75W140 (PAO)	80W90 (MIN)
Density @ 15°C	g/cm^3	ASTM D4052	0,866	0,885	0,886
Viscosity @ 40°C	cSt	ASTM D445	101	183	115
Viscosity @ 100°C	cSt	ASTM D445	15	26,3	14,1
Viscosity Index	/	ASTM D2270	157	178	123
Pour Point	°C	ASTM D97	-51	-36	-33

3.1. Oil Analysis - Physical Properties

Before any test was made using the oils provided, their physical properties needed to be measured in order to confirm the information provided by the manufacturer. Also, a preliminary particle analysis was made to verify that the oils weren't contaminated before being submitted to the test procedures using cylindrical roller thrust bearings.

In this stage, the tests performed were density measurement (Densimeter), viscosity measurement (Engler viscometer, Rheometer, Vibrational viscometer), ferrography analysis (Direct Reading Ferrography and Analytical Ferrography) and FTIR Analysis.

3.1.1. Density

It is important to know the density of the oils at different temperatures. Knowing this parameter makes it possible to calculate a good approximation of the thermal expansion coefficient and the dynamic viscosity. To measure the density of the oils a densimeter was used.

To obtain the density, 2 ml of an oil sample are extracted by the densimeter at three different temperatures, and based on those three measurements, it is possible to obtain a good approximation of the density variation with the temperature. The value of the inclination of the linear function that is obtained is the thermal expansion coefficient which can be expressed using equation (3.1).

$$\rho = \rho_{ref} \cdot (1 - \alpha(T_{ref} - T)) \tag{3.1}$$

In this equation ρ represents the density at a temperature T, ρ_{ref} the density at the reference temperature T_{ref} (usually 15 °C) and α the thermal expansion coefficient.

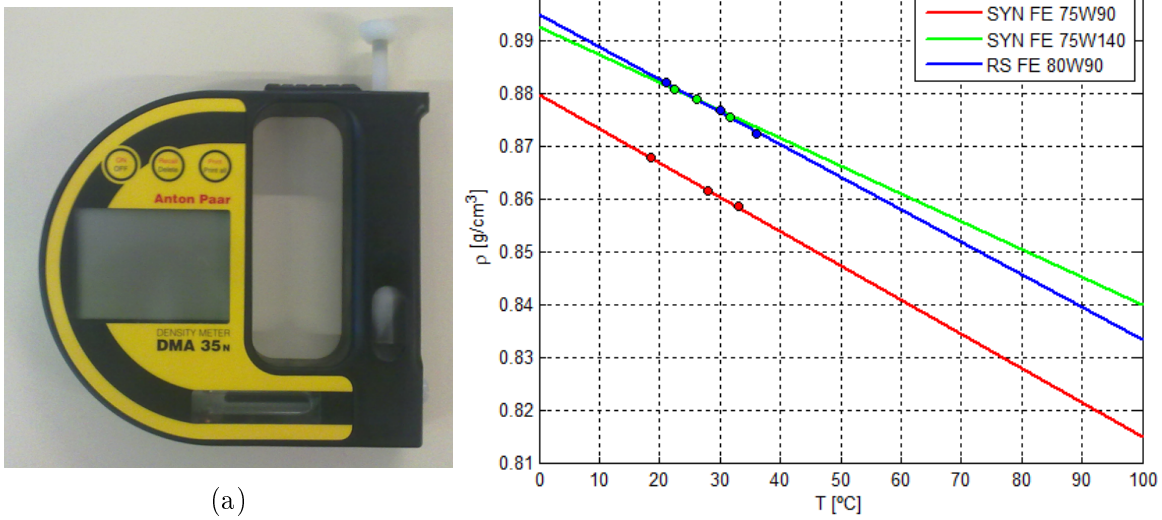

(a) (b)

Figure 3.1.: Anton Paar DMA 35_N Densimeter (a) and density variation with the temperature of the tested oils (b)

It is important to note that the densimeter used can only measure density on fluid temperatures lower than 40 °C with great accuracy.

The values obtained for the density of the three oils at 15 °C, as well as the values of the thermal expansion coefficient are presented in Table 3.4.

Analysing the results, it is possible to observe in Figure 3.1b or comparing the values of the thermal expansion coefficient in Table 3.4, that the SYN FE 75W90 oil is the one that has an higher density decrease with the temperature, which means its volume variation is bigger than the other oils. SYN FE 75W90 is also the oil with the lowest density at the working temperatures.

3.1.2. Viscosity - Engler Viscometer

To obtain the viscosity variation with temperature, the viscosity for different temperatures needs to be experimentally determined in order to apply Vogel's Law or the ASTM D341 Standard. To determine the kinematic viscosity, it was used the Engler's viscometer. The working principle of this viscometer is described in the IP 212/92 Standard and viscosity's calculation is based on the time a given volume of oil takes to fill a recipient at a certain temperature.

In the Engler's viscometer, the oil sample which will be analysed is inside a cylindrical container that as a hole in the bottom which is obstructed with a wooden pointer. The cylindrical container is imersed in an oil bath that is heated with an electrical resistance and will heat the oil sample to be analysed. The temperature of the oil sample and the oil bath is controlled with two mercury thermometers and once the desired measuring temperature of the oil sample is reached, the hole in the container is disobstructed and the time the oil takes to drain a defined volume is measured.

To obtain the values of the kynematic viscosity at each temperature, equations (3.2) and (3.3) are used considering the values presented in Table 3.2.

$$^{\circ}Engler = \frac{time\ that\ 200\ mL\ of\ oil\ takes\ to\ flow\ at\ the\ tested\ temperature}{time\ that\ 200\ mL\ of\ water\ takes\ to\ flow\ at\ 20^{\circ}C} \tag{3.2}$$

Table 3.2.: Values used to convert the kinematic viscosity from ° Engler to cSt

	k_1	k_2	k_3
$^{\circ}Engler < 3$	14,867	75,568	-6,198
$^{\circ}Engler \geq 3$	7,624	-2,717	-1,522

$$\nu(cSt) = k_1 \cdot \left(^{\circ}Engler + \frac{k_2}{^{\circ}Engler + k_3} \right) \tag{3.3}$$

Table 3.3.: Conversion from ° Engler to cSt of the three tested oils at the tested temperatures

	75W90 (PAO)		75W140 (PAO)		80W90 (MIN)	
	° Engler	cSt	° Engler	cSt	° Engler	cSt
40 °C	15,21	115,77	27,25	207,63	16,76	127,57
70 °C	5,23	38,23	8,60	64,20	4,94	36,54
100 °C	2,63	17,13	3,73	27,22	2,33	15,15

Table 3.4.: Oil properties experimentally measured

Parameter	Unit	Standard	75W90 (PAO)	75W140 (PAO)	80W90 (MIN)
Density @ 15°C	g/cm^3	/	0,870 (0,866)	0,885 (0,885)	0,886 (0,886)
Thermal Expansion Coefficient $\times 10^4$	$°C^{-1}$	/	$-7,46$	$-5,98$	$-6,98$
Viscosity @ 40°C	cSt	ASTM D341	115,77 (101)	207,63 (183)	127,57 (115)
Viscosity @ 70°C	cSt	ASTM D341	38,23	64,20	36,54
Viscosity @ 100°C	cSt	ASTM D341	17,13 (15)	27,22 (26,3)	15,15 (14,1)
m	/	ASTM D341	7,4576	7,0893	8,3460
n	/	ASTM D341	2,8618	2,6942	3,2143
Viscosity Index	/	ASTM D2270	162 (157)	167 (178)	122 (123)
Thermoviscosity @ 40°C	K^{-1}	ASTM D341	0,0437	0,0461	0,0501
Thermoviscosity @ 70°C	K^{-1}	ASTM D341	0,0311	0,0331	0,0345
Thermoviscosity @ 100°C	K^{-1}	ASTM D341	0,0230	0,0247	0,0249

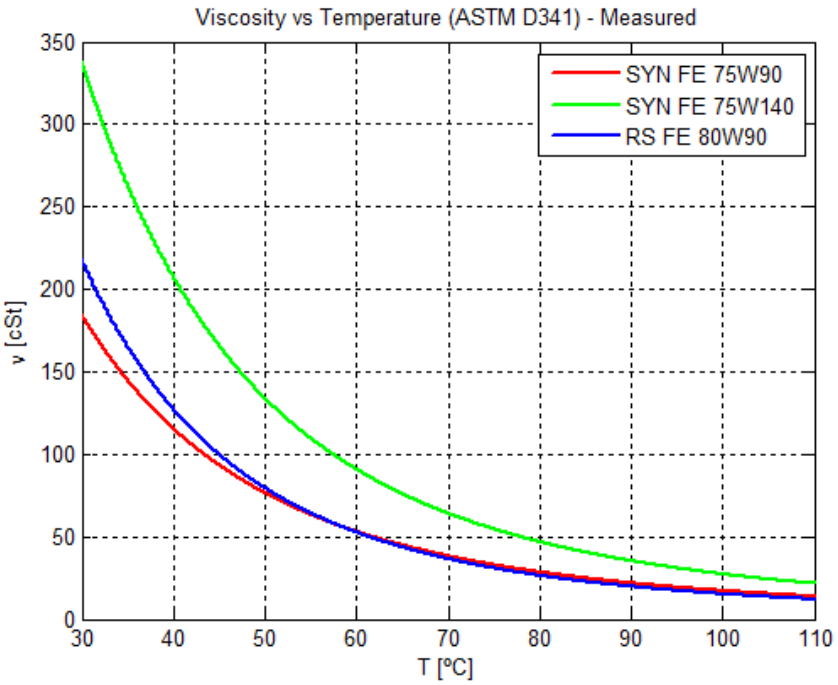

Figure 3.2.: Viscosity variation with the temperature for the tested oils based on the Engler's viscometer measurements

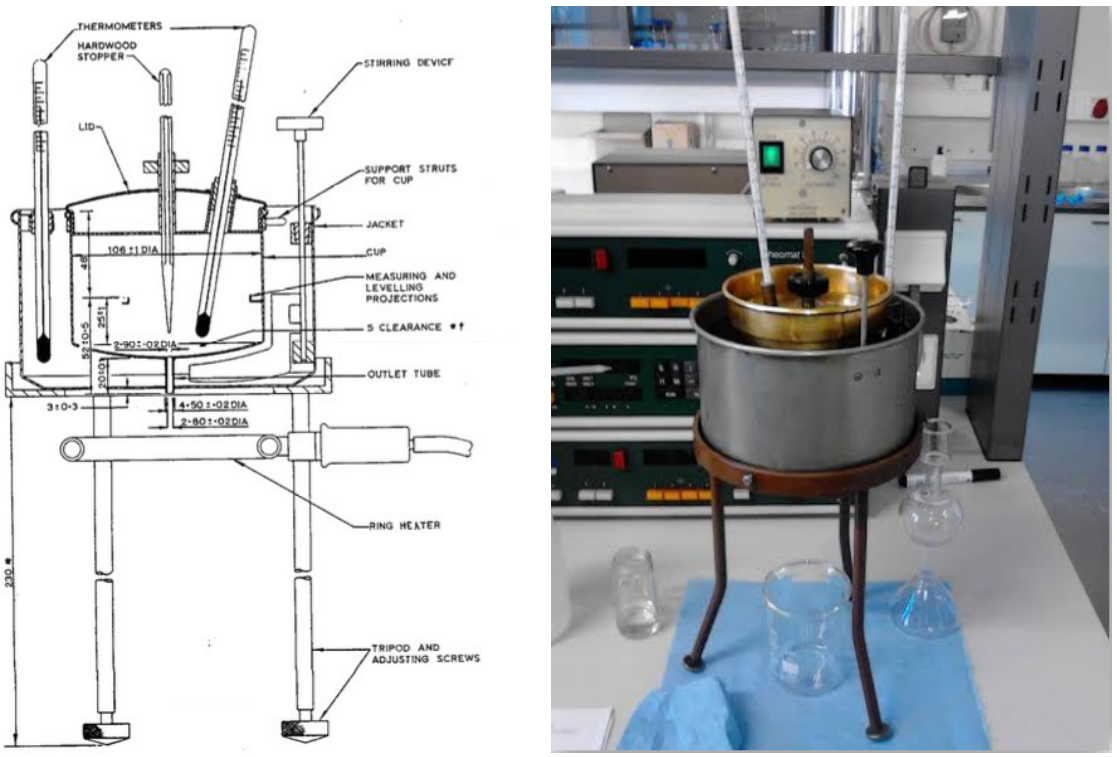

Figure 3.3.: Engler Viscometer

For the Engler viscometer used the water's time to flow is 49,3 seconds, and once knowing the time the oil takes to drain the predefined volume, it is possible to obtain the kynematic viscosity of each oil at the tested temperatures as shown in Table 3.3. Once the viscosity for each temperature is obtained it is possible to determine the constants which are used in ASTM D341 Standard and Vogel's Law, and compare both solutions. Observing that the viscosity-temperature curves obtained using the ASTM D341 Standard or Vogel's Law are pratically identical, the ASTM D341 will be used for calculations as displayed in Table 3.4. Values between brackets in Table 3.4 show the values from the manufacturers data sheets.

It is observed through the Viscosity Index that the RS FE 80W90 oil is the oil who shows bigger viscosity variation with the temperature (semi-synthetic oil), and the viscosity variations of the other two oils are very similar despite having different viscosities at the tested temperatures.

3.1.3. Viscosity - Rheometer

The rheometer RHEOMAT 115 (Figure 3.4a) is a rotational viscometer that measures the braking torque exerted on the rotating shaft by the fluid which the bob is inserted in, and displays its value on a control instrument. By measuring the braking torque at different shear rates (different rotational speeds of the shaft) and different temperatures, it is possible to obtain the shear stress and the dynamic viscosity and observe the behaviour of the fluid (Newtonian or Non-Newtonian) at different temperatures.

To obtain the graphics that show the evolution of viscosity (η [mPa·s]) and shear stress (τ [mPa]) with the shear rate, equations (3.4) and (3.5) were used.

$$\eta = \eta‰ \cdot torque\ read\text{-}out \tag{3.4}$$

$$\tau = \tau‰ \cdot torque\ read\text{-}out \tag{3.5}$$

The *torque read-out* is the value observed in the control instrument for each measurement while $\eta‰$ [mPa·s] and $\tau‰$ [mPa] are values for a given step module (77) and measuring system (DIN 145). The shear rate D [$1/s$] is also tabled for each step module.

For the tested oils, measurements were made at three different temperatures, and at each temperature the *torque read-out* is annotated for five different rotational speeds of the rheometer's shaft.

The measurements performed with the rheometer (Figure 3.4b) showed that all three oils have a newtonian behaviour at 70°C and 100°C. At 40°C, SYN FE 75W90 and RS FE 80W90 also show a newtonian behaviour, but for SYN FE 75W140 the decrease in dynamic viscosity with the increase in shear rate suggests that at this temperature it has a non-newtonian behaviour. However, observing rheometer measurements it is noticed that at the last speed measurement, the temperature increased slightly, which is translated in a decrease of viscosity. Summarizing, the probable reason for the decrease in viscosity between the two last speeds for the 75W140 oil is an increase in temperature instead of an increase in shear rate.

(a)

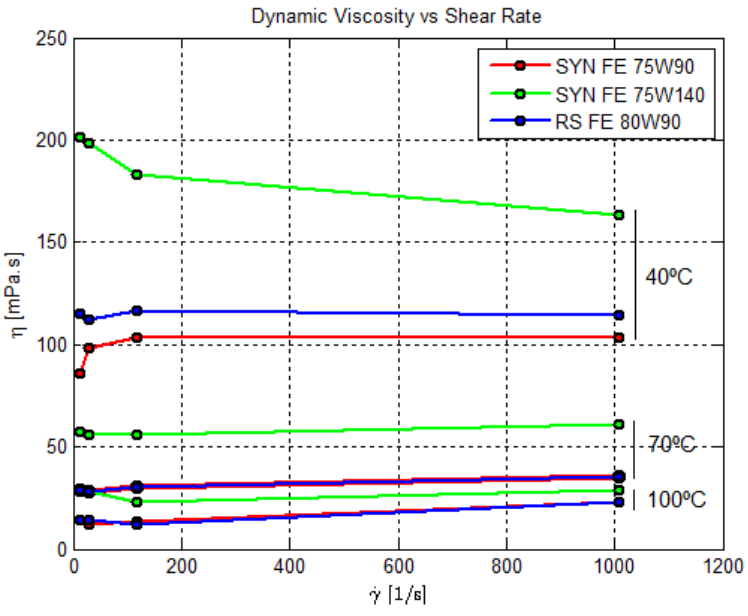

(b)

Figure 3.4.: Contraves RHEOMAT 115 rheometer (a) and Dynamic viscosity variation with the shear rate of the tested oils at three different temperatures (b)

3.1.4. Viscosity - Vibrational Viscometer

Another method to obtain the viscosity is utilizing the vibrational viscometer SV10 (Figure 3.5a). This viscometer has two paddles that vibrate with a frequency of 30 Hz and an amplitude inferior to 1 mm, and are inserted into a container with a sample of the lubricant to be tested. In the tests, both the frequency and amplitude are kept constant. While measuring, the viscosity of the lubricant provokes damping on the vibration, however the amplitude must remain the same and for that purpose a current is given to the paddles to keep the amplitude constant. The values of the current are continuously measured and converted to viscosity values, and the graphic obtained is the viscosity as function of the temperature. Dividing the dynamic viscosity with the density at a given temperature, it is possible to obtain the kynematic viscosity and compare the values with the ones provided by the manufacturer and the ones obtained with the Engler viscometer. For this viscometer there are no calculations applied as the viscosity for each temperature is directly obtained from the graphic. Observing the data obtained with the vibrational viscometer (Figure 3.5b and Table 3.5) and converting the dynamic viscosity in kynematic viscosity, it is observed that this values are similar to the ones obtained with the Engler viscometer, the biggest difference being at 40°C, where viscosity variations with temperature are bigger.

(a)

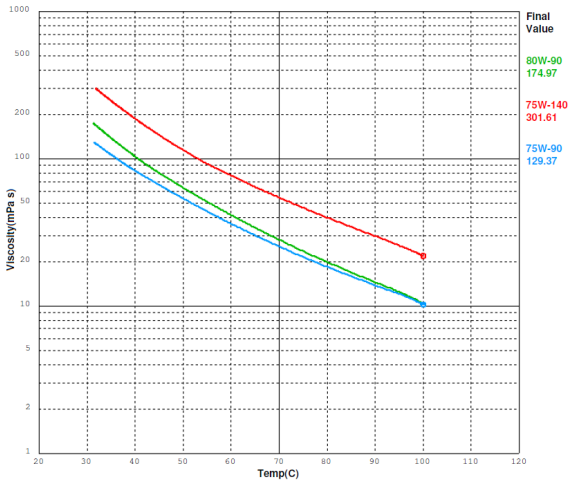

(b)

Figure 3.5.: SV10 Viscometer (a) and dynamic viscosity variation with the temperature of the tested oils (b)

Table 3.5.: Comparison of viscosities obtained with the SV10 viscometer and the Engler viscometer for the three tested oils

	75W90 (PAO)		75W140 (PAO)		80W90 (MIN)	
	SV10	Engler	SV10	Engler	SV10	Engler
40 °C	96,66	115,77	213,76	207,63	118,47	127,57
70 °C	29,17	38,23	62,94	64,20	31,11	36,54
100 °C	12,55	17,13	25,96	27,22	12,40	15,15

3.2. Oil Analysis - Oil Quality

To analyse the quality of the oils before being tested, two types of tests were performed: FTIR analysis and ferrography analysis (Direct Reading Ferrography and Analytical Ferrography).

3.2.1. FTIR Analysis

FTIR analysis, or *Fourier Transform Infrared Spectroscopy*, is a method of spectroscopy used to evaluate the changes in an oil after being submitted to use. When the infrared radiation goes through a sample, some of the radiation is absorbed, and some is transmited through the sample. The obtained spectra of transmitance and absorption represents a molecular fingerprint of the sample, therefore, when analysing the obtained graph and its peaks, it is possible to know which molecules are present in the sample. The size of the peaks represents the amount of a particular material present in the sample. To obtain the transmitance spectra, an *Agilent Cary 630* device (Figure 3.6) was used. The result is displayed on a computer and presented for the user for its analysis.

The FTIR analysis was taken for the oils before being used to serve as reference values to a posterior analysis of the oils after being used. The different peaks present in the spectra in Figure 3.7 show that the three oils have similar composition. The peak between 3000 and 2800 cm^{-1} represents the hydrocarbon group in the oils (C-H), the peak of 1742,2 cm^{-1} indicates the presence of an ester (C=O) that is evident in the fully synthetic oils, and the peaks with a wavenumber inferior to 1500 cm^{-1} shows the additives existant in the three oils. If a posterior analysis of the oil after being tested is to be made, changes in the peaks of the spectra indicate signs of degradation or additive consumption.

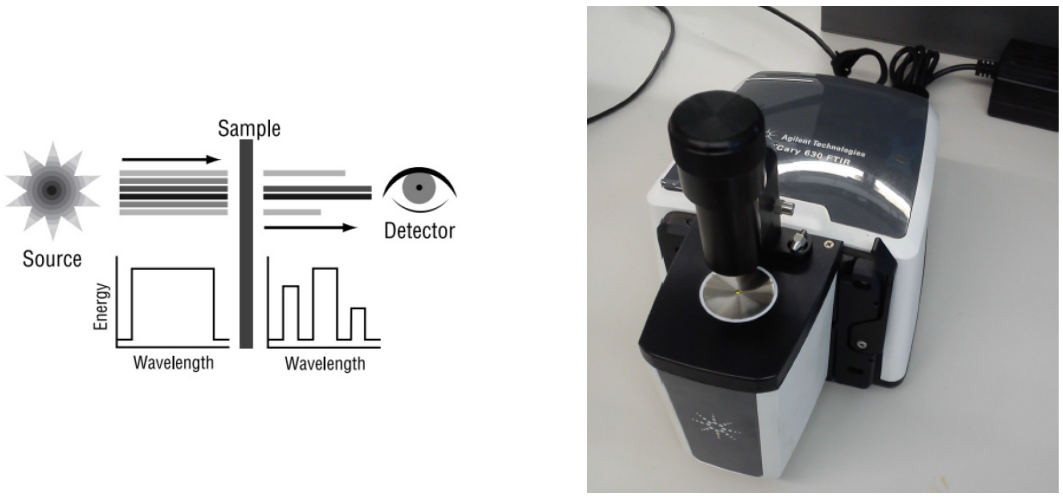

Figure 3.6.: FTIR working principle and *Agilent Cary 630*

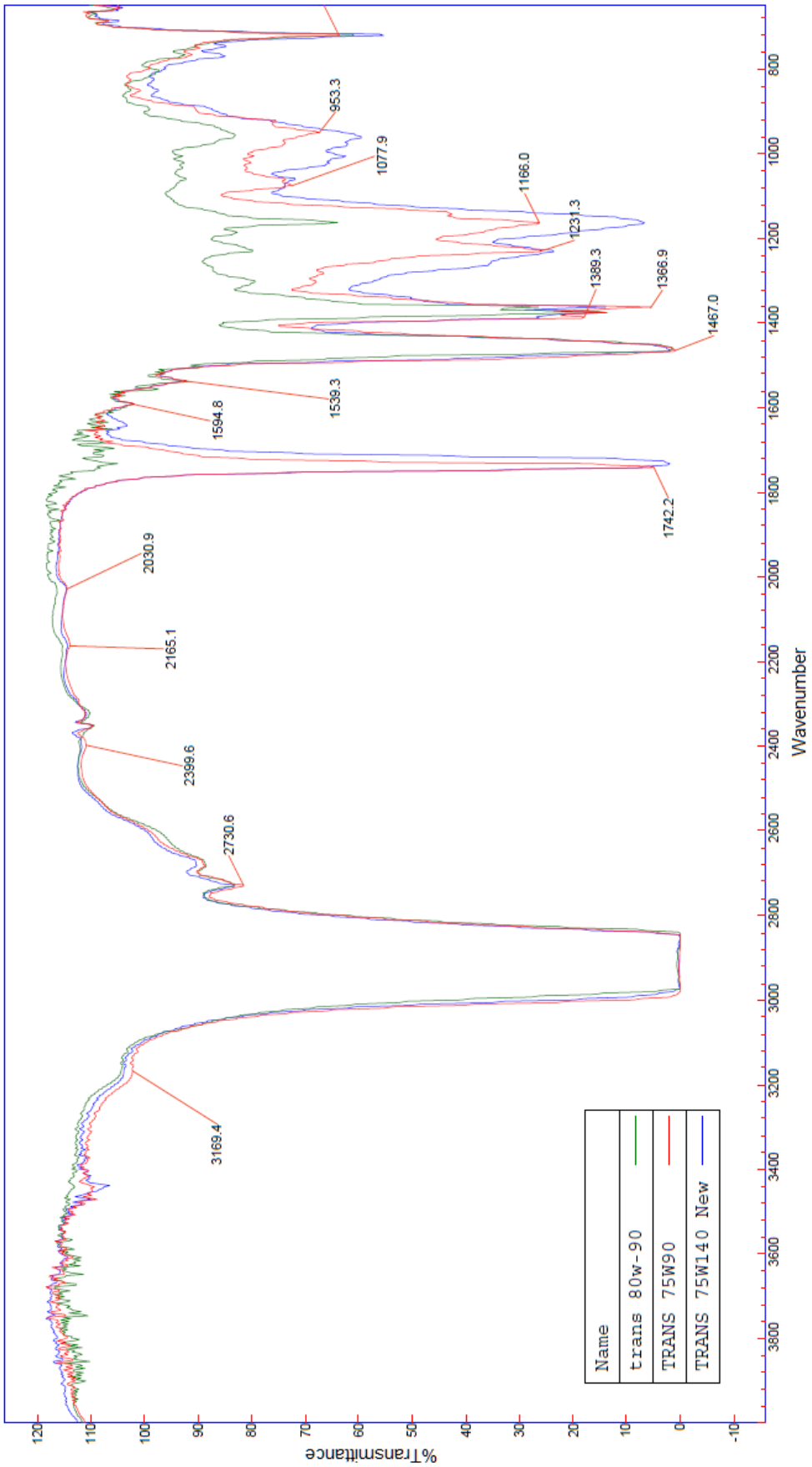

Figure 3.7.: FTIR spectra of the three tested oils before being used

3.2.2. Direct Reading Ferrography

The purpose of direct reading ferrography is to quantify the amount of ferrous particles existent in a given volume of oil using a *DR-III Direct Reading Ferrograph*.

In the process (Figure 3.8a), 1 ml of oil goes through a capillary tube which is subjected to a magnetic field and two light beams. The ferrous particles in the oil are deposited in the tube because of sedimentation or the magnetic field. When the light beams go through the tubes, they are atenuated by the existing particles and are read by an optical detector, which will send a sign to a processor and display the results in a reader (Figure 3.8b). The intensity of the light beams is proportionally inverse to the amount of particles deposited. The two results that are shown are D_L, that represents the amount of large particles (larger than 5 μm), and D_S which is the amount of small particles (smaller than 5 μm).

Knowing the values of D_L and D_S it is possible to calculate two wear indexes: $CPUC$ (Concentration of Wear Particles Index) and $ISUC$ (Severity of Wear Particles Index), which are presented in equations (3.6) and (3.7) respectively.

$$CPUC = \frac{D_L + D_S}{d} \tag{3.6}$$

$$ISUC = \frac{D_L^2 - D_S^2}{d^2} \tag{3.7}$$

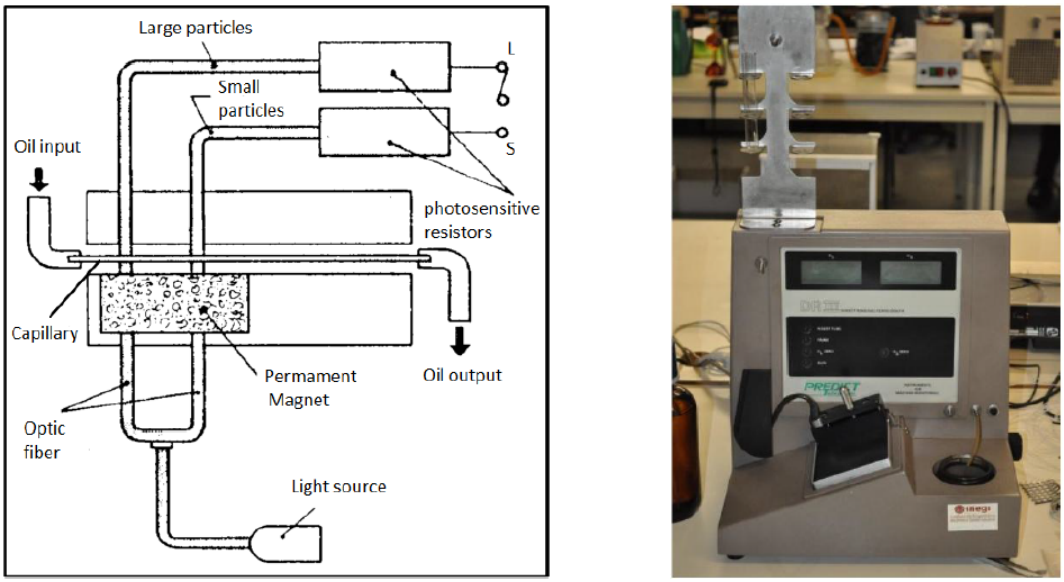

(a) (b)

Figure 3.8.: DR-III Direct Reading Ferrography

Table 3.6.: Direct Reading Ferrography results for the tested oils before being used

Parameter	75W90 (PAO)	75W140 (PAO)	80W90 (MIN)
D_L	0,5	1,4	1,4
D_S	0,6	2,6	0,7
Dillution Factor	1	1	1
$CPUC$	1,1	4,0	2,1
$ISUC$	-0,11	-4,8	1,47

The variable d represents the dillution factor that needs to be used if the sample of oil analysed is excessively contaminated. For a regular sample, d is equal to 1. The values obtained of CPUC and ISUC are represented in Table 3.6 and display very low values, which indicate that the three oils have insignificant contamination.

3.2.3. Analytical Ferrography

Analytical Ferrography is a procedure whose purpose is to evaluate the quality of an oil based on the colour, size, shape, surface, distribution and concentration of particles in a ferrogram. To prepare a ferrogram with oil for analysis, a *FM-III Ferrograph* (Figure 3.9b) is used.

The process of particle deposition and fixation is the same as the described on the direct reading ferrography, but in this case the particles are deposited in a ferrogram (Figure 3.9a). The particles of bigger dimensions are usually deposited at the entrance of the ferrogram and as they advance in the ferrogram their size diminishes. It is import-

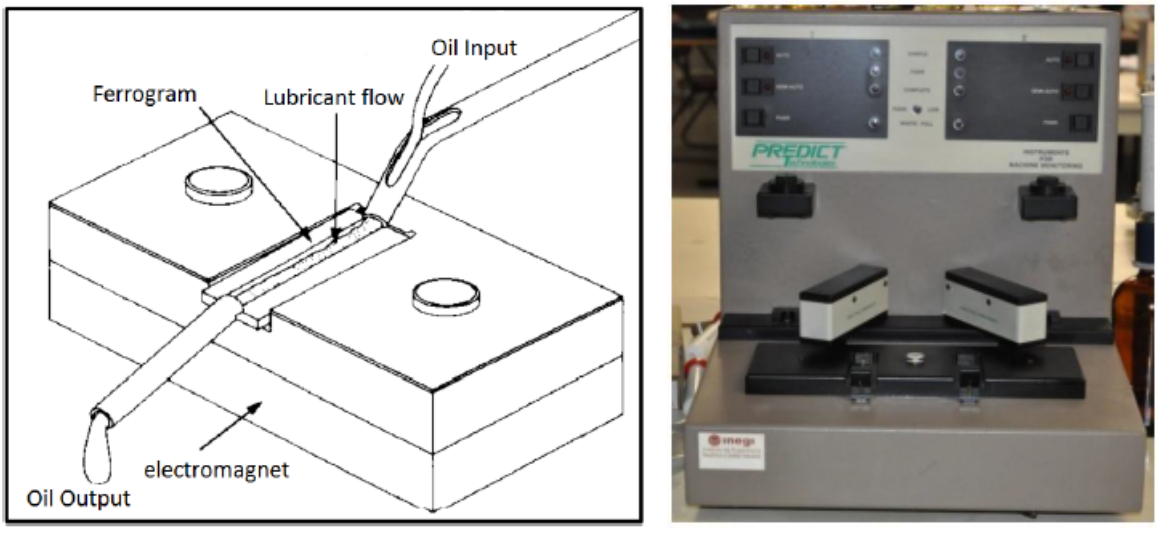

(a) (b)

Figure 3.9.: Analytical Ferrography

ant to notice that magnetic particles besides the size distribution along the ferrogram, are also aligned perpendicularly with the magnetic field. Non-magnetic particles (copper,aluminum,...) are also deposited on the ferrogram through the action of gravity or mechanically trapped, but their distribution is dispersed, which means they are not aligned with the magnetic field.

Observing the ferrogram on the microscope, it is possible to evaluate not only the type of particles that are deposited in the ferrogram (ferrous particles, non-ferrous particles, contaminants,...), but also the possible causes of the degradation of the surface and eventually of the oil (sliding, fatigue, corrosion, excessive load...). The analytical ferrography (view Appendix D) showed no significant contamination of any of the oils.

4. Film Thickness and Traction Curves of Axle Gear Oils

In order to characterize the ability of the axle gear oils to generate a lubricating film and avoid friction, a set of film thickness, traction coefficient and stribeck curves measurements were performed on a ball-on-disc test rig (EHD2 machine from PCS Instruments) under different operating conditions according to each test. In the particular case of this thesis, it is of great interest to know the traction properties of these oils to predict the friction coefficients obtained in posterior rolling bearing tests, as well as the lubrication regime under a broad range of temperatures.

Figure 4.1.: EHD2 ball-on-disc test rig from PCS Instruments

4.1. Film Thickness

4.1.1. Theoretical Film Thickness - Elliptical Contact

According to Hamrock and Dowson [22], the centre film thickness in elliptical contacts, which will be used as a term of comparison with the experimental measurements

is given by equation (4.1).

$$h_0 = 2,69 \cdot R^* \cdot U^{0,67} \cdot G^{0,53} \cdot W^{-0,067} \cdot (1 - 0,61e^{-0,73k}) \tag{4.1}$$

Equation (4.1) is useful as it takes into account the lubricant's viscosity variation with pressure through the material parameter G.

U, G and W are given by equations (4.2), (4.3) and (4.4) respectively, and the ellipticity k has the value of 1 since the elliptical contact in the particular case of the experimental procedure is a point contact.

$$U = \frac{\eta_0 U}{R^* E^*} \tag{4.2}$$

$$G = \alpha E^* \tag{4.3}$$

$$W = \frac{F_n}{(R^*)^2 E^*} \tag{4.4}$$

The corrected film thickness (h_{0C}) takes into account the inlet shear heating of the lubricant as presented in equation (4.5). The thermal correction factor (ϕ_T) was proposed by Gupta *et al.* [23] and is given by equation (4.6).

$$h_{0C} = \phi_T \cdot h_0 \tag{4.5}$$

$$\phi_T = \frac{1 - 13,2 \cdot (p_0/E^*) \cdot (L^*)^{0,42}}{1 + 0,213 \cdot (1 + 2,23 \cdot S^{0,83} \cdot (L^*)^{0,64})} \tag{4.6}$$

Where the Hertz's maximum pressure p_0 and the parameter L^* are given by equations (4.7) and (4.8) respectively.

$$p_0 = \frac{3 \cdot k \cdot F_n}{2 \cdot \pi \cdot a^2} \tag{4.7}$$

$$L^* = \frac{\beta_L \cdot \eta \cdot U_S}{k_L} \tag{4.8}$$

Having defined all the parameters that allow the calculation of the centre film thickness in point contacts, it is possible to predict the film thickness that will be obtained in the experimental results with some degree of certainty as it will be described further ahead. The prediction of the film thickness is useful to determine the maximum and

minimum rolling speed that can be used in the experimental procedure since the used machine can't measure film thicknesses above 1000 nm and a minimum film thickness must be ensured to separate the ball and disc surfaces.

4.1.2. Experimental Procedure

Table 4.1.: Ball and disc data for film thickness measurements provided by the manufacturer

	Ball	Disc
Young Modulus (E) [GPa]	210	64
Poisson's Coefficient (ν)	0,29	0,2
Radius (R) [mm]	19,05	50
Surface roughness (Ra) [nm]	≈ 20	≈ 5
Spacer layer thickness [nm]	-	≈ 500
Spacer layer refractive index	-	$\approx$ 1,4785

Film thickness measurements were performed on ball-on-disc test apparatus (EHD2 machine, from PCS Instruments) equipped with optical interferometry, which allows the measurement of the lubricant film thickness in the contact between a steel ball and a rotating glass disc in the presence of a lubricant fluid.

The ball used has a diameter of 19,05 mm, is made of carbon chrome steel and has a high grade surface finish to ensure good reflectivity. The roughness of the balls and disc is presented in Table 4.1. The discs are made of glass, coated with approximately 20 nm of chromium and 500 nm of silica. The disc supports a maximum Hertz pressure of approximately 0,7 GPa (corresponding to 50 N), and the silica spacer layer has a refractive index of 1,4785.

The film thickness measurements were made with three different operating temperatures (40 °C, 70 °C and 100 °C) and an applied load of 50 N. For each temperature, two different slide to roll ratios (SRR(%)) were tested (3% and 30%). The slide to roll ratio is given by equation (4.9).

$$SRR(\%) = 2 \times \frac{(U_{disc} - U_{ball})}{(U_{disc} + U_{ball})} \times 100 \tag{4.9}$$

For every tested temperature, the maximum rolling speed obtained is of 2 m/s, but the minimum rolling speed is variable in order to ensure a minimum film thickness of approximately 50 nm for each temperature and every tested oil. So, the minimum rolling speeds for 40 °C, 70 °C and 100 °C are 0,1 m/s, 0,25 m/s and 0,5 m/s respectively. For each operating temperature, the film thickness is measured from the highest to the lowest rolling speed, and then from the lowest to the highest rolling speed. This procedure allows to check the repeatability of the measurements, and the results obtained show very similar values at the same rolling speed for both measurements.

The lubricant parameter (LP) values shown on Table 4.3 are useful to predict the film thickness obtained, since for the same conditions of geometry and speed, the film thickness only changes with the piezoviscosity coefficient and the oil's viscosity.

The piezoviscosity's coefficient is a parameter that depends on the lubricant and the temperature. Various equations have been developed to determine this coefficient (Klaus and So equation [20], Gold's equation [21]). However, only Gold's equation will be presented due to its accuracy and simplicity. The piezoviscosity coefficient according to Gold is given by equation (4.10), and the values obtained for the three oils at the three different temperatures use the viscosity obtained with the Engler viscometer measurements and are shown on Table 4.3.

$$\alpha = s \cdot \nu^t \times 10^{-9} \tag{4.10}$$

Table 4.2.: s and t constants for each lubricant type

Type of Oil		Mineral	PAO	Ester
0,2 GPa	s	9,904	7,382	6,605
	t	0,1390	0,1335	0,1360
0,6 GPa	s	8,097	7,008	5,897
	t	0,1534	0,0984	0,1173

Combining the values of the viscosity and the piezoviscosity coefficient, it is possible to predict which oil will have the highest and lowest values of the film thickness using the lubricant parameter as shown on Table 4.3. For every temperature, since $LP^{75W140} > LP^{80W90} > LP^{75W90}$, then it is predicted that $FT^{75W140} > FT^{80W90} > FT^{75W90}$. It can also be concluded that despite having the highest values of the piezoviscosity coefficient, the 80W90 oil has a lower LP than the 75W140 oil due to its lower viscosity.

Table 4.3.: Piezoviscosity Coefficient ($\alpha \times 10^8$) and Lubricant Parameter ($\alpha \cdot \eta \times 10^{10}$) for the three tested oils

	75W90 (PAO)	75W140 (PAO)	80W90 (MIN)
s @ 0,2 GPa	7,382	7,382	9,904
t @ 0,2 GPa	0,1335	0,1335	0,1390
α @ 40°C	1,392	1,505	1,943
α @ 70°C	1,201	1,287	1,633
α @ 100°C	1,079	1,147	1,445
LP @ 40 °C	13,76	27,24	21,58
LP @ 70 °C	3,83	7,07	5,08
LP @ 100 °C	1,51	2,62	1,82

4.1.3. Experimental Film Thickness Measurements

The experimental measurements of the film thickness presented in Figure 4.2 for every test performed, show that as expected the 75W140 oil has the highest values of the film thickness mainly due to its higher viscosity at the working temperatures (highest lubricant parameter despite not having the highest piezoviscosity coefficient - Table 4.3), and the 75W90 oil has the lowest film thickness because it has the lower values of both the viscosity and the piezoviscosity coefficient at the working temperatures (lowest lubricant parameter - Table 4.3). The value of the slide to roll ratio (SRR) doesn't have a major influence in the values obtained for the film thickness, a fact corroborated by the Hamrock and Dowson equation where this parameter as a very small influence (see equation (4.6)). Comparing the theoretical film thickness with the experimental values, it is observed that the predicted film thickness is slightly higher than the experimentally obtained for every test, so the difference between these values will be minimized optimizing the piezoviscosity coefficient for every test performed, as it will be shown in a following section.

4.1.4. Optimization of the piezoviscosity coefficient

When applying the Hamrock and Dowson equation to obtain the centre film thickness in a point contact, it is observed in Figure 4.2 that the predicted values of the film thickness are generally slightly higher than the values obtained from experimental evidence. So, in order to minimize the difference between theoretical and experimental results, the piezoviscosity coefficient will be optimized for each result obtained, as it is a parameter that clearly depends on the oil's formulation when applying Gold's equation [21]. The values obtained for the piezoviscosity coefficient applying Gold's equation (α_{GOLD}) and after optimization for every test (α_{FTM}) are presented in Table 4.4.

Analysing the values obtained for (α_{FTM}), it is observed that, as expected, they are generally lower than the values obtained with Gold's equation. Comparing the

Table 4.4.: Piezoviscosity coefficients ($\alpha \times 10^8$) determined based on film thickness measurements α_{FTM} and Gold's equation α_{GOLD}

		75W90 (PAO)	75W140 (PAO)	80W90 (MIN)
40 °C	α_{FTM} (SRR=3%)	1,305	1,110	1,791
	α_{FTM} (SRR=30%)	1,211	1,127	1,573
	α_{GOLD}	1,392	1,505	1,943
70 °C	α_{FTM} (SRR=3%)	1,057	1,035	1,258
	α_{FTM} (SRR=30%)	1,089	1,038	1,282
	α_{GOLD}	1,201	1,287	1,633
100 °C	α_{FTM} (SRR=3%)	1,093	0,883	1,402
	α_{FTM} (SRR=30%)	1,000	0,977	1,149
	α_{GOLD}	1,079	1,147	1,445

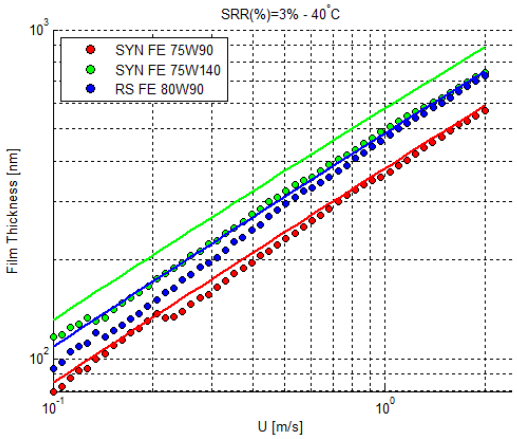

(a) T = 40 °C ; SRR = 3%

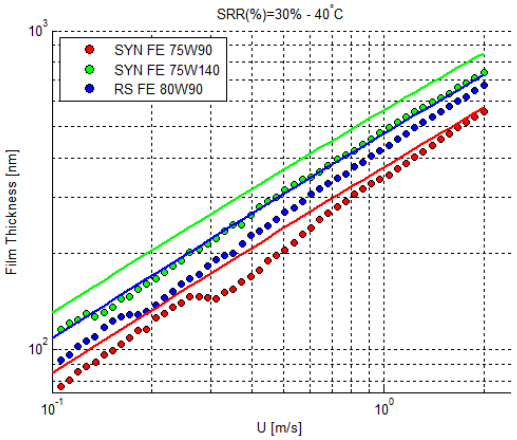

(b) T = 40 °C ; SRR = 30%

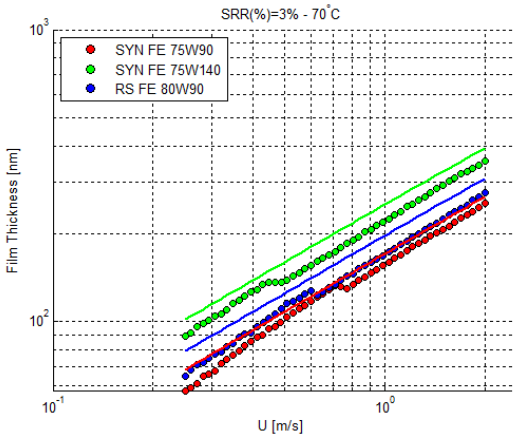

(c) T = 70 °C ; SRR = 3%

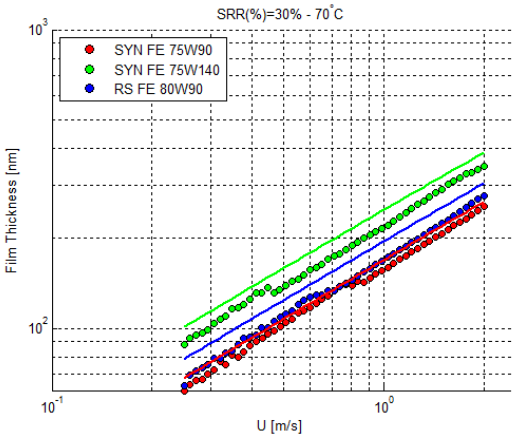

(d) T = 70 °C ; SRR = 30%

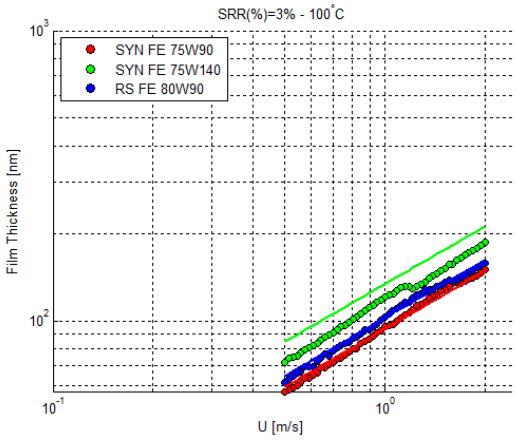

(e) T = 100 °C ; SRR = 3%

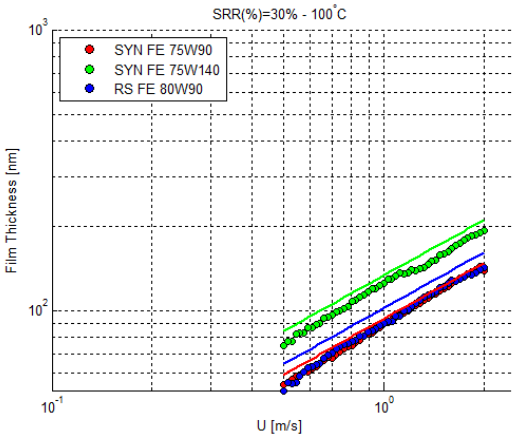

(f) T = 100 °C ; SRR = 30%

Figure 4.2.: Film Thickness obtained for the three tested oils and comparison with the predicted film thickness obtained with Hamrock and Dowson equations

coefficients with different values of SRR(%), no significant conclusions can be obtained since there are cases where the difference between (α_{FTM}) and (α_{GOLD}) is smaller with SRR=3% and some cases where it is smaller with SRR=30%. The evolution of the piezoviscosity coefficient with the temperature is also inconsistent, as in some cases the piezoviscosity coefficient increases with the increase in temperature (α_{FTM} (SRR=3%) from 70 °C to 100 °C in the 75W90 and 80W90 oils) instead of decreasing as predicted by Gold's equation. This behaviour might have to do with the additives behaviour for different temperatures.

Calculating the error between the optimized values of the piezoviscosity coefficient and the values obtained with Gold's equation, it is verified that the error can go from 1% (α_{FTM} (SRR=3%) in the 75W90 at 100 °C) to 26% (α_{FTM} (SRR=3%) in the 75W140 at 40 °C).

4.2. Traction Curves

4.2.1. Experimental Procedure

Table 4.5.: Ball and disc data for traction coefficient measurements provided by the manufacturer

	Ball	Disc (SD002)	Disc (SD003)
Young Modulus (E) [GPa]	210	210	210
Poisson's Coefficient (ν)	0,29	0,29	0,29
Radius (R) [mm]	19,05	50	50
Surface roughness (σ) [nm]	≈ 20	≈ 300	≈ 15

The measurement of the traction coefficients for the axle gear oils were made on a ball-on-disc apparatus (Thin Film Measurement System, model EHD2, from PCS Instruments), for three different operating temperatures (40 °C, 70 °C and 100 °C). During traction measurements the ball runs against the disc and the load is applied by moving the ball upwards towards disc. Both the ball and the disc are made of steel and the contact pressure may rise to 1.11 GPa (corresponding to a 50 N load). For traction coefficient measurements, two steel discs were used, where the difference between them is the roughness as shown on Table 4.5. In traction coefficient measurements, the rolling speed is kept constant (three different rolling speeds were tested at each temperature: 2 m/s, 1 m/s and 0,5 m/s) while the SRR increases from 1% to 50% and then decreases to 1% again to verify the repeatability of the results.

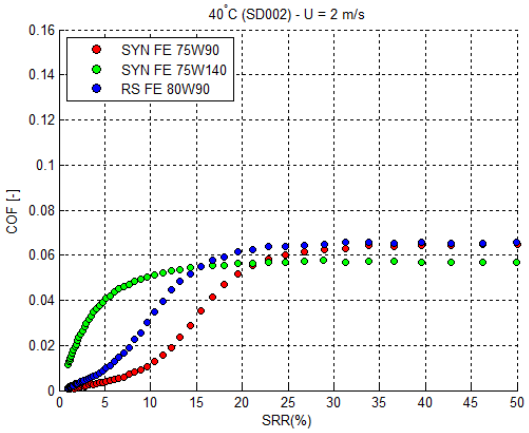

(a) U = 2 m/s ; σ^{disc} = 300 nm

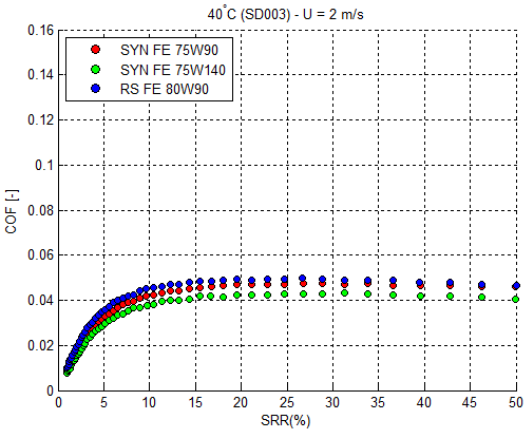

(b) U = 2 m/s ; σ^{disc} = 15 nm

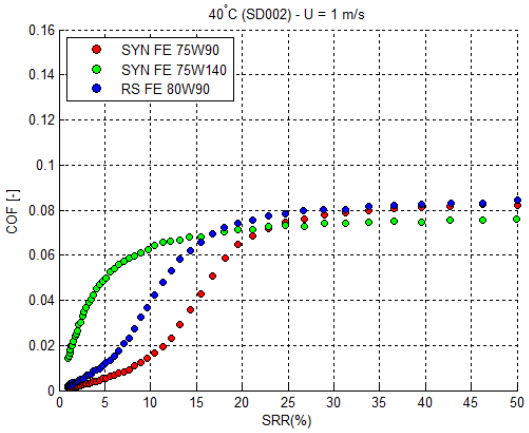

(c) U = 1 m/s ; σ^{disc} = 300 nm

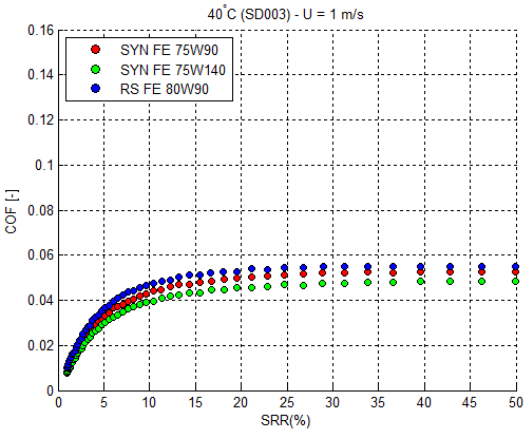

(d) U = 1 m/s ; σ^{disc} = 15 nm

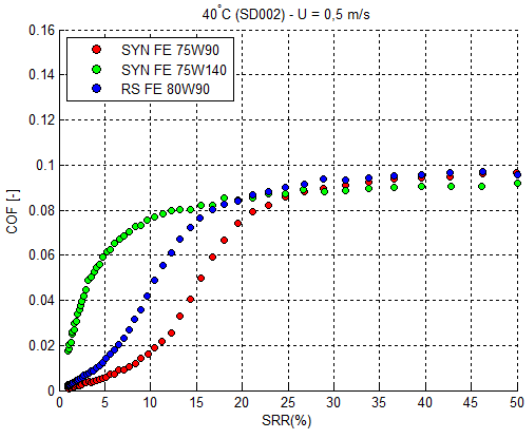

(e) U = 0,5 m/s ; σ^{disc} = 300 nm

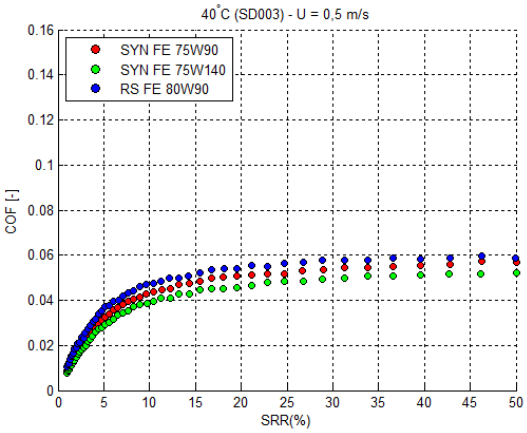

(f) U = 0,5 m/s ; σ^{disc} = 15 nm

Figure 4.3.: Traction Curves obtained at 40 °C for the three tested oils using different discs and rolling speeds

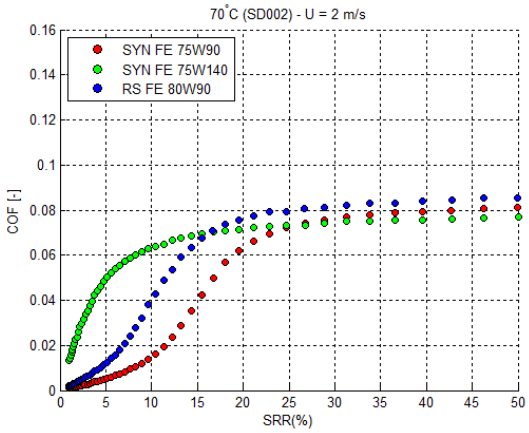

(a) U = 2 m/s ; σ^{disc} = 300 nm

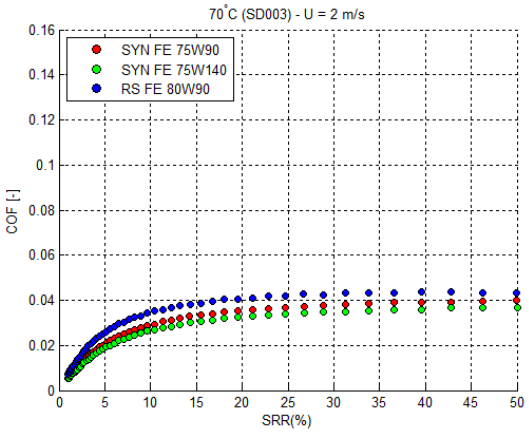

(b) U = 2 m/s ; σ^{disc} = 15 nm

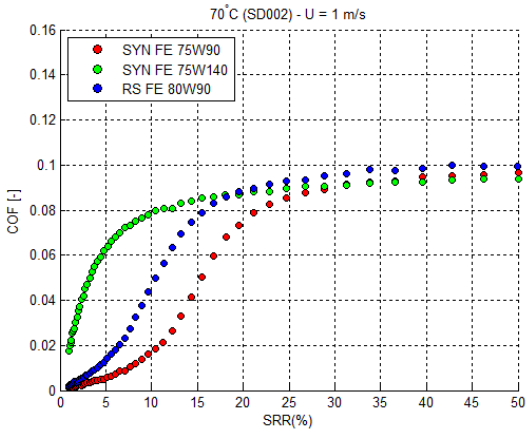

(c) U = 1 m/s ; σ^{disc} = 300 nm

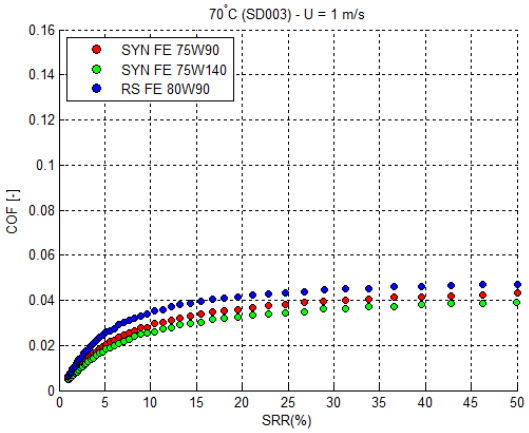

(d) U = 1 m/s ; σ^{disc} = 15 nm

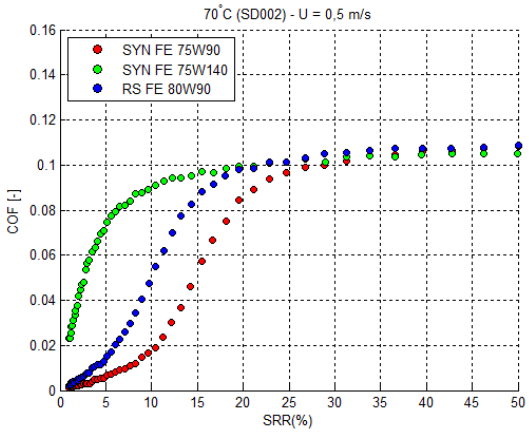

(e) U = 0,5 m/s ; σ^{disc} = 300 nm

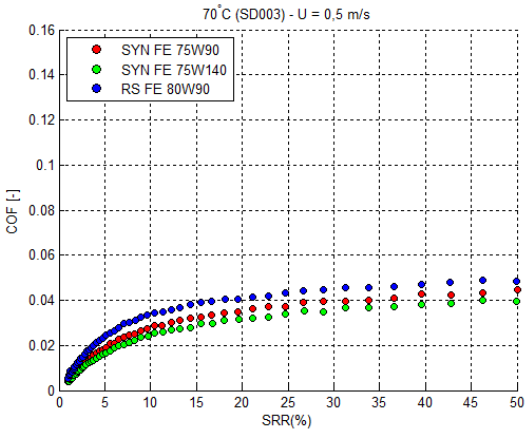

(f) U = 0,5 m/s ; σ^{disc} = 15 nm

Figure 4.4.: Traction Curves obtained at 70 °C for the three tested oils using different discs and rolling speeds

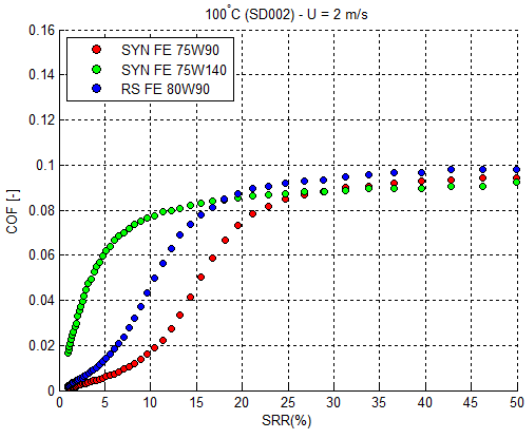

(a) U = 2 m/s ; σ^{disc} = 300 nm

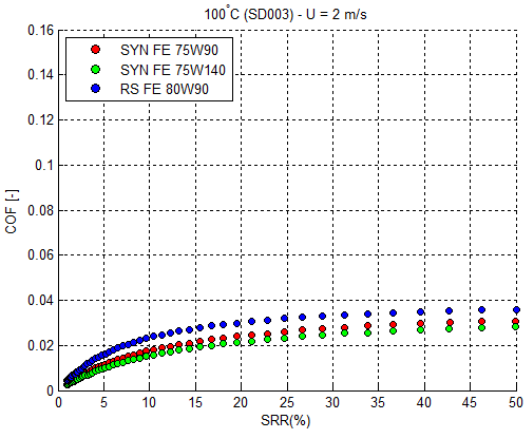

(b) U = 2 m/s ; σ^{disc} = 15 nm

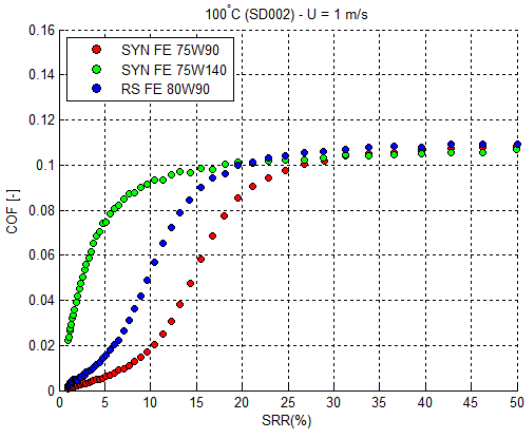

(c) U = 1 m/s ; σ^{disc} = 300 nm

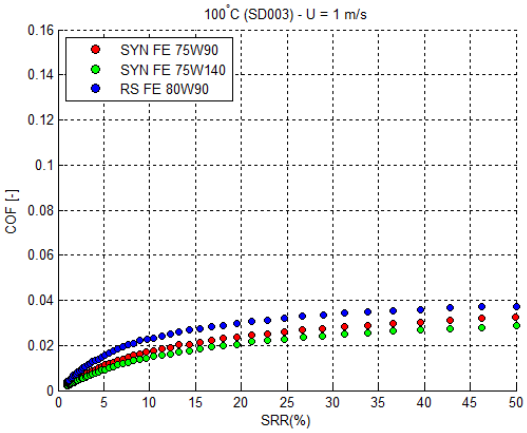

(d) U = 1 m/s ; σ^{disc} = 15 nm

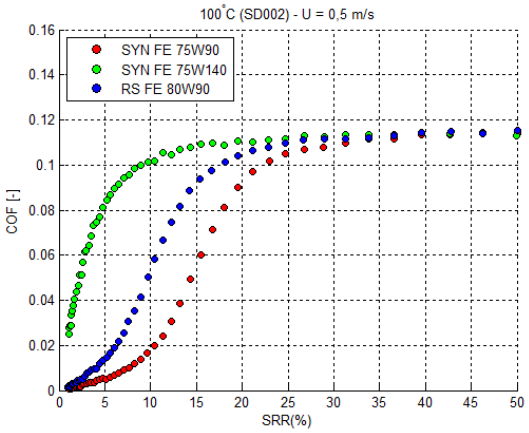

(e) U = 0,5 m/s ; σ^{disc} = 300 nm

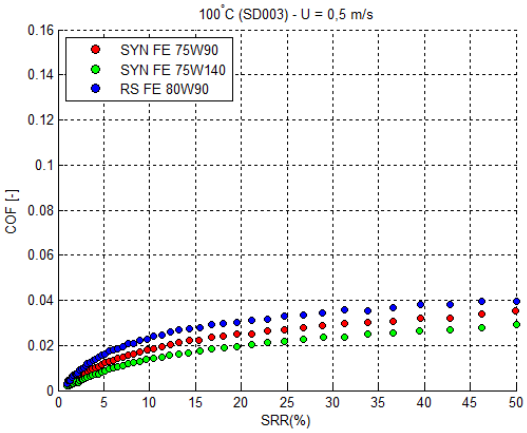

(f) U = 0,5 m/s ; σ^{disc} = 15 nm

Figure 4.5.: Traction Curves obtained at 100 °C for the three tested oils using different discs and rolling speeds

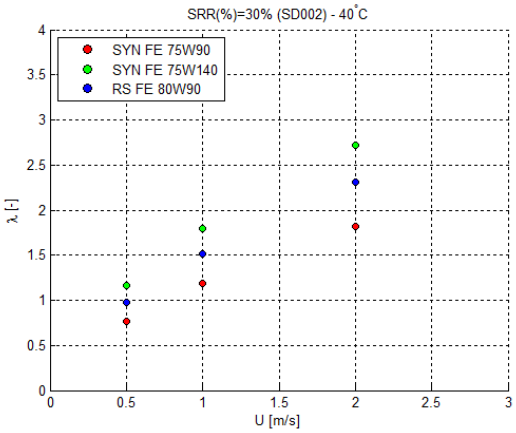

(a) T = 40 °C ; σ^{disc} = 300 nm

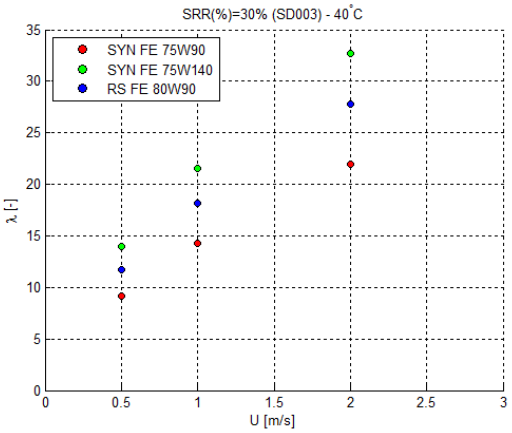

(b) T = 40 °C ; σ^{disc} = 15 nm

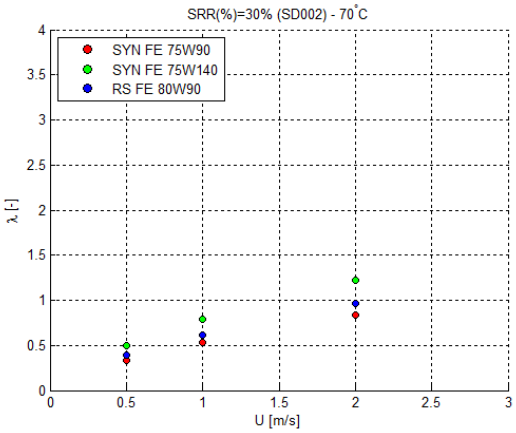

(c) T = 70 °C ; σ^{disc} = 300 nm

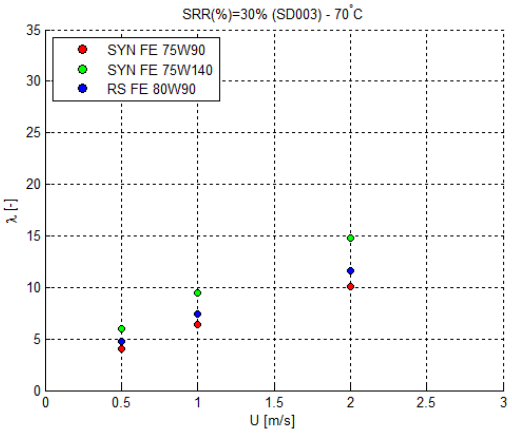

(d) T = 70 °C ; σ^{disc} = 15 nm

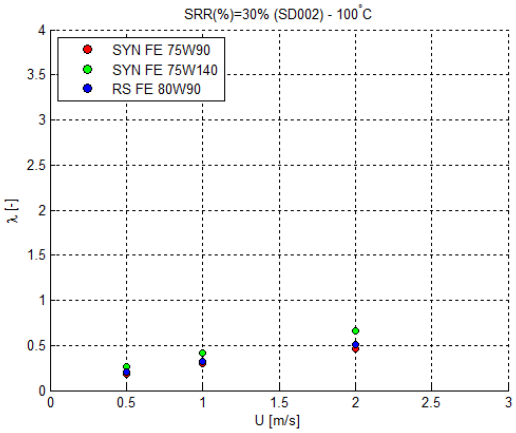

(e) T = 100 °C ; σ^{disc} = 300 nm

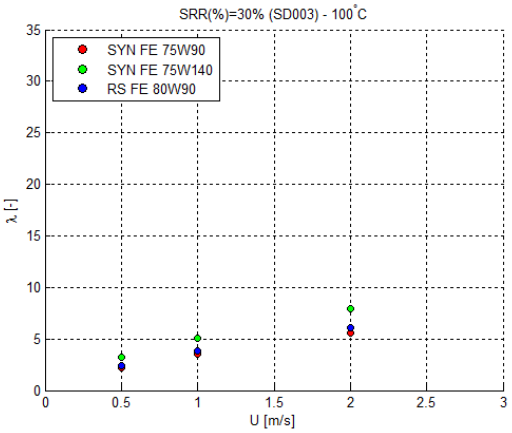

(f) T = 100 °C ; σ^{disc} = 15 nm

Figure 4.6.: Predicted specific film thickness for the traction coefficient measurements made for the three tested oils

4.2.2. Experimental Results

The experimental measurements of the traction coefficient for the three different oils are displayed in Figure 4.3, Figure 4.4 and Figure 4.5 for the oil temperatures of 40 °C, 70 °C and 100 °C, respectively. These results show significant differences when changing the temperatures, speeds and the roughness of the steel disc.

Firstly, in all the tests performed the 80W90 oil always has the highest values of the traction coefficient, followed by the 75W90 oil and then the 75W140 oil. The 80W90 values of the traction coefficient may be caused by its lower viscosity and the fact that it is a semi-synthetic oil (partially mineral), while the 75W140 values of the traction coefficient are caused by its higher viscosity and its synthetic nature. Brandão *et al.* [24] showed that oils with higher piezoviscosity coefficient have higher values of the coefficient of friction, a fact that is verified in the tests when comparing oils with similar viscosities (75W90 and 80W90). It is also verified that the oils with higher Viscosity Index have lower values of the coefficient of friction.

Observing the tests made with the steel disc with higher roughness (graphics in the left column in Figure 4.3, Figure 4.4 and Figure 4.5) it is observed that the traction coefficient increases with the decrease in rolling speed for every tested temperature. Comparing tests made with different temperatures and the same speed, it can be seen an increase in the traction coefficient with the increase in rolling speed.

With the steel disc with a smoother surface, the values of the traction coefficient are smaller than the values obtained for the same tests with the rougher disc (graphics in the right column in Figure 4.3, Figure 4.4 and Figure 4.5).

Maintaining a constant temperature, it is observed that with the smoother disc the values of the traction coefficient do not change so much with speed as the rougher disc.

Comparing again tests with different temperatures and the same rolling speed, it is observed that, opposite to the rougher disc, the traction coefficient decreases with the increase in temperature, which implies the presence of full-film conditions as shown by Brandão *et al.* [24].

The conclusion obtained with the different roughnesses in the existing contacts and comparing with predicted specific film thickness of the oils for each test (Figure 4.6), is that when using the rougher disc, the lubrication regime is boundary lubrication regime for the higher temperatures and lower speeds ($\lambda < 0,5$). Using the smoother disc, it becomes aparent the change in the lubrication regime to mixed or even full-film conditions due to the significant decrease in the traction coefficient and significant increase in the predicted specific film thickness for all the tests. For a better analysis of the lubrication regime, the Stribeck curves of each oil will be obtained at the tested operating temperatures using again both steel discs SD002 and SD003.

It becomes apparent in these tests that the axle gear oils, given that they are considered "fuel-economy" oils, have values of the traction coefficient under full-film conditions that can be considered high (between 0,03 and 0,06 in the tests).

4.3. Stribeck Curves

4.3.1. Experimental Procedure

The experimental procedure to obtain the Stribeck curves is similar to the procedure described to obtain the traction coefficient (same operating temperatures, same load and same ball and discs). To obtain the stribeck curves, the slide to roll ratio is kept constant (30%) and the rolling speed is varying as the test is being made. The rolling speed increases from 0,01 m/s to 3 m/s, and then decreases from 3 m/s to 0,01 m/s. Measurements are taken in both situations to ensure the repeatability of the results. The modified Hersey parameter used to obtain the curves is based on the parameter obtained by Brandão [25] and given by equation (4.11).

$$S_p = \frac{U_S \eta \alpha^{\frac{1}{2}}}{F_n^{\frac{1}{2}}} \tag{4.11}$$

4.3.2. Experimental Results

The Stribeck curves obtained with the rough disc (SD002), show that for every tested temperature, full-film conditions are never achieved. With the lower temperature (Figure 4.7a) it is evident that the predominant regime is mixed lubrication due to the decrease in the traction coefficient with the increase in speed, while at the highest temperature (Figure 4.7e) boundary regime is predominant and mixed lubrication only starts to become evident at the higher speeds. Under boundary conditions, the 75W140 oil generally has the higher values of the traction coefficient and the 75W90 and 80W90 oils have the lower values of the traction coefficient. However, the difference between the three oils isn't very significant.

With the smooth disc (SD003), full-film conditions are achieved in every operating temperature (the smoother surface means an higher specific film thickness). In fact, only at the temperature of 100 °C there is evidence of a mixed lubrication regime at lower speeds (Figure 4.7f). At the lower temperatures (Figure 4.7b and Figure 4.7d), full-film conditions occupy pratically 100% of the duration of the test. Under full-film conditions, the 80W90 oil has higher values of the traction coefficient, while the 75W90 and the 75W140 oil have lower values of the traction coefficient. This fact suggests the importance of the oil's formulation under full-film conditions, since the 80W90 is a partially synthetic oil and the other two oils are fully synthetic.

Comparing the temperatures, it is observed that with the rough disc, the traction coefficient under boundary conditions doesn't suffer significant changes, but with the smoother disc, the traction coefficient decreases with the increase in temperature, as verified by Brandão *et al.* [24].

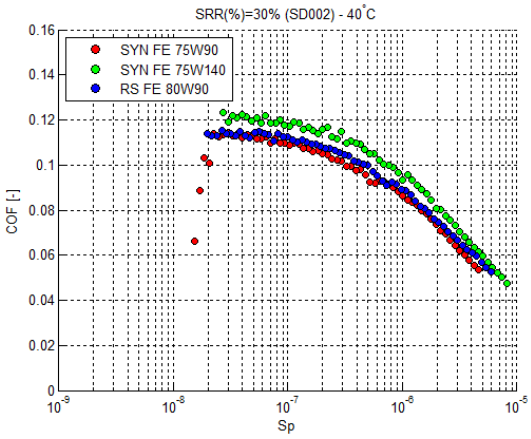

(a) T = 40 °C ; σ^{disc} = 300 nm

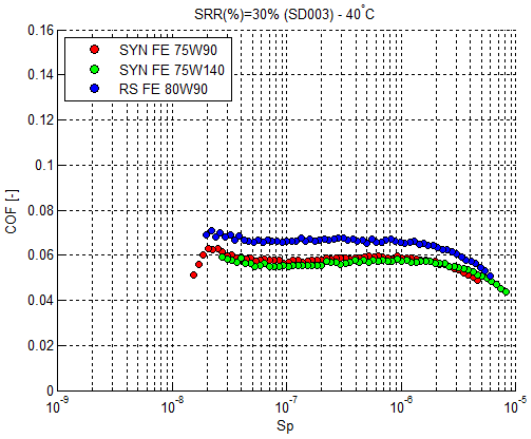

(b) T = 40 °C ; σ^{disc} = 15 nm

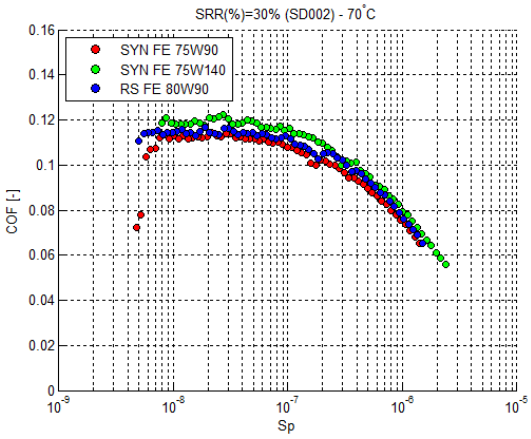

(c) T = 70 °C ; σ^{disc} = 300 nm

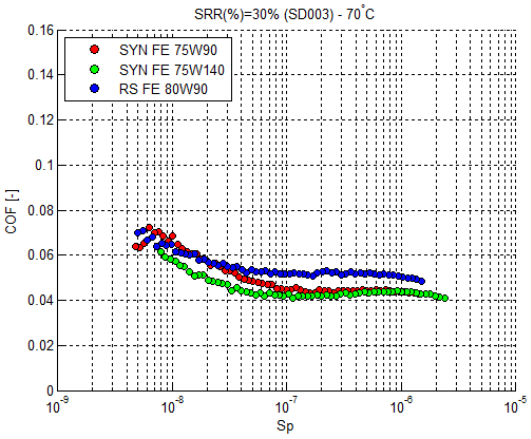

(d) T = 70 °C ; σ^{disc} = 15 nm

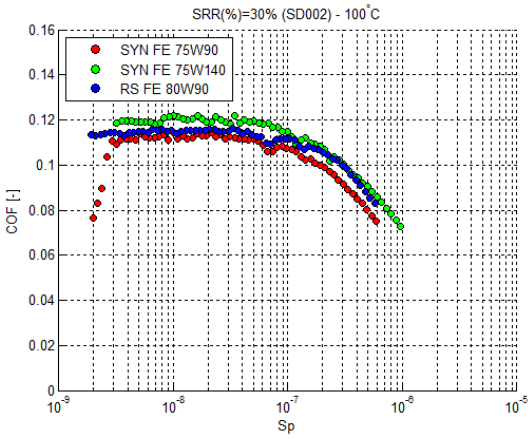

(e) T = 100 °C ; σ^{disc} = 300 nm

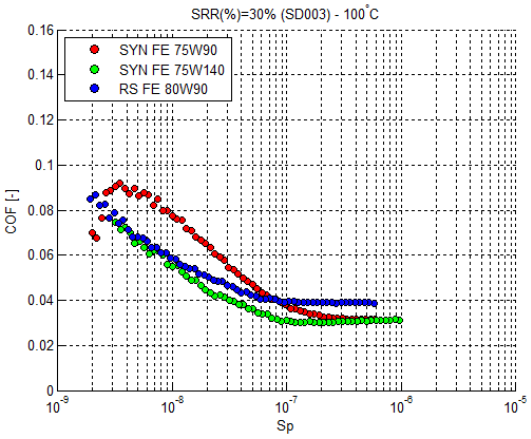

(f) T = 100 °C ; σ^{disc} = 15 nm

Figure 4.7.: Stribeck Curves obtained for the three tested oils

Part II.

Development of the Friction Torque Model

5. Elastohydrodynamic Lubrication

Elastohydrodynamic lubrication (or EHD lubrication) is defined as a form of hydrodynamic lubrication where the elastic deformation of the bodies in contact, as well as the changes in viscosity with pressure can't be ignored [17].

The introduction of the concept of EHD lubrication was important to understand the lubrication of highly loaded non-conformal contacts (gears, rolling bearings, cams,...) because the wear rate of these types of mechanisms was very low, which implied the existence of a lubricant film thickness much higher than the predicted when using the concept of hydrodynamic lubrication.

The first model that obtained an accurate approximation of the elastohydrodynamic film thickness was published by Grubin in 1949 [26], and took into account the hydrodynamics, the elastic deformation of the bodies in contact and the increase in the oil's viscosity due to extreme pressures. The development of EHD lubrication theory was continued by Dowson and Higginson [27], Crook [28], Cameron and Gohar [29], among others.

To sum up, EHD lubrication is important to understand lubrication and friction phenomena in Hertzian contacts, and it is useful to determine the film thickness between two surfaces with elastic deformation of the corresponding solids, to evaluate the friction existent in the contact due to the viscoelastic deformation of the lubricant film taking into account the lubricant's rheological properties, and to represent the energetic balance in the contact taking into account the power loss in the lubricant film due to shear stress and heat evacuation due to the lubricant's flow in the contact.

5.1. Film Thickness in Thrust Roller Bearings

EHD lubrication is the type of lubrication commonly observed in mechanical components, which include gears and bearings. To predict the film thickness in cylindrical roller thrust bearings, it will be taken into account the fact that the contact between the surfaces is linear, and then the film thickness will be estimated utilizing the Dowson and Higginson equation [27].

5.1.1. Hertzian Linear Contact

Linear contact occurs when two cylinders are in contact, forming a rectangular contact area when submitted to a normal load. Knowing both solids curvature radius (equation (5.1)), material (equation (5.2)) and the applied load, it is possible to determine Hertz's maximum pressure (equation (5.3)) and Hertz's semi-width (equation (5.4)).

$$\frac{1}{R_x} = \frac{1}{2}\left(\frac{1}{R_{x1}} + \frac{1}{R_{x2}}\right) \tag{5.1}$$

$$\frac{1}{E^*} = \left(\frac{1-\nu_1^2}{E_1} + \frac{1-\nu_2^2}{E_2}\right) \tag{5.2}$$

$$p_0 = \sqrt{\frac{2}{\pi} \cdot \frac{F_n}{l} \cdot \frac{E^*}{R_x}} \tag{5.3}$$

$$a = \sqrt{\frac{2}{\pi} \cdot \frac{F_n}{l} \cdot \frac{R_x}{E^*}} \tag{5.4}$$

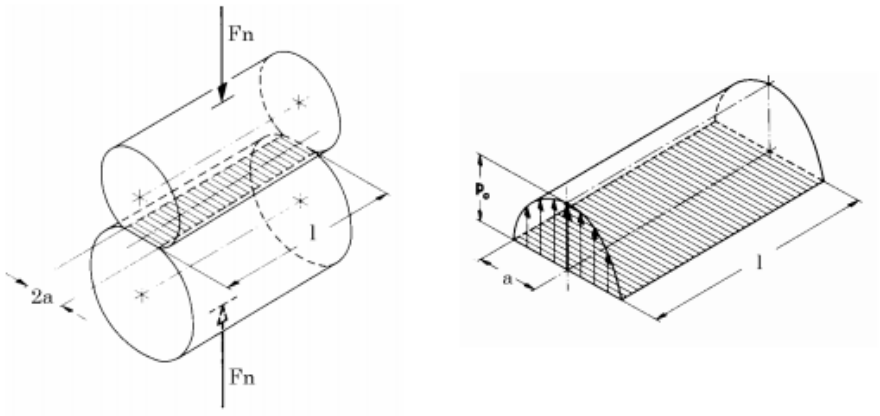

Figure 5.1.: Linear contact between two surfaces

5.1.2. Bearing Contact Kynematics

To determine the film thickness in the contact of a bearing, it is necessary to know the roller bearing's kynematics [30]. In the figure is represented a scheme of the velocity distribution in a cylindrical thrust roller bearing, where the peripheric speed is

represented by U_e, the interior speed of the roller is given by U_i and the speed on the center of the roller is given by U_g.

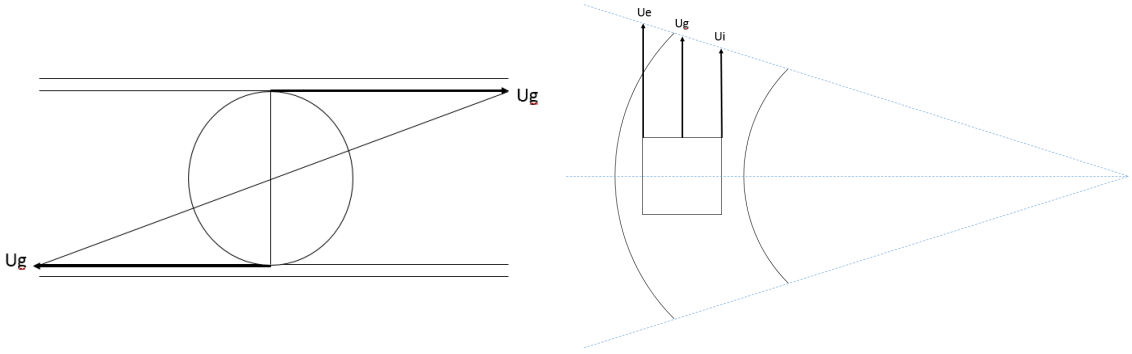

Figure 5.2.: Schematic representation of the cylindrical thrust roller bearing kynematics

To determine the film thickness it is necessary to know the sliding speed in the contact existant between the surfaces of the roller and races. Observing Figure 5.2, the speed on the center of the roller U_g is easily obtained as the average of the interior and peripheric speed of the roller (for calculation purposes it is obtained knowing the bearing's mean diameter). It is important to notice that in equation (5.5) the rotational speed appears divided in half because it assumes both races are rotating and the relative motion between them must be equal to the input rotational speed (Figure 5.2 shows an example where it is assumed a stationary cage). If it was assumed a stationary lower race and the upper race with rotational movement, U_g would be considered in the center of the rolling element and having half of the input rotational speed, therefore validating equation (5.5).

$$U_g = \frac{U_e + U_i}{2} = \frac{d_m}{4} \cdot \frac{2 \cdot \pi \cdot n}{60} \tag{5.5}$$

Knowing U_g and U_i, it is possible to obtain the sliding speed in the contact which will be used in the calculation of the bearing's film thickness and is given by equation (5.7).

$$U_i = \frac{d_i}{4} \cdot \frac{2 \cdot \pi \cdot n}{60} \tag{5.6}$$

$$V_e = \frac{|U_g - U_i|}{U_g + U_i} \tag{5.7}$$

5.1.3. Film Thickness Calculation

To calculate the film thickness, the method used is the model developed by Dowson and Higginson for linear contacts [27]. This model assumes isothermal contact between smooth surfaces and fully flooded lubrication.

The Velocity (U), Material (G) and Load (W) parameters are given respectively by equations (5.8), (5.9) and (5.10).

$$U = \frac{\eta_0(U_g + U_i)}{2R_x E^*} \tag{5.8}$$

$$G = 2\alpha E^* \tag{5.9}$$

$$W = \frac{F_n}{R_x E^* l} \tag{5.10}$$

Where η_0 is the lubricant's dynamic viscosity at the feeding temperature and α is the lubricant's piezoviscosity coefficient at the feeding temperature.

Knowing the three previously mentioned parameters, it is possible to know the center and minimum film thickness which are given by equations (5.11) and (5.12), respectively.

$$h_0 = 0,975 \cdot R_x \cdot U^{0,727} \cdot G^{0,727} \cdot W^{-0,091} \tag{5.11}$$

$$h_m = 1,325 \cdot R_x \cdot U^{0,70} \cdot G^{0,54} \cdot W^{-0,13} \tag{5.12}$$

The value of h_0 represents the theoretical value of the film thickness at a given temperature. This value needs, however, to be corrected to take in consideration the lubricant's shear heating, the feeding conditions in the contact and the roughness of both contact surfaces.

The corrected film thickness [31] can be calculated using equation (5.13) which is obtained from equations (5.14), (5.15) and (5.16).

$$h_{0C} = \phi_T \cdot \phi_A \cdot \phi_R \cdot h_0 \tag{5.13}$$

$$\phi_T = [1 + 0,1(1 + 14,8V_e^{0,83})L^{0,64}]^{-1} \tag{5.14}$$

$$V_e = \frac{|U_g - U_i|}{U_g + U_i} \tag{5.15}$$

$$L = \frac{\beta \eta_0 (U_g + U_i)^2}{K} \tag{5.16}$$

Where ϕ_T, ϕ_A and ϕ_R are the correction factors due to the heating, feeding conditions and roughness respectively, V_e is the sliding velocity between the solids, β is the thermoviscosity's coefficient of the lubricant and K is the thermal conductivity of the lubricant. In calculations, the factors ϕ_A and ϕ_R are not considered due to the difficulty in obtaining both parameters. Also, to serve as reference, it is known that the value of the sliding speed V_e is generally situated between 3 and 5%.

The specific film thickness can be calculated using the Tallian concept [32] presented in equation (5.17).

$$\lambda = \frac{h_{0C}}{\sqrt{\sigma_1^2 + \sigma_2^2}} \tag{5.17}$$

Where σ_1 and σ_2 are the roughnesses of each of the surfaces of the solids in contact. Typical values for composite roughness in rolling bearings are presented in Table 5.1.

Table 5.1.: Composite Roughness of different types of bearings [31]

Type of Bearing	Composite Roughness ($\sigma = \sqrt{\sigma_1^2 + \sigma_2^2}$)
Precision Balls	0,05
Balls	0,18
Cylindrical Rollers	0,36
Tapered Rollers	0,23

The specific film thickness is a parameter that allows to identify the lubrication regime by expressing the relation between film thickness and the composite roughness of the surfaces in contact.

5.2. Lubrication Regimes

In elastohydrodynamic lubrication, three different lubrication regimes can be defined: full film, mixed film and boundary film. The lubrication regime is directly related to the value of the specific film thickness, and for bearings it can be specified as [33]:

- $\lambda \geq 3,0$ - full film lubrication (the surfaces in contact are completely separated by the lubricant film).
- $1,0 < \lambda < 3,0$ - mixed film lubrication (the surfaces in contact are partially separated by the lubricant film and there may be some metal to metal contact).
- $\lambda \leq 1,0$ - boundary film lubrication (there is no lubricant film separating the surfaces in contact and metal to metal contact is predominant).

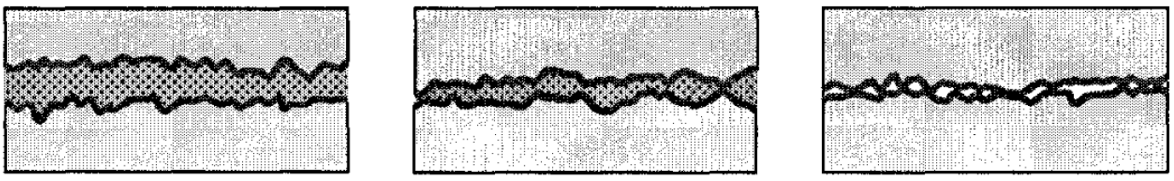

Figure 5.3.: Full film, mixed film and boundary film lubrication regimes [15]

To better understand the lubrication when transitioning from boundary film conditions to mixed film and then full film conditions, it will be introduced the concept of the Stribeck curve.

5.3. Stribeck Curve

The Stribeck curve shows the evolution of the coefficient of friction in steady state conditions with a dimensionless number known as the Hersey number [34] which is given by equation (5.18).

$$H_s = \frac{\eta\omega}{p} \tag{5.18}$$

Where η is the lubricant's dynamic viscosity [Pa·s], ω the rotational speed [s^{-1}] and p the pressure [Pa]. If the Hersey number is very low, the predominant phenom observed is asperity contact and no significant lubricant film is formed, thus resulting in higher friction. The friction maintains its high value up to a point where it decreases rapidly due to the increase in film thickness, entering in the mixed lubrication regime. After entering full film conditions, the friction increases again but at a low rate. This happens because the lubricant's film size is limited by the geometry of the solids in contact, and there's an increase in shear strength, even though its contribution is relatively low.

As EHD lubrication is being analysed through all the lubrication regimes, the lubricant's piezoviscosity must be taken into account as it influences the film thickness and

the coefficient of friction. So, in calculations it will be used instead of the Hersey number, a Modified Hersey Parameter proposed by Brandão [25] that is given by equation (5.19).

$$S_p = \frac{U_S \eta \alpha^{\frac{1}{2}}}{F_n^{\frac{1}{2}}} \tag{5.19}$$

Where U is the rolling speed [m/s], η the lubricant's dynamic viscosity at the operating temperature [Pa·s], α the lubricant's piezoviscosity coefficient at the operating temperature [Pa^{-1}] and F_n the normal applied load [N]. It is important to notice that this parameter also takes into account the oil's nature (Mineral,PAO,...) if Gold's Law for the calculation of the piezoviscosity coefficient is applied.

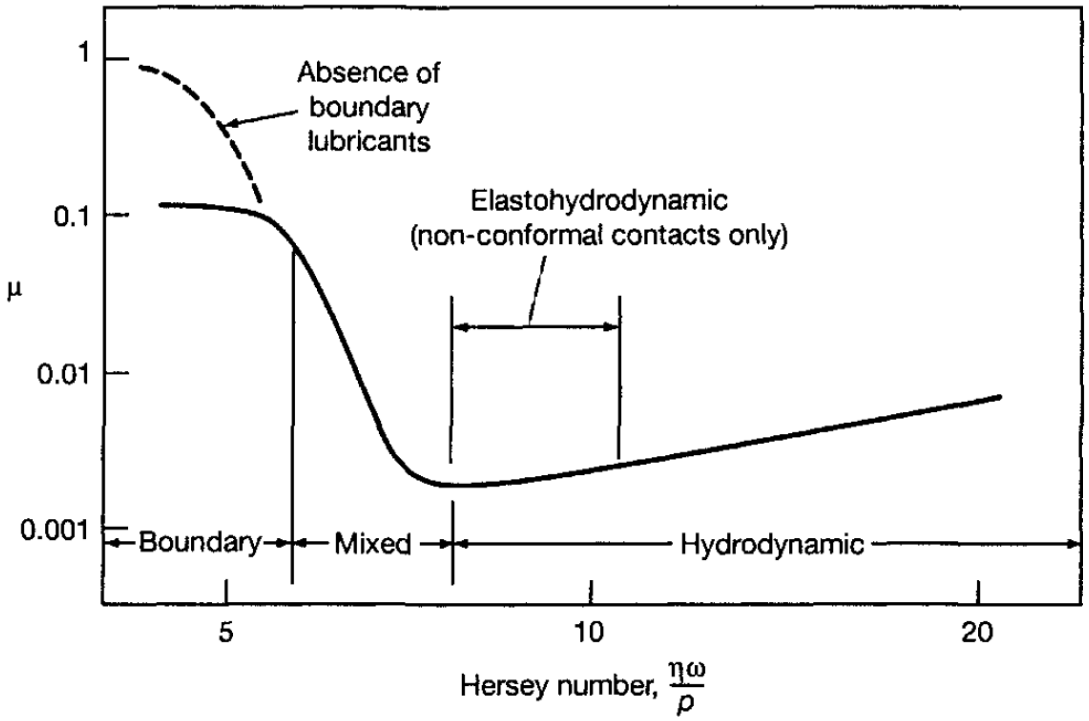

Figure 5.4.: Stribeck curve [15]

6. Friction Torque/Power Loss in Cylindrical Roller Thrust Bearings

The main motive that usually explains the choice of a cylindrical roller thrust bearing for a determined application, is its higher load capacity due to a larger contact area. Therefore, it is important to study the power losses associated with the bearings so optimal performance can be achieved. For most axle applications tapered roller bearings are used. However in the experimental work presented in this thesis, the tested bearings are cylindrical thrust roller bearings since the contact between the rollers and race is very similar to the existing contact in tapered roller bearings.

Analysing the power losses in a vehicle axle, there is a component that is attributed to losses in bearings, that when combined with gear losses represent the vast majority of losses in the axle. The losses in bearings can be classified as no-load losses and load dependent losses as represented in Figure 6.1 [9] [35].

No-load losses are the ones that happen without power transmission in the axle, and depend on the rotational speed, the bearing used (type and size), the bearing assembly and the lubricant's viscosity, quantity and supply. Load dependent losses in the axle bearings are related to bearing sliding and rolling friction.

When the vehicle is in motion, a pre-load (thrust load) is applied to the bearings creating an interference fit. This guarantees the absence of radial and axial clearance, that if existed would influence the vibration, noise and fatigue-life of the bearing.

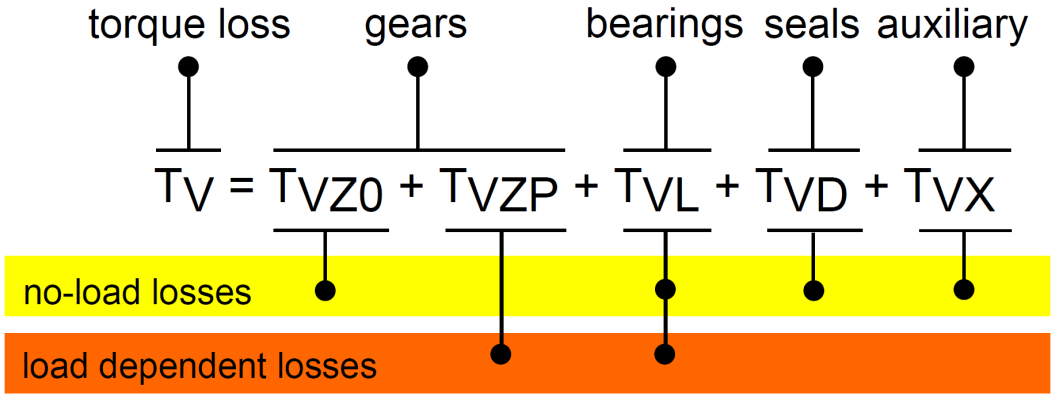

Figure 6.1.: No-load losses and load dependent power losses in a vehicle axle [35]

To predict the power loss in rolling bearings, models based on a large number of measurements have been developed by bearing manufacturers such as SKF and FAG. For the purpose of this thesis, the model selected to analyse the results obtained will be the SKF Friction Torque Model [36], which will be calibrated for cylindrical thrust roller bearings using three different oils. It is expected that a better understanding of the oil's formulation in the bearing's power loss is displayed after the calibration of the model.

6.1. SKF Friction Torque Model

The SKF Friction Torque Model to predict the power loss in a bearing is of great interest, because it divides the total friction torque in the bearing in its true physical forms. The model takes into account four different torque losses as presented in equation (6.1).

$$M_t = M_{rr} + M_{sl} + M_{seal} + M_{drag} \tag{6.1}$$

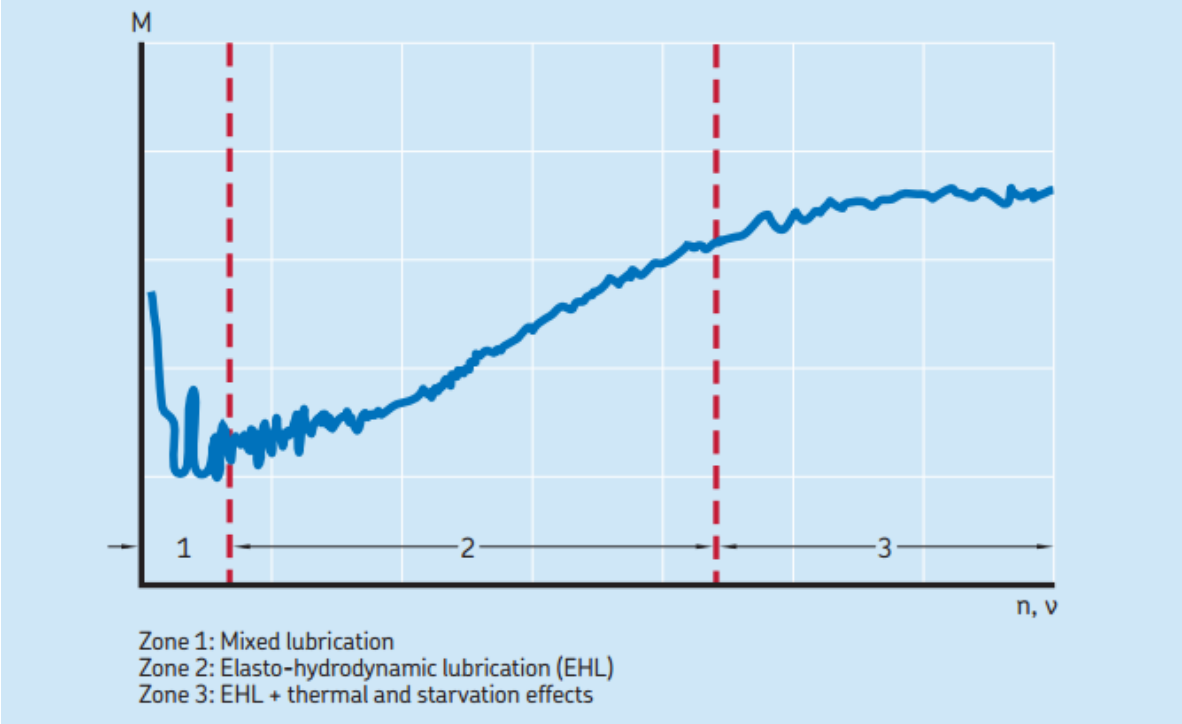

Figure 6.2.: Friction torque variation with rotational speed or viscosity [36]

Where M_t represents the total value of the friction torque, M_{rr} the rolling friction torque, M_{sl} the sliding friction torque, M_{seal} the friction torque on seals and M_{drag} the

friction torque from drag losses (churning, splashing). Knowing the rotational speed n of the bearing, it is possible to obtain the total power loss in bearings, which is given by equation (6.2).

$$P_{VL} = M \cdot n \cdot \left(\frac{\pi}{30}\right) \cdot 10^{-3} \approx 1,05 \times 10^{-4} \cdot M \cdot n \tag{6.2}$$

In Figure 6.2, the friction torque as function of the rotational speed or fluid's viscosity is analysed. In the beginning of the rotation, the friction moment decreases with the increase of rotational speed and viscosity because the fluid film is still being formed. With the continuing increase of speed and viscosity, the lubrication enters a full elasto-hydrodinamic state and the film thickness increases, causing an increase in friction torque.

If the increase in speed and viscosity continues, the friction torque will eventually remain constant or even decrease due to the effects of inlet shear heating and kinematic starvation.

In the following sections each of the components of the total friction torque will be explained. More detailed information with actual values and the calculation of M_{seal} and M_{drag} (which won't be used in the friction torque model as it will be explained further ahead) is presented in Appendix E.

6.1.1. Rolling Friction Torque

In rolling contacts, rolling friction is always present. Energy is dissipated while introducing the lubricant in the contact and removing the excess, in the deformation process and adhesion between surfaces. To establish the formula that calculates the total rolling friction torque M_{rr} three factors must be taken into account:

1. Load distribution in the rolling contacts

In the SKF model the load distribution in bearings is represented by the variable G_{rr} which is function of the bearing type, the bearing mean diameter, the radial load and the axial load. The calculation of G_{rr} is presented on Appendix E.

2. Inlet Shear Heating

This occurs because only a small amount of lubricant is used to produce the film in the contact, causing some of the oil near the contact to reverse its course. This reverse flow shears the lubricant and generates heat, that lowers the viscosity of the oil and

consequently decreases film thickness and the rolling torque. The inlet shear heating reduction factor (ϕ_{ish}) is given by equation (6.3).

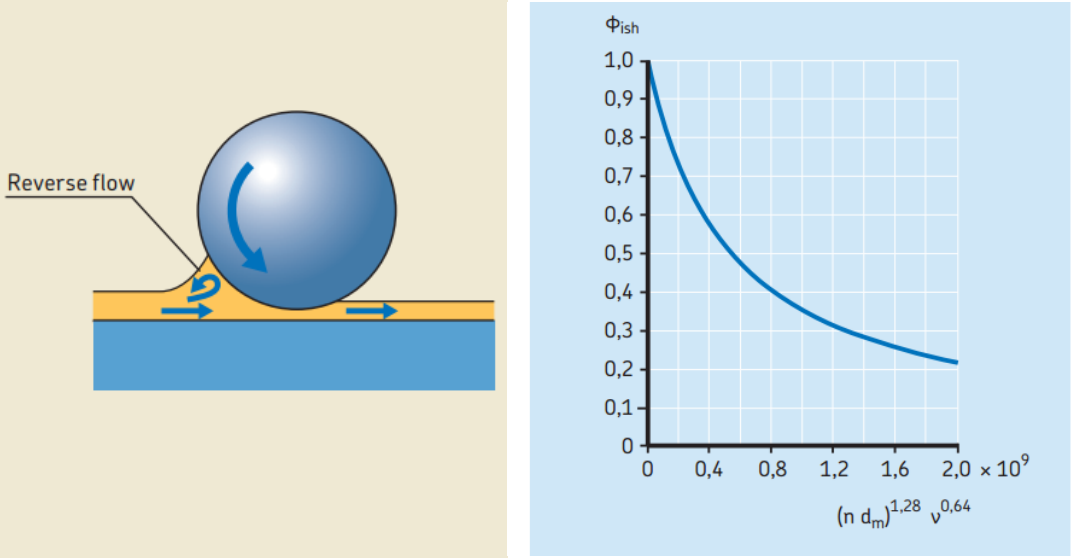

Figure 6.3.: Lubricant recirculation in the inlet (left) and Inlet shear heating factor (right) [36]

$$\phi_{ish} = \frac{1}{1 + 1,84 \times 10^{-9} \cdot (n \cdot d_m)^{1,28} \cdot \nu^{0,64}} \tag{6.3}$$

Where n represents the rotational speed [rpm], d_m the bearing mean diameter [mm] and ν the kinematic viscosity at the operating temperature of the fluid [mm^2/s].

3. Kinematic Replenishment/Starvation

This occurs when the bearing is rotating at high speeds or the lubricant as an high viscosity, and consists in the fact that the replacement of lubricant in the bearing's raceway isn't effective the lubricant doesn't have time to flow from the sides to the center of the railway. This causes a reduction of fluid available (hence the name *"starvation"*) in the inlet of the contact, and provokes the decrease in film thickness and in rolling friction torque. The kynematic replenishment reduction factor (ϕ_{rs}) is given by equation (6.4).

$$\phi_{rs} = \frac{1}{e^{\left[K_{rs} \cdot \nu \cdot n \cdot (d+D) \cdot \sqrt{\frac{K_Z}{2(D-d)}}\right]}} \tag{6.4}$$

Where K_{rs} is a starvation constant that depends on the lubricating method (3×10^{-8} for low level oil bath and oil jet lubrication, and 6×10^{-8} for grease and oil-air lubrication), K_Z is a bearing type constant, d is the bearing bore diameter and D is the bearing outside diameter.

As all the parameters have been defined, the total rolling friction torque is given by equation (6.5).

$$M_{rr} = \phi_{ish} \cdot \phi_{rs} \cdot G_{rr} \cdot (\nu \cdot n)^{0,6} \tag{6.5}$$

6.1.2. Sliding Friction Torque

In a rolling contact, sliding friction is caused by two major factors: macrosliding which is caused by the contact between two surfaces of bigger geometries (e.g. the contact between the balls and the raceway in ball bearings), and micro-sliding that occurs when there is distortion caused by elastic deformation. There are two ways to produce sliding friction losses:

1. Lubricant Shearing

Lubricant shearing occurs when the film thickness is thick enough to completely separate the surfaces in contact. The friction coefficient due to lubricant shearing (μ_{EHL}) is given by equation (6.6).

$$\mu_{EHL} = \frac{1}{Q} \int_A \tau \cdot dA \tag{6.6}$$

Where Q is the normal load applied in the contact, A is the area of the contact and τ is the shear stress in the lubricant. The value of τ depends on the sliding speed and the lubricant's rheology.

2. Asperity Contacts

Asperity contact between the surfaces occurs if the film thickness is not thick enough to completely separate the surfaces. This increases sliding friction losses and as a larger influence in the losses than lubricant shearing. Putting together lubricant shearing and asperity contacts, it is possible to obtain the coefficient of friction for sliding torque losses (μ_{sl}), as given by equation (6.7).

$$\mu_{sl} = \phi_{bl} \cdot \mu_{bl} + (1 - \phi_{bl}) \cdot \mu_{EHL} \tag{6.7}$$

Where μ_{bl} is a coefficient of friction under boundary lubrication that depends on the lubricant's additives, and ϕ_{bl} is a weighting factor for the sliding coefficient of friction given by equation (6.8).

$$\phi_{bl} = \frac{1}{e^{[2{,}6 \cdot 10^{-8} \cdot (n \cdot \nu)^{1{,}4} \cdot d_m]}} \tag{6.8}$$

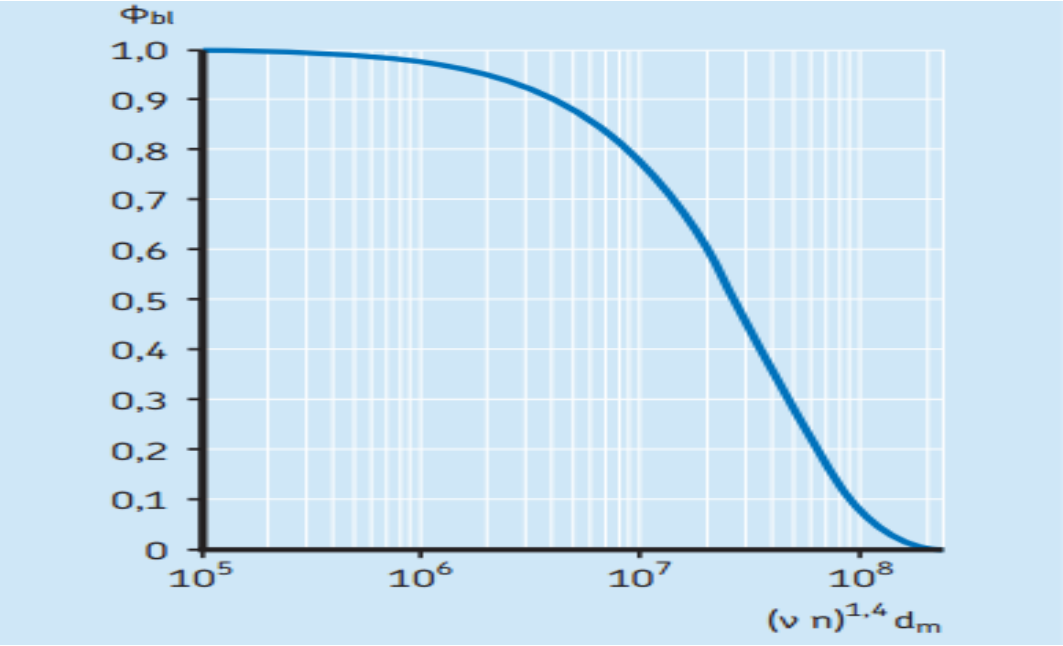

Figure 6.4.: Influence of rotating speed and viscosity on the weighting factor [36]

For lower viscosities and rotating speeds, it is observed that the value of ϕ_{bl} tends to 1, so, the sliding coefficient of friction due to asperity contacts is dominant (there may be metal to metal contact between surfaces). On the other hand, for higher viscosities and rotating speeds (full elastohydrodynamic lubrication), the value of ϕ_{bl} tends to 0, and the primary source of sliding friction is lubricant shearing.

To obtain the expression that defines the sliding torque losses, all that is left is to define the variable G_{sl} that refers to the bearing load and depends on the bearing type, the bearing mean diameter, and radial and axial forces (presented in Appendix E). Knowing this, the expression for the sliding friction torque is given by equation (6.9).

$$M_{sl} = G_{sl} \cdot \mu_{sl} \tag{6.9}$$

6.1.3. Seals Friction Torque

When bearings have contact seals, the frictional losses generated by the seals may be higher than the ones generated by the bearings. However, since the bearings which are used in the experimental tests don't have any seals, this component will be disregarded in the calculations.

6.1.4. Drag Losses

When in the presence of oil bath lubrication, drag losses occur when the oil is rotating in the oil bath. Drag losses are influenced by the bearing speed, the oil's viscosity and level and the size and geometry of the oil reservoir. The drag losses can also be disregarded in the calculations since the bearings' mean diameter is very small as well as the tested operating speeds.

6.2. Tested Roller Bearings

As mentioned previously, the bearings used in the experimental work are cylindrical roller thrust bearings, more particularly SKF 81107 TN bearings. The dimensions and characteristics of the bearings are presented in Figure 6.5 and Table 6.1.

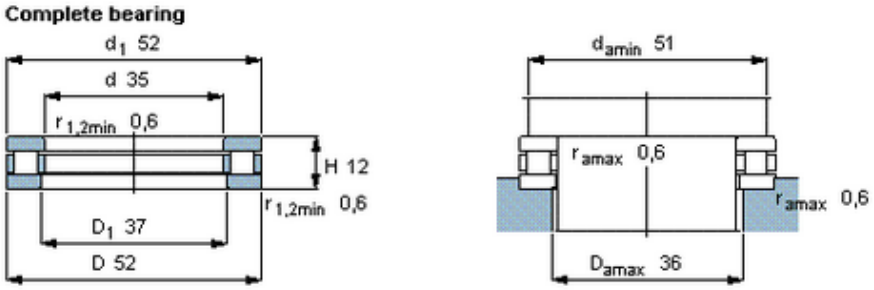

Figure 6.5.: Cylindrical Roller Thrust Bearing 81107 TN design [36]

Table 6.1.: Cylindrical Roller Thrust Bearing 81107 TN characteristics [36]

Dimensions [mm]			Load Ratings [kN]		Speed Ratings [rpm]		Designation	
			Dynamic	Static	Reference Speed	Limiting Speed	Complete Bearing	Thrust Assembly
d	D	H	C	C_0				
35	52	12	29,00	93,00	2800	5600	81107 TN	K 81107 TN

6.3. Determination of the sliding coefficient of friction

The friction torque that is obtained in the experimental measurements made can be considered equal to the total friction torque in the SKF model. Taking into account that the seals friction torque doesn't exist and drag losses are considered very small in comparison to other losses, it is possible to obtain equation (6.10).

$$M_t = M_t^{exp} = M_{rr} + M_{sl} \tag{6.10}$$

The experimental measures besides giving directly the total friction torque, also shows the oil temperature, so it is possible to obtain through simple calculations the rolling friction torque M_{rr}. Therefore, the sliding friction torque is given by equation (6.11).

$$M_{sl}^{exp} = M_t^{exp} - M_{rr} \tag{6.11}$$

Knowing the value of the sliding friction torque, it is possible to obtain the sliding coefficient of friction by applying equation (6.12).

$$\mu_{sl}^{exp} = \frac{M_{sl}^{exp}}{G_{sl}} \tag{6.12}$$

However, as mentioned in the description of the SKF model, there is a formula that allows the direct calculation of the sliding coefficient of friction. In that formula, the value of μ_{sl} is dependent on the value of two coefficients, μ_{bl} that is related to the additive package of the oil and advised to be given the value 0,15 in the SKF Handbook, and μ_{EHL} that can be related to the type of bearing or lubricant. Using the provided values of the coefficient of friction it is verified that the SKF model value may be slightly different to the value obtained experimentally, so the coefficents μ_{bl} and μ_{EHL} in equation (6.7) will be optimized in order to approximate the values of μ_{sl} obtained by the SKF model to the values obtained experimentally. This methodology was proposed by Fernandes *et al.* [38].

6.4. Viscosity Ratio

To evaluate the film thickness and lubrication regime in rolling bearings, the concept of viscosity ratio is used to evaluate a lubricant's efectiveness in forming a sufficient

lubricant film to separate the surfaces in contact. The viscosity ratio (k) is given by equation (6.13).

$$k = \frac{\nu}{\nu_1} \tag{6.13}$$

Where ν represents the lubricant's kinematic viscosity at the operating temperature, and ν_1 the viscosity required to have an adequate lubrication in the contact, taking into account the bearing's mean diameter and the rotational speed (view Figure E.1). In other words, to have a degree of separation between the surfaces (mixed lubrication), $k \geq 1$ is required. According to the SKF catalogue, for $k \geq 4$ full-film conditions are achieved, for $k < 1$ metal to metal contact (boundary lubrication) may occur, and for $k \leq 0,4$ the oil used in those operating conditions needs to have EP additives.

According to ISO 281 [39], the relationship between the viscosity ratio and the specific film thickness can be defined by equation (6.14).

$$k = \lambda^{1,3} \tag{6.14}$$

Part III.

Roller Bearings Experimental Results

7. Roller Bearings Experimental Results

7.1. Experimental Procedure

To measure the total friction torque on the cylindrical roller thrust bearings, a modified four-ball machine was used. In this machine, the four-ball arrangement was replaced with a rolling bearing assembly in order to test the behaviour of bearings lubricated with an oil or grease. This assembly allows the measurement of the total friction torque and the temperature in different points with the aid of a torque cell and seven thermocouples respectively. The procedure used to measure the friction torque is the one described by Cousseau *et al.* [40].

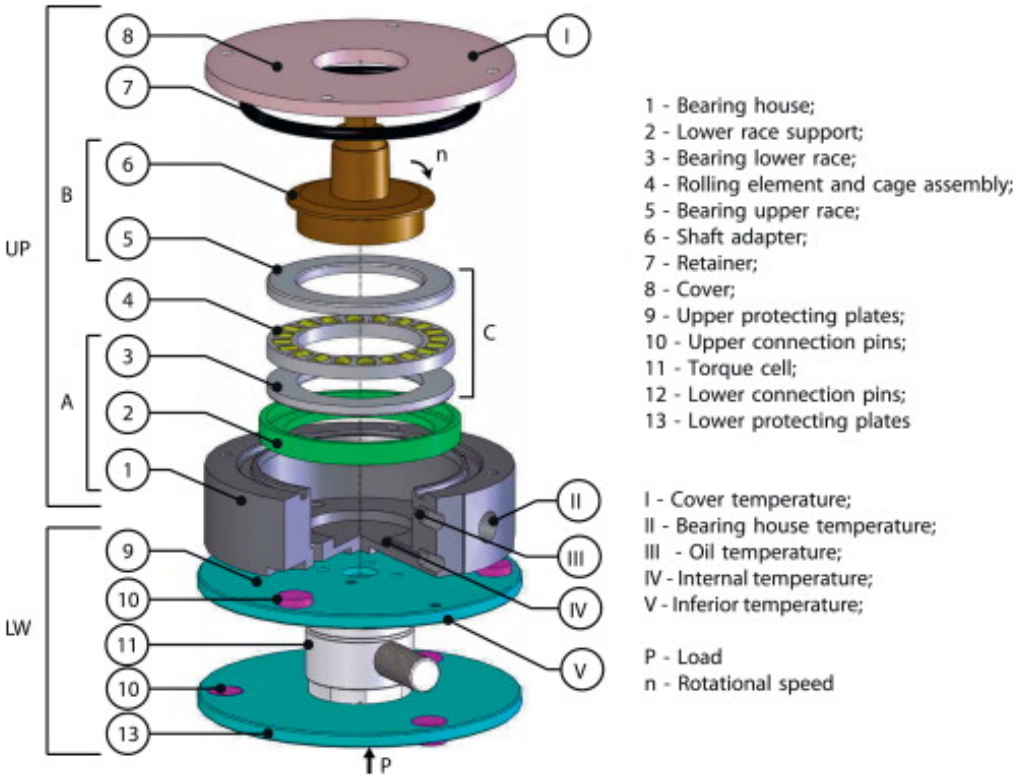

Figure 7.1.: Rolling Bearing Assembly [40]

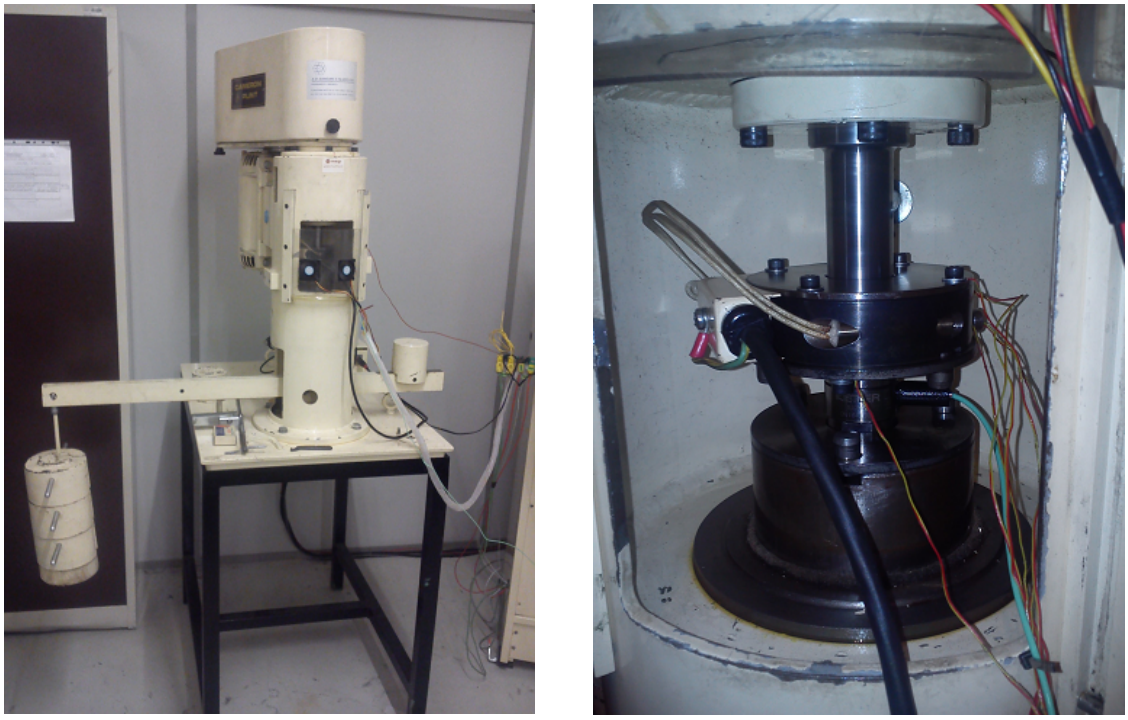

Figure 7.2.: Modified four-ball machine and overview of the rolling bearing assembly

The mounting phase of the rolling bearing assembly consists of:

1. The lower race (3) is fitted on the spacer (2) with J6/p5 tolerance. This set (3+2) is fitted on the bearing house (1) with H6/j5 tolerance. The tight fit used among these parts of the group (A) ensures that there is no relative motion between them.

2. The upper race (5) is mounted on the shaft adapter (6) with P5/j6 tolerance, also to prevent relative motion between them, composing the group (B).

3. To prevent contamination by external particles due to the mounting operations (groups A and B), and also to remove the oil film protection of the bearing package, the groups A and B and the rolling elements and cage (4) are washed with solvent in an ultrasonic bath before assembly on the test rig.

4. Bath oil lubrication: The oil level should reach the centre of the lowest rolling element when the bearing is stationary. For the cylindrical roller thrust bearing 81107, the oil volume required is approximately 14 ml. During this operation the rolling elements and cage (4) are already on the lower race (3) and the thermocouples (III, IV) should be assembled on the bearing house (1), preventing oil leakage through the thermocouple holes.

5. To complete the assembly of the upper set (UP), the retainer (7), the cover (8) and the thermocouples I and II are mounted.

6. The lower set (LW) was previously assembled (and does not need to be reassembled for each test), and is composed by six connection pins (10 and 12) clamped to the torque cell protecting plates (9 and 13) and a torque cell (11). The lower plate (9) is mounted on the lower non-rotating shaft of the Four-Ball Machine, which applies the load to the bearing. The three lower pins (12) assure that there is no relative rotation. The three upper pins (10) are used to connect the UP to the lower set (UP $\rightarrow$ LW) preventing any relative rotation. The thermocouple V is permanently mounted on the protecting plate (9).

7. The final phase is to install UP and LW into the Four-Ball Machine. First, UP is connected to the rotating shaft, and then the LW is mounted below. The conjunction will be locked by the lower shaft of the Four-Ball Machine, which is moved up to apply the load.

When the four-ball machine is operating, a load (P) is applied on the lower plate (13) while the rotational speed (n) is applied to the machine's shaft and transmitted to the shaft adapter (6). The rotating motion is conducted through the upper race (5) to the rolling elements and cage assembly (4). This motion generates the bearing internal friction torque, which is transmitted through the lower race (3) to the bearing house (1), to the upper plate (9) and to the torque cell (11), which are all clamped together.

While the machine is operating, two fans submit the bearing assembly to forced air convection to keep the air temperature steady during the test. Also, to make measurements with controlled temperature, the bearing assembly is mounted with two heaters which are controlled with a PID control system with feedback, whose feedback is given by thermocouple III.

The four-ball machine allows measurements with four different types of roller bearings whose dimensions are limited by the bearing housing and the four-ball machine.

Table 7.1.: Rolling Bearings that can be used on the four-ball machine

Dimensions [mm]			Dynamic Load [kN]	Limiting Speed [rpm]	SKF Designation
d	D	H	C		
Thrust Ball Bearings					
17	30	9	11,14	12000	51103
35	52	12	19,90	7500	51107
Cylindrical Roller Thrust Bearings					
17	28	9	11,20	8500	81102 TN
35	52	12	29,00	5600	81107 TN
Angular Contact Ball Bearings					
17	40	12	11,00	22000	7203
20	47	14	13,30	18000	7204
Tapered Roller Bearings					
15	42	14,25	22,40	18000	30302 J2
17	40	13,25	19,00	18000	30203 J2

The torque cell used to measure the rolling bearings friction torque is a piezoelectric torque cell KISTLER® 9339A. By applying a mechanical excitation in the torque cell, the piezoelectric crystals change the electric current, whose variation is very small and must be amplified and conditioned with an amplifier KISTLER® 5015A. The output signal is displayed and registered in the computer. The changes in the output signal ("*drift*") must be avoided by making measurements in short periods of time (120 s) under stabilized temperatures (±2 °C).

To measure the temperature at different points, seven thermocouples are used. Five of those thermocouples (I-V) measure the temperature inside the bearing, in the neighbourhood of the bearing and of the lubricant. The other two thermocouples measure the chamber and the room temperatures. These thermocouples have a measuring range of −40 °C to 200 °C and a sensibility of 41 $\mu V°C^{-1}$. The reference temperature for the tests that were made, is the temperature registered by thermocouple III.

7.2. Operating Conditions

As mentioned in the previous section, the rolling bearing tests were performed on a modified four-ball machine in order to measure the friction torque. Three oils (SYN FE 75W90, SYN FE 75W140 and RS FE 80W90) were tested under different load (4000 N and 7000 N) and temperature (70 °C, 90 °C and 110 °C) conditions (Table 7.2) with a RTB 81107 bearing, and the friction torque was measured for different rotational speeds between 75 and 1200 rpm for each test. For every speed, four measurements of friction torque were made, and the friction torque considered is the average of the three closest values. In Table 7.3 are represented the characteristics of the contact of each roller with the race for the two selected axial loads. Roughness measurements of the roller and race before being used were not made, as it has been done in previous works [37] for RTB 81107 bearings in new conditions. Since the friction torque tests made were of short duration, roughness measurements of the rollers and race were also not made after being submitted to the tests. Table 7.4 shows the viscosity, piezoviscosity coefficient and lubricant parameter of each oil at the selected testing temperatures.

Temperature values for the measurements were chosen based on results obtained by Kolekar et al. [41], while the value of the axial load was chosen knowing typical values of bearing preload on vehicle's axles [7] [42]. Numerical results of each test performed are presented from Table F.2 to Table F.21

Table 7.2.: Battery of tests at constant temperature performed on the modified four-ball machine for each of the three oils

	70 °C	90 °C	110 °C
4000 N	✓	✓	✓
7000 N	✓	✓	✓

Table 7.3.: Roller-Raceway contact parameters for the 81107 RTB Bearing at the load conditions applied in the tests

	4000 N	7000 N
Number of Rollers	20	20
R_x [m]	0,005	0,005
l [m]	0,005	0,005
a [μm]	32,9	43,5
p_0 [MPa]	759,3	1004,4
σ [μm]	0,14	0,14

Table 7.4.: Kinematic viscosity, piezoviscosity coefficient and lubricant parameter of the three oils at the three operating temperatures

	70 °C	90 °C	110 °C
ν^{75W90} [cSt]	38,23	21,80	13,75
ν^{75W140} [cSt]	64,20	35,25	21,51
ν^{80W90} [cSt]	36,54	19,69	11,95
α^{75W90} $\times 10^8$ [Pa^{-1}]	1,201	1,114	1,047
α^{75W140} $\times 10^8$ [Pa^{-1}]	1,287	1,187	1,112
α^{80W90} $\times 10^8$ [Pa^{-1}]	1,633	1,499	1,398
LP^{75W90} $\times 10^{10}$ [s]	3,83	2,00	1,16
LP^{75W140} $\times 10^{10}$ [s]	7,07	3,54	2,00
LP^{80W90} $\times 10^{10}$ [s]	5,08	2,48	1,38

7.3. Experimental Measurements

7.3.1. Operating Temperature

Before starting the analysis, it is important to mention that for the testing conditions performed, it was impossible in the majority of the tests to keep the temperature stabilized at the desired value. Figure 7.3 shows the average temperature in the friction torque measurements made in every tested conditions.

Under a 7000 N load, the temperature remained stable only until 600 rpm for both 70 °C and 90 °C cases and until 900 rpm for measurements at 110 °C. Above the mentioned speeds the temperature always increased. With measurements performed with a 4000 N load, for measurements at 70 °C the temperature suffered an increase only above 900 rpm, and at 90 °C and 110 °C the temperature remained stable throughout all the speeds. The dashed black line in all the graphics represented in the following sections represents the last measurement speed at which the temperature remained constant.

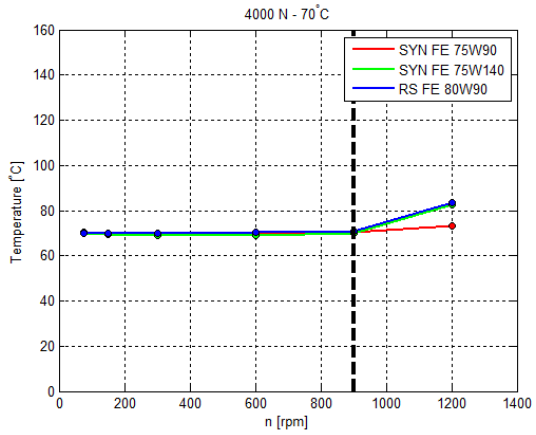

(a) 4000 N/70 °C

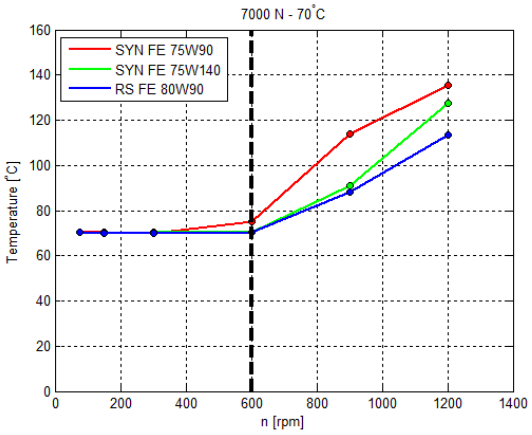

(b) 7000 N/70 °C

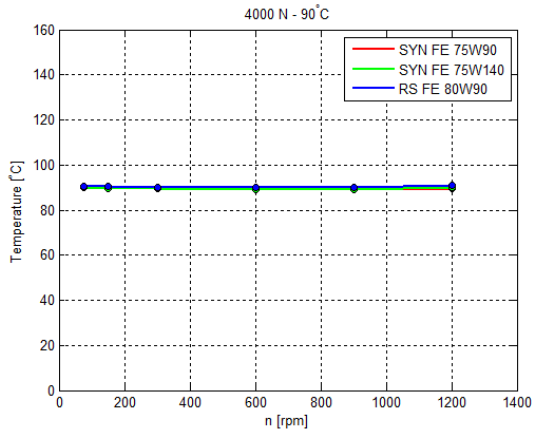

(c) 4000 N/90 °C

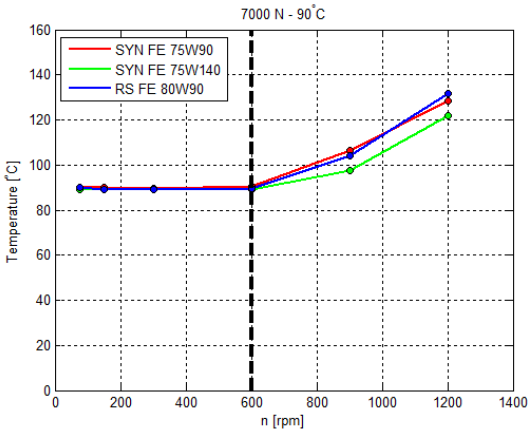

(d) 7000 N/90 °C

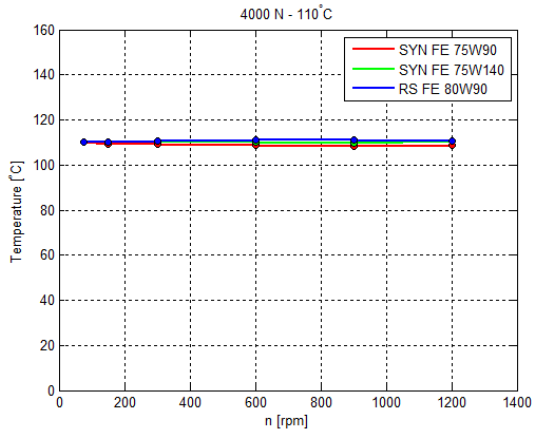

(e) 4000 N/110 °C

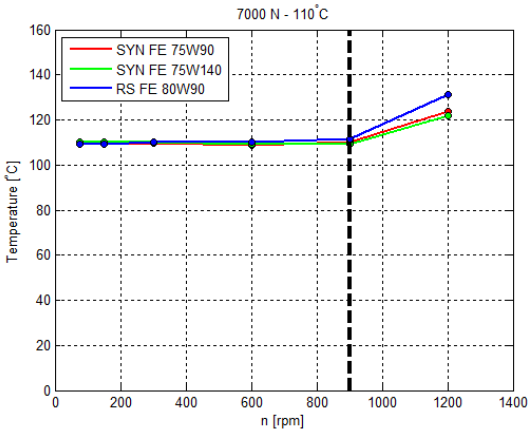

(f) 7000 N/110 °C

Figure 7.3.: Temperature [θ / °C] evolution in the constant temperature measurements for each oil in every tested condition

7.3.2. Total Friction Torque Measurements

In Figure 7.4a, it is possible to observe that under a 4000 N load at 70 °C the torque loss decreases with an increase in rotational speed. With these testing conditions, the 75W90 oil presents lower values of torque loss than the 75W140 and 80W90 oils. This is the result of being the oil with the lowest viscosity at the working temperature, being a fully synthetic oil, and the film thickness being sufficient to completely separate the contact surfaces, as shown ahead. Curiously, the 75W140 and the 80W90 oils present similar values of friction torque at any rotational speed. This may be because that while the 75W140 oil is fully synthetic and typically presents better properties under shear than a mineral oil, the 80W90 oil is less viscous at the working temperature, therefore offering less resistance to the bearing's rotation.

Figure 7.4c shows that at 90 °C the friction torque values are generally slightly higher than at 70 °C for the higher speeds (above 600 rpm). In fact, the 75W140 shows lower values of the friction torque because it has a lower viscosity than at 70 °C, while maintaining sufficient film thickness in the contact. It is also observed that the 80W90 oil increases friction torque at higher speeds (combined effect of a possible metal to metal contact and its mineral nature), and that for rotational speeds lower than 600 rpm, the values of torque loss for the three oils are identical.

With 4000 N and 110 °C (Figure 7.4e) it is observed that the trend is similar to the one observed in Figure 7.4c (after 600 rpm the friction torque decreases in the synthetic oils and increases in the mineral oil) with the values of the measured friction torque being slightly higher than at 70 °C due to a decrease in film thickness in all the oils.

In Figure 7.4b, it is observed that with a higher load of 7000 N, while the temperature remains at 70 °C the torque loss decreases with the increase in rotational speed. For these conditions, the 75W90 oil produced the highest value of friction torque for every rotational speed, while the 75W140 and the 80W90 oils presented lower and similar values. The higher value of the friction torque in the 75W90 oil can be explained by low values of the film thickness, which means metal to metal contact may occur.

Comparing Figure 7.4d with Figure 7.4b, it is verified an increase in friction torque with the increase in temperature for all the three oils. The 80W90 oil is the oil that displays the highest increase, while the 75W90 and the 75W140 oil suffer smaller and similar increases. It is interesting to notice that while at 75 and 150 rpm the difference in friction torque can be clearly seen, from 300 rpm to 600 rpm (while the temperature remains constant), the three oils present the same values of friction torque. This may imply that at 300 rpm the oils with lower viscosity (75W90 and 80W90) were able to produce an adequate film thickness to separate the contacting surfaces. It is also noticeable that after the temperature control was lost, all the oils but the 75W90 presented a decrease in the friction torque at the higher speeds.

Observing Figure 7.4f it is possible to verify that the three oils have the same tendency observed in Figure 7.4d, with the 75W90 oil apparently having better behaviour at this higher temperature above 300 rpm. Comparing all three temperatures tests made at 7000 N, it is noticeable that the 80W90 oil has a bigger increase in friction torque than the 75W90 and the 75W140 oils.

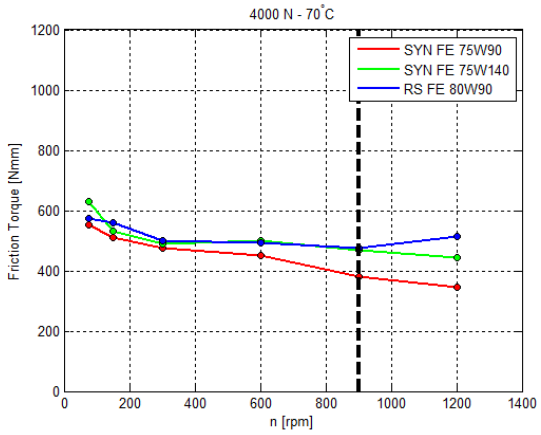

(a) 4000 N/70 °C

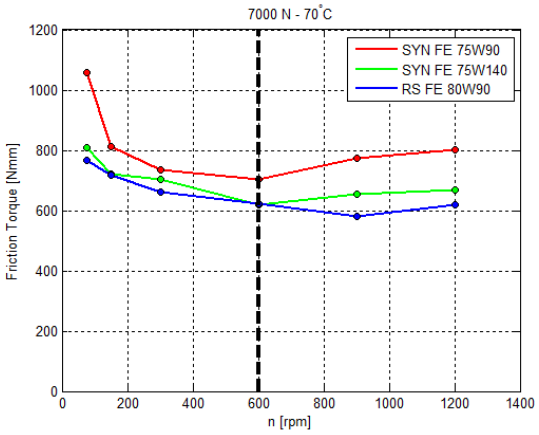

(b) 7000 N/70 °C

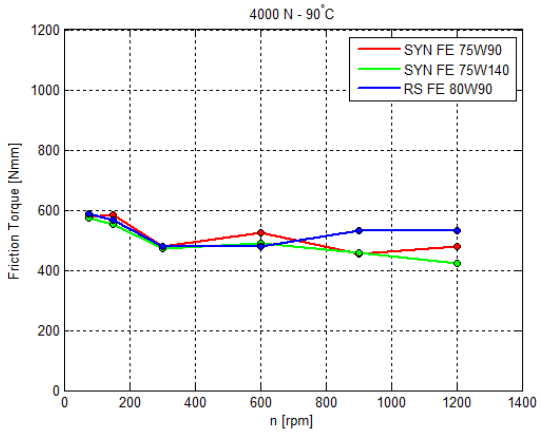

(c) 4000 N/90 °C

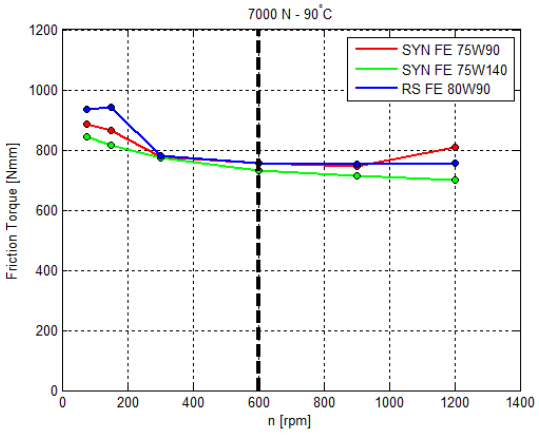

(d) 7000 N/90 °C

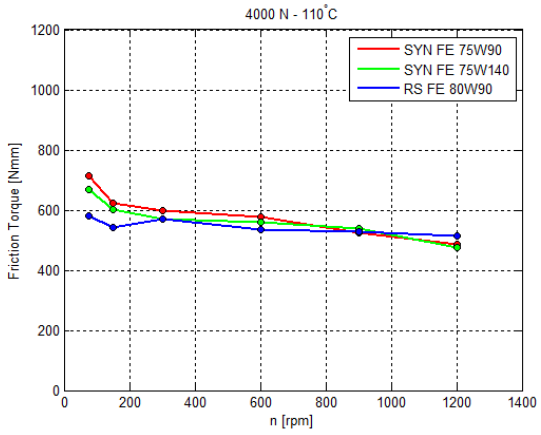

(e) 4000 N/110 °C

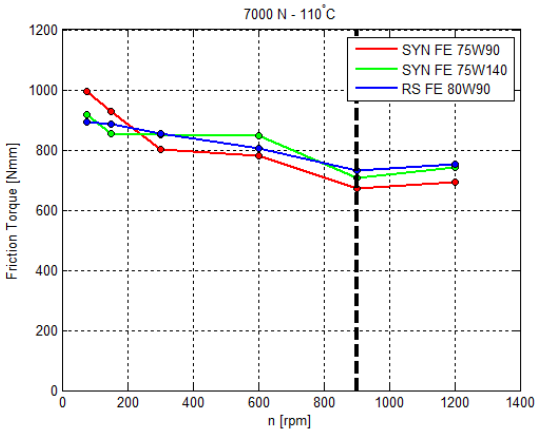

(f) 7000 N/110 °C

Figure 7.4.: Experimental friction torque [M_t^{exp} / Nmm] measurement results for each oil in every tested condition

7.4. Rolling and Sliding Friction Torque

One of the main advantages of the friction torque model proposed by SKF for roller bearings, is the fact that the total friction torque can be separated in four different components: rolling friction torque, sliding friction torque, seals friction torque and drag losses. In calculations only the rolling and sliding friction torque will be analyzed because the bearing has no seals, and due to its small size drag losses can be disregarded.

The rolling friction torque evolution in all the tested conditions for the three oils is very similar as represented in Figure 7.5. In all cases, the rolling torque increases with the increase in speed while the temperature remains constant, and the values are also generally higher with lower temperatures and higher loads applied. It is also noticed that the 75W140 oil always presents the highest rolling torque values while the 75W90 and 80W90 oil present lower and almost identical values. This is due to the fact that the main parameter that differentiates each oil in the calculation of the rolling torque is the viscosity at the working temperature.

As expected, the sliding torque values are higher than the ones obtained for the rolling torque, and the tendency of its value decreasing with the increase in rotational speed (in the majority of the cases) is also the expected for low viscosity oils and verified on Figure 7.6.

The analysis made for the sliding friction torque is pratically identical to the one made for the total friction torque measured, as the shape of the curves in each test is the same. Figure 7.6a shows that at 4000 N and 70 °C, the mineral oil (80W90) has higher sliding torque than the synthetic oils (75W90 and the 75W140). At an higher temperature (Figure 7.6c) the behaviour of the oils is the same until 600 rpm. At higher speeds, the viscosity of the oils plays a greater role since the sliding torque decreases for the oil with higher viscosity and remains more or less constant for the lower viscosity oils. With a temperature of 110 °C (Figure 7.6e) it is observed that all oils present similar values of sliding friction torque.

Increasing the load, it is observed that the sliding torque values are much higher at all temperatures. Observing Figure 7.6b it is verified that the 75W90 oil presents higher values of sliding friction torque. With the higher load and temperature conditions (Figure 7.6d) the 80W90 oil suffers the biggest increase in the sliding torque while the 75W90 and 75W140 oils also increase but in a lower degree. At these conditions it can also be viewed that after temperature control was lost, the values of the sliding friction torque suffered little or no change in the three oils.

At 110 °C (Figure 7.6f) it is again observed that the 75W90 oil and 75W140 oil behave better in these conditions than the 80W90 oil (as observed in Figure 7.6d) and that the values of sliding friction torque at 110 °C are close to the ones observed at 90 °C. The small changes are due to the fact that from 90 °C to 110 °C there are smaller changes in the value of the viscosity of the oils since the three of them have high values of the Viscosity Index.

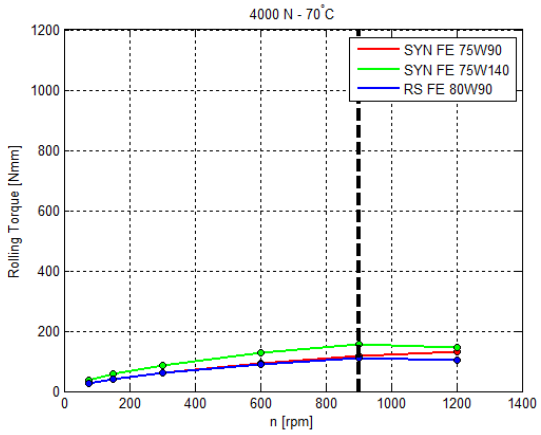

(a) 4000 N/70 °C

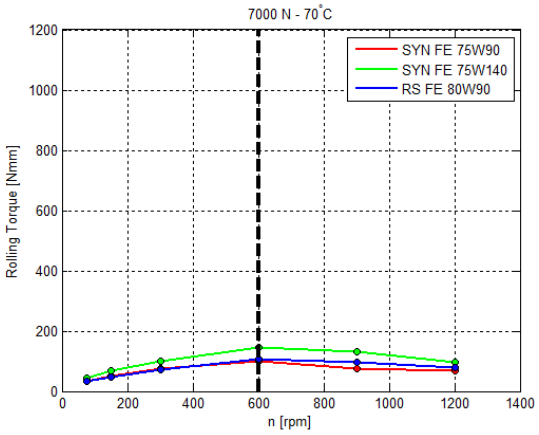

(b) 7000 N/70 °C

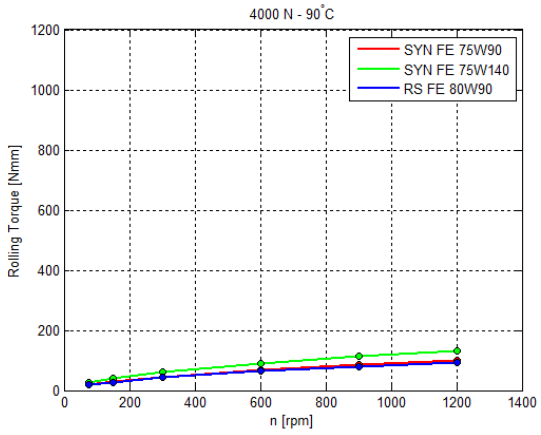

(c) 4000 N/90 °C

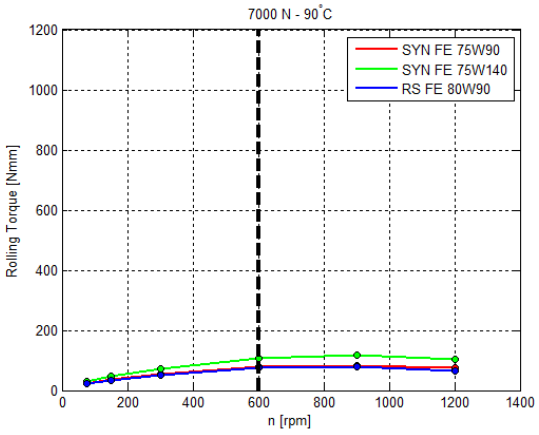

(d) 7000 N/90 °C

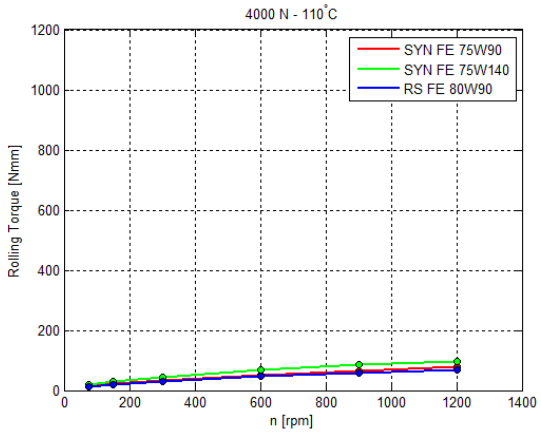

(e) 4000 N/110 °C

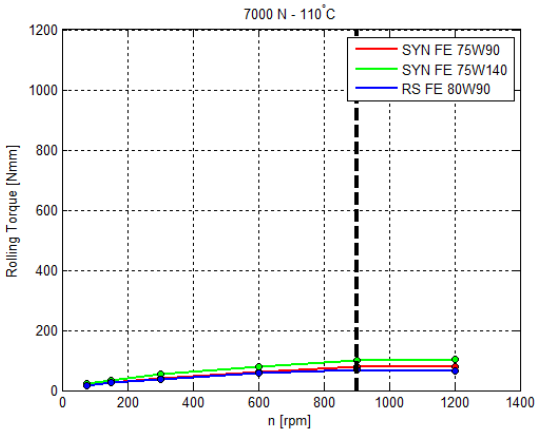

(f) 7000 N/110 °C

Figure 7.5.: Rolling friction torque [M_{rr} / Nmm] measurement results for each oil in every tested condition

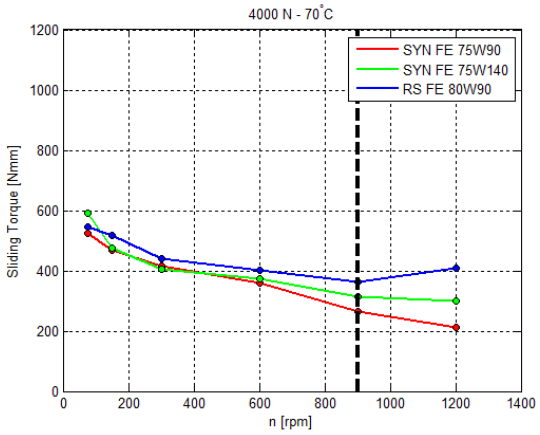

(a) 4000 N/70 °C

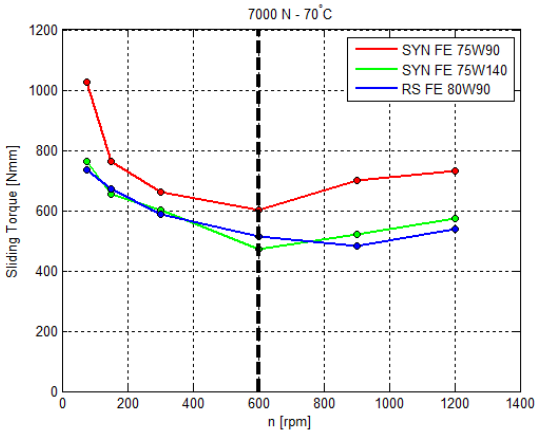

(b) 7000 N/70 °C

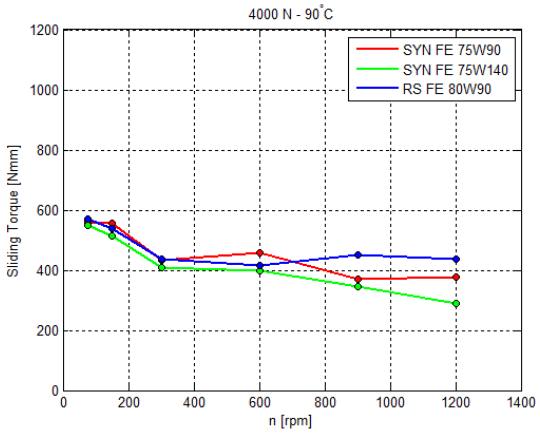

(c) 4000 N/90 °C

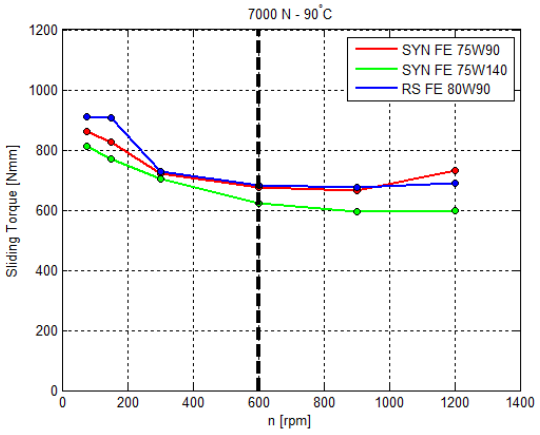

(d) 7000 N/90 °C

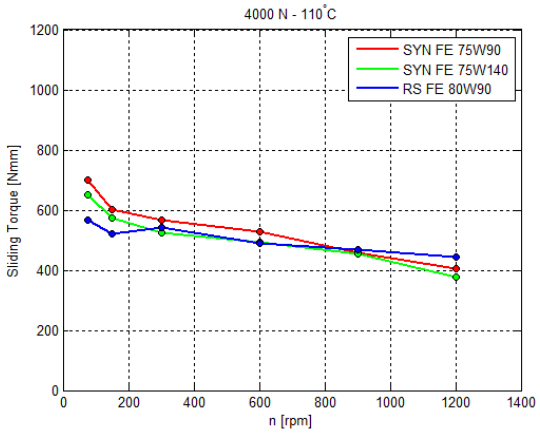

(e) 4000 N/110 °C

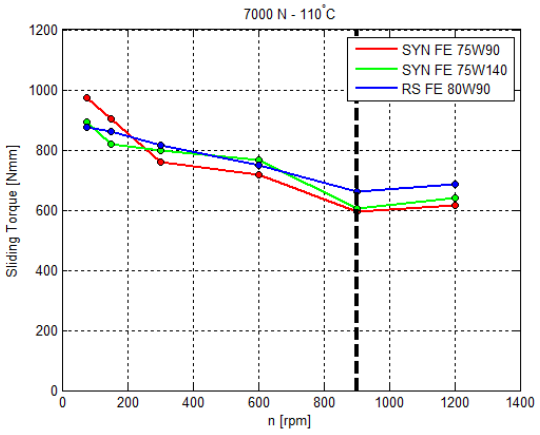

(f) 7000 N/110 °C

Figure 7.6.: Sliding friction torque [M_{sl}^{exp} / Nmm] measurement results for each oil in every tested condition

7.5. Specific Film Thickness and Viscosity Ratio

Using the Dowson and Higginson model for linear contacts, it is possible to calculate the specific film thickness for each oil at each tested conditions. In this model, the piezoviscosity coefficients used were the ones obtained by Gold's equation.

It is possible to observe that at every temperature and load tested, the 75W90 oil presents always the lowest values of specific film thickness because not only it has the lower viscosity at the working temperatures it also has the lower piezoviscosity coefficient. The 75W140 oil, despite having a lower piezoviscosity coefficient than the 80W90 oil, presents higher values of specific film thickness due to its higher viscosity.

It is also of obvious comprehension that when increasing the temperature, the oils specific film thickness decreases due to the decrease in the viscosity of every oil, and that when the load increases the specific film thickness also decreases.

Comparing the calculated specific film thickness with the measurements of friction torque, some interesting conclusions can be obtained. For example, with a 4000 N load and the two lower temperatures, it is observed that despite having an higher specific film thickness than the 75W90 oil, the torque losses in the 80W90 oil are generally higher than the 75W90 oil, which implies that the synthetic nature or the additive package in the 75W90 oil provide better performance with a 4000 N load. At 110 °C with the 4000 N load, the 75W90 only at higher speeds has lower losses than the 80W90 oil. Also at the tested speeds in almost every condition, it appears that the 75W140 oil is a better choice than the other two oils because it forms a thicker film. At 4000 N and 70 °C (Figure 7.4a and Figure 7.7a) the 75W90 oil presents the lowest friction torque since a sufficient film thickness is formed (higher viscosity and lower load).

Another way to estimate the lubrication regimes present in the tests, is by using the SKF abacus that determines the viscosity ratio (k). Using this concept, it is possible to observe that at low rotational speeds (75 and 150 rpm), the three oils are in the boundary lubrication regime in every test performed. Comparing Figure 7.5 with Figure 7.8, a direct relationship between the viscosity ratio and the rolling torque can be observed, as both parameters only depend on the oil's viscosity.

With a working temperature of 70 °C, it is possible to see that the 75W140 oil, mixed lubrication regime is entered at 300 rpm ($k > 1$), while the other two oils only surpass that barrier at 600 rpm (Figure 7.8a and Figure 7.8b). At 90 °C, the 75W140 enters mixed lubrication at 600 rpm and the 75W90 and 80W90 at 900 rpm (Figure 7.8c and Figure 7.8d). With a temperature of 110 °C, the 75W140 only enters mixed lubrication at 900 rpm, and the other two oils never completely achieve that lubrication stage. These relationships confirm the tendency observed in the Stribeck curves, so, the relationship between the specific film thickness and the lubrication regime for bearings mentioned in section 5.2, can be seen as an indication for a broad range of bearings available rather than an actual accurate value. In the tests performed, full film lubrication was generally not achieved due to temperature increase at higher rotational speeds.

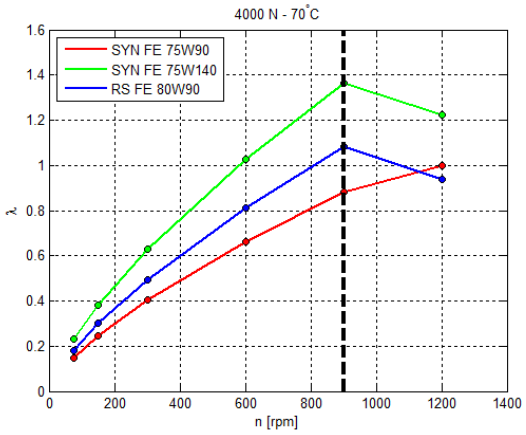

(a) 4000 N/70 °C

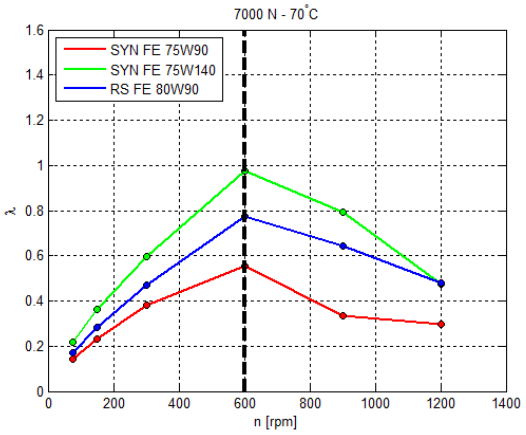

(b) 7000 N/70 °C

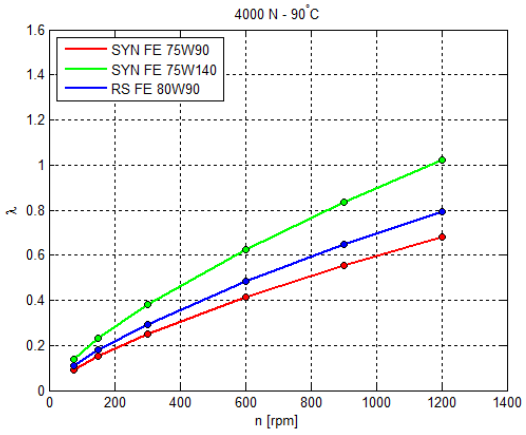

(c) 4000 N/90 °C

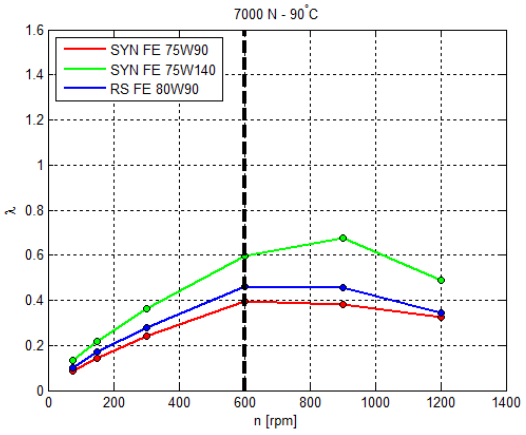

(d) 7000 N/90 °C

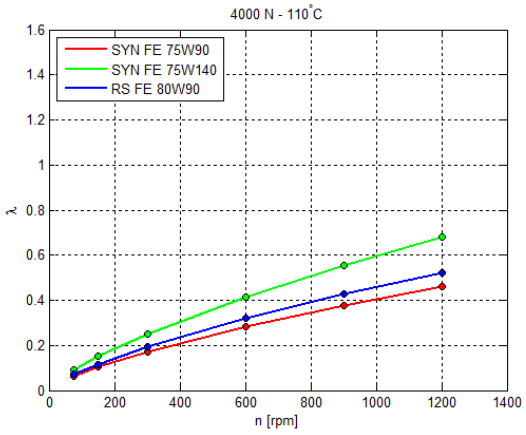

(e) 4000 N/110 °C

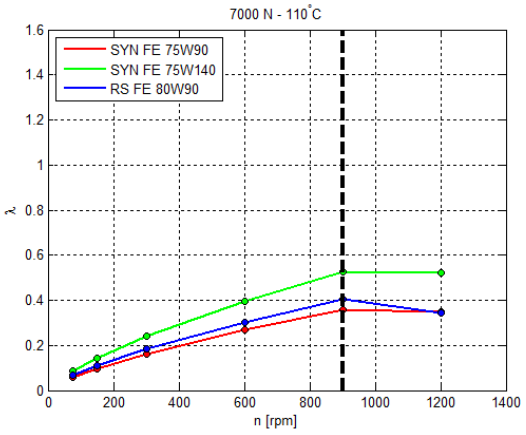

(f) 7000 N/110 °C

Figure 7.7.: Specific film thickness [λ / -] calculated using the Dowson and Higginson model for linear contacts for each tested oil in every tested conditions

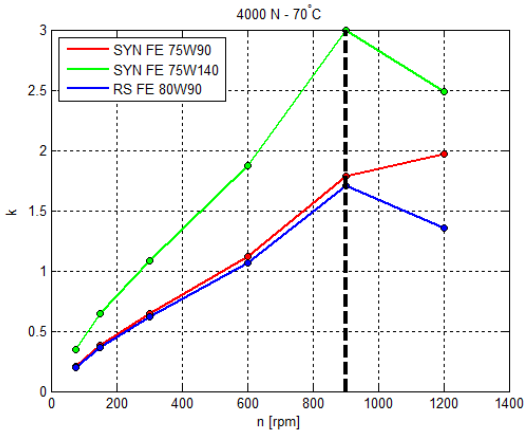

(a) 4000 N/70 °C

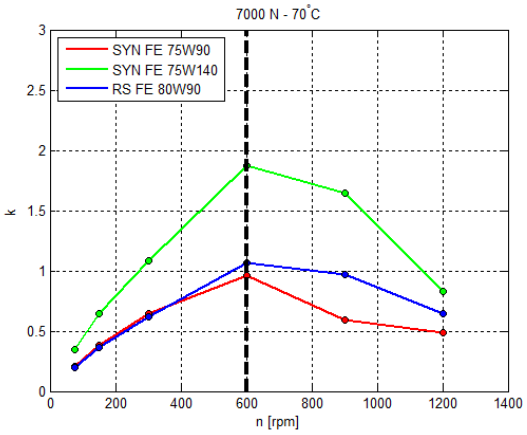

(b) 7000 N/70 °C

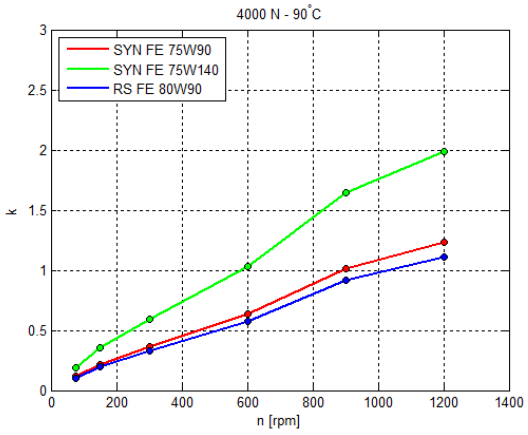

(c) 4000 N/90 °C

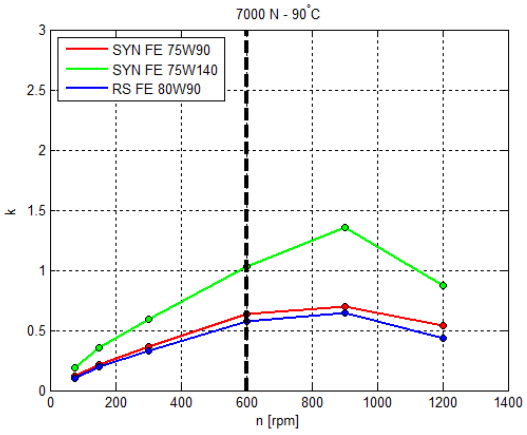

(d) 7000 N/90 °C

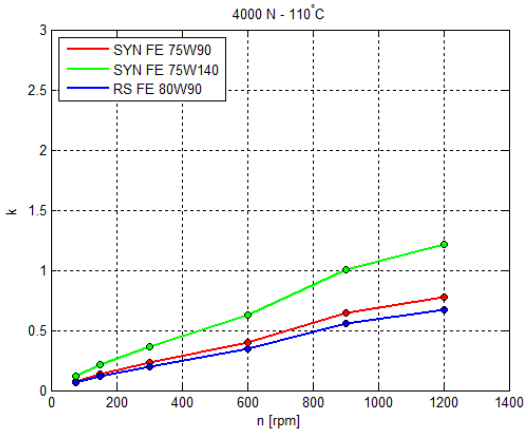

(e) 4000 N/110 °C

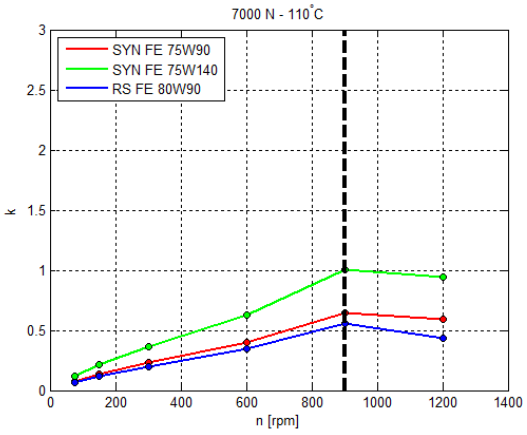

(f) 7000 N/110 °C

Figure 7.8.: Viscosity ratio [k = ν/ν_0 / -] calculated for the three tested oils in every tested conditions

7.6. Sliding Coefficient of Friction

The sliding coefficient of friction can be determined through the application of equation (7.1) to the experimental results. The sliding coefficient of friction results are displayed in Figure 7.9. It can be observed that while the temperature remains stabilized, the sliding coefficient of friction decreases with the increase in rotational speed in almost all the tests performed (the evolution is the same of the sliding friction torque). This is in accord with the evolution of the lubrication regime with the increase in speed, in other words, boundary lubrication at the lower speeds and mixed lubrication at higher speeds.

$$\mu_{sl}^{exp} = \frac{M_t^{exp} - M_{rr}}{G_{sl}} = \frac{M_{sl}^{exp}}{G_{sl}} \tag{7.1}$$

At Figure 7.9a it is observed that the three oils have similar values of the sliding coefficient of friction at lower speeds, but at higher speeds the 75W90 oil presents the lowest values of μ_{sl} while the 80W90 oil presents the highest.

Comparing Figure 7.9a with Figure 7.9b, it is possible to see that the three oils evolved differently with the increase in load. The values of μ_{sl} increased in the 75W90 oil (lower specific film thickness) and decreased in the 75W140 and 80W90 oils (higher specific film thickness). In sum, since both the M_{sl} and G_{sl} parameters in equation 6.12 increase when increasing the load, it is the rate of increase in sliding friction torque that will determine if the parameter μ_{sl} will increase or decrease with an higher load.

Comparing the tests performed at 70 °C (Figure 7.9a and Figure 7.9b) with the tests performed at 90 °C (Figure 7.9c and Figure 7.9d) it is possible to observe that generally μ_{sl} increases with the increase in temperature. With a 4000 N load the values of μ_{sl} increase more in the 75W90 oil than the other two (Figure 7.10d, Figure 7.10e and Figure 7.10f), which may be caused by its lower specific film thickness at 90 °C.

At 7000 N from 70 °C to 90 °C, μ_{sl} clearly increases in the 75W140 and 80W90 oils (Figure 7.10h and Figure 7.10i), being more accentuated in the 80W90 due to its lower viscosity. With the 75W90 oil, the value of μ_{sl} for these conditions doesn't display an increase (Figure 7.10g), probably because the film thickness at both temperatures is already very low.

Observing the tests performed at 110 °C (Figure 7.9e and Figure 7.9f) and comparing them with the tests made at 90 °C, it is possible to see that the values of μ_{sl} increase with a higher degree with a 4000 N load than with a 7000 N load. This may be due to the change in lubrication regime when changing the temperature with both loads. While at 4000 N and 90 °C mixed lubrication is predominant and when increasing the temperature to 110 °C the regime may change into boundary lubrication, with a 7000 N load and these same temperatures boundary lubrication is the dominant lubrication regime.

With Figure 7.10 it is possible to observe that for every oil tested the sliding coefficient of friction decreases with the increase in load, (the increase in the parameter G_{sl} is greater than the increase in M_{sl} - Figure 7.10a to Figure 7.10c), and increases with the

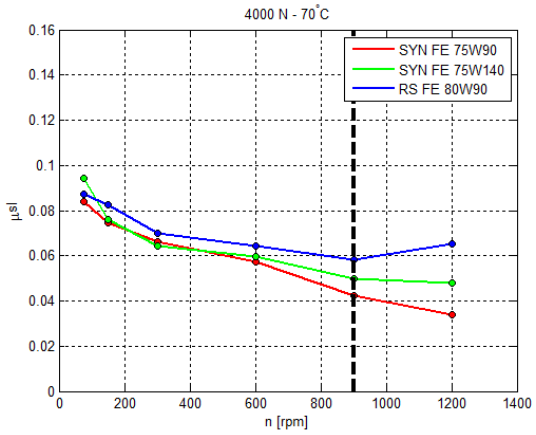

(a) 4000 N/70 °C

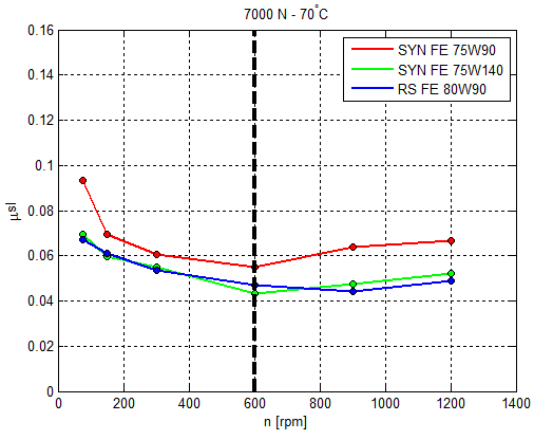

(b) 7000 N/70 °C

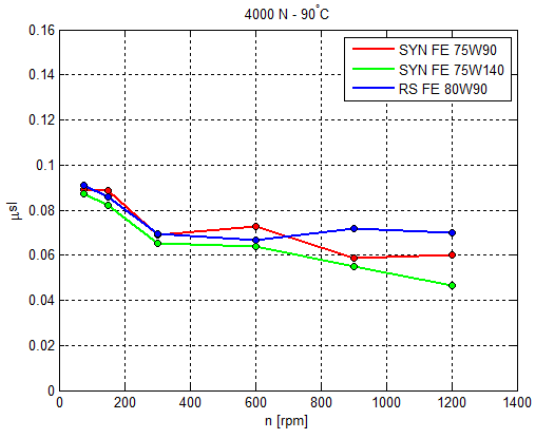

(c) 4000 N/90 °C

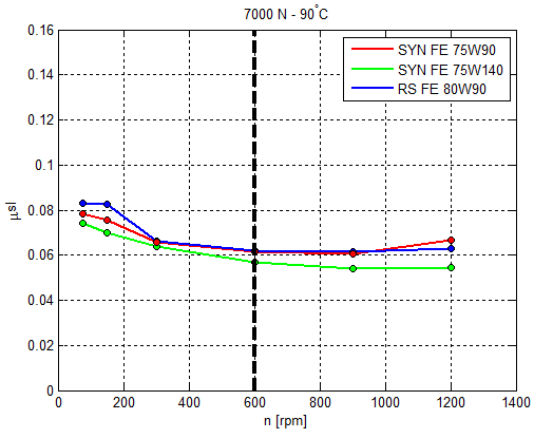

(d) 7000 N/90 °C

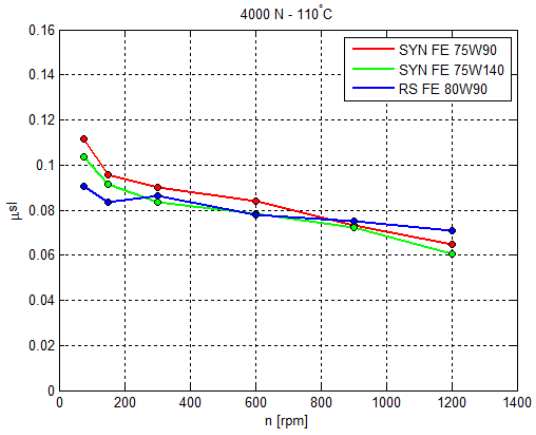

(e) 4000 N/110 °C

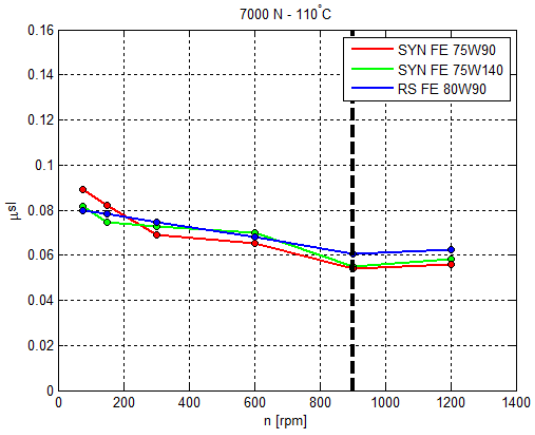

(f) 7000 N/110 °C

Figure 7.9.: Sliding coefficient of friction $[\mu_{sl}^{exp}$ / -] measured for the three tested oils in every tested conditions

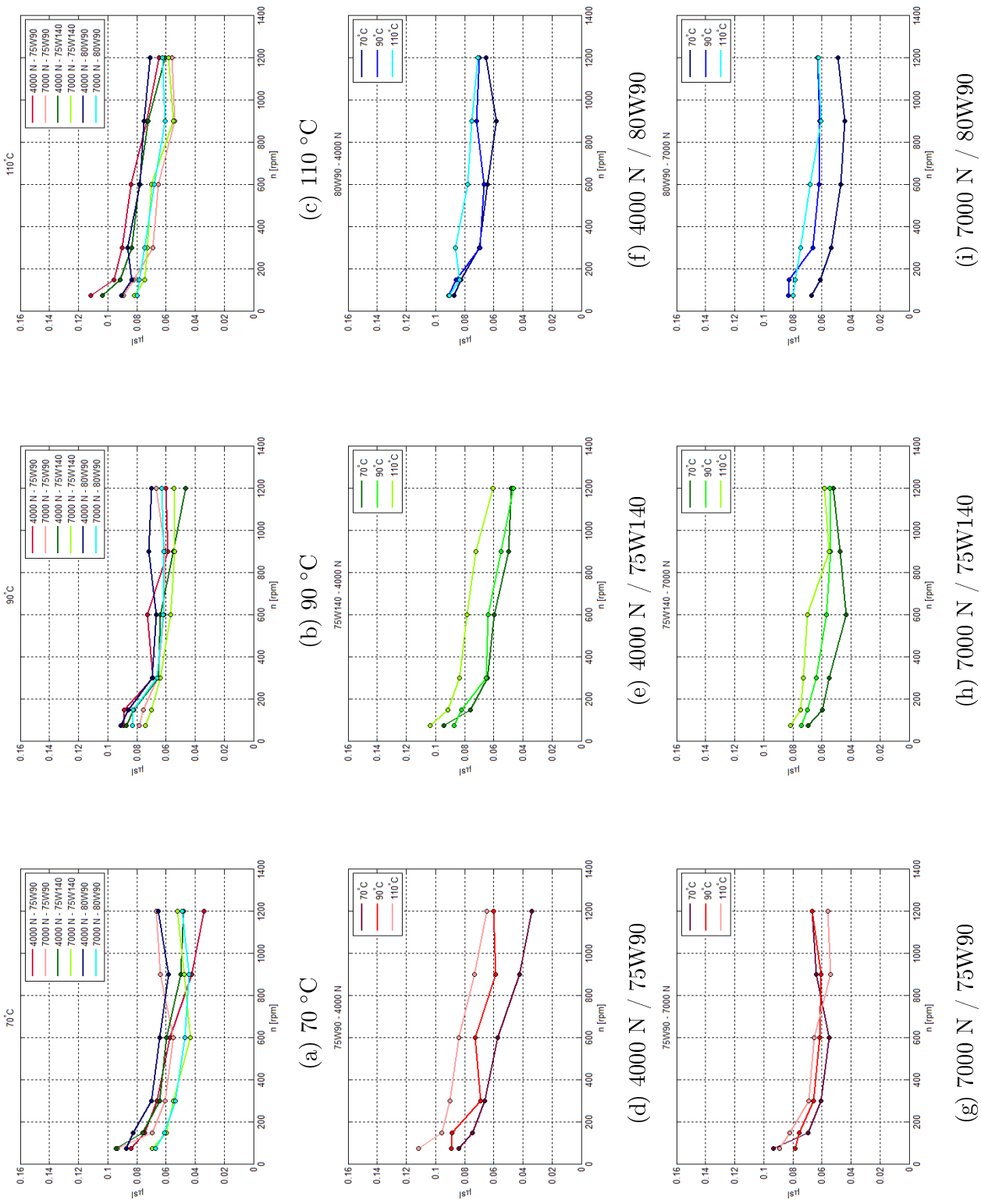

(a) 70 °C (b) 90 °C (c) 110 °C

(d) 4000 N / 75W90 (e) 4000 N / 75W140 (f) 4000 N / 80W90

(g) 7000 N / 75W90 (h) 7000 N / 75W140 (i) 7000 N / 80W90

Figure 7.10.: Sliding coefficient of friction [μ_{sl}^{exp} / -] measurements at the same temperature ((a) to (c)) and at the same load ((d) to (i)) for the three tested oils

increase in temperature due to the decrease in viscosity (Figure 7.10d to Figure 7.10i).

7.7. Stribeck Curves

As mentioned previously, the Stribeck curves show the evolution of the sliding coefficient of friction with a dimensionless parameter known as the modified Hersey parameter. The shape of the curve (see Figure 5.4) allows to clearly see the predominant regime of lubrication in a contact (boundary, mixed or full-film lubrication). It is important to mention that to obtain the Stribeck curves, only measurements at constant temperature are considered, and that the curves represented are obtained using the sliding coefficient of friction calculated with the optimized values of the parameters μ_{bl} and μ_{EHL} that are represented in section 7.8.

Observing the Stribeck curves obtained for the tests performed for every oil represented in Figure 7.11, it can be seen that at every tests performed the oils are either under boundary lubrication regime (lower speeds) or mixed lubrication regime (higher speeds). Under the tested conditions, full film lubrication is never achieved. In fact, in the only case where it could be expected to happen (the 75W140 oil at 4000 N and 70 °C) the predominant regime is mixed lubrication. For every test performed, the 75W140 is the oil that is always closest to achieve full film lubrication due to its higher viscosity and consequent higher film thickness. The other two oils, which are less viscous appear to be always under boundary lubrication (lower speeds) or in the beginning of mixed lubrication (higher speeds), except at the lower load and temperature conditions (Figure 7.11a).

Observing each tested conditions individually, it is observed that at lower temperatures (Figure 7.11a and Figure 7.11b) mixed lubrication is the predominant regime due to the oils higher film thickness, while at higher temperatures (Figure 7.11c and Figure 7.11d) boundary lubrication appears to exist at least up to 300 rpm (lower film thickness and possible metal to metal contact). At 110 °C (Figure 7.11e and Figure 7.11f), boundary lubrication is almost always present, with mixed lubrication only starting to be seen with rotational speeds above 900 rpm. This is because at this working temperature, the viscosity of the three tested oils is very low and metal to metal contact is inavoidable at any of the tested rotational speeds.

7.8. Boundary and EHL friction coefficients (μ_{bl} and μ_{EHL})

Using equations (7.1) and (7.2), it is possible, using a non-linear least squares fitting, to obtain the values of μ_{bl} and μ_{EHL} that minimize the error between the values of the sliding friction torque predicted by the SKF model (μ_{sl}) and the experimentally determined values (μ_{sl}^{exp}).

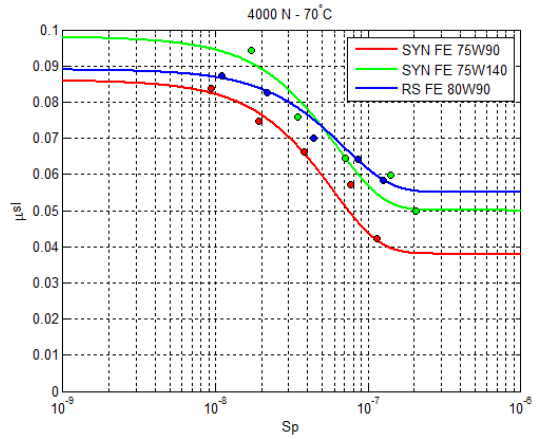

(a) 4000 N/70 °C

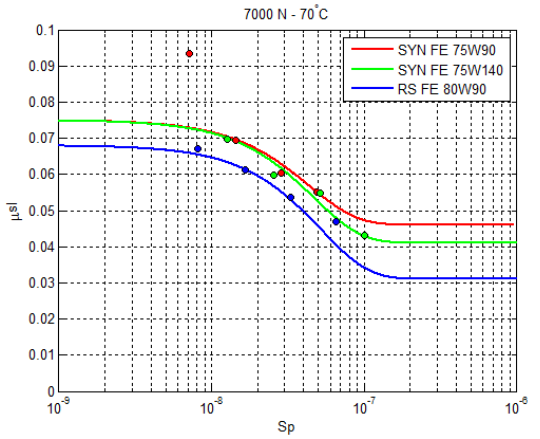

(b) 7000 N/70 °C

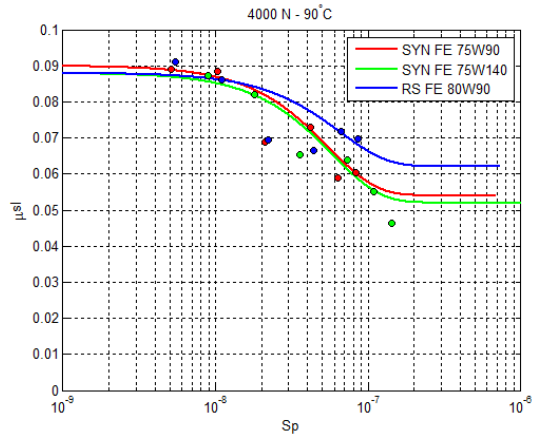

(c) 4000 N/90 °C

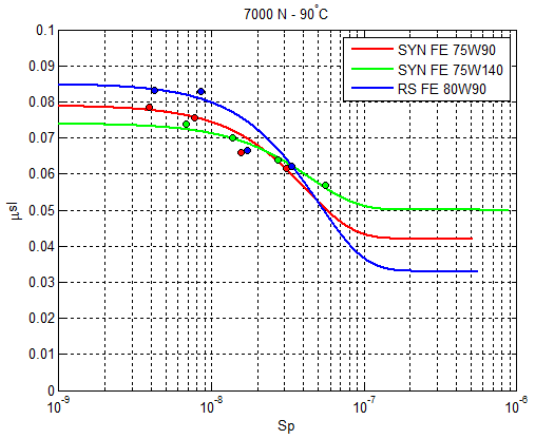

(d) 7000 N/90 °C

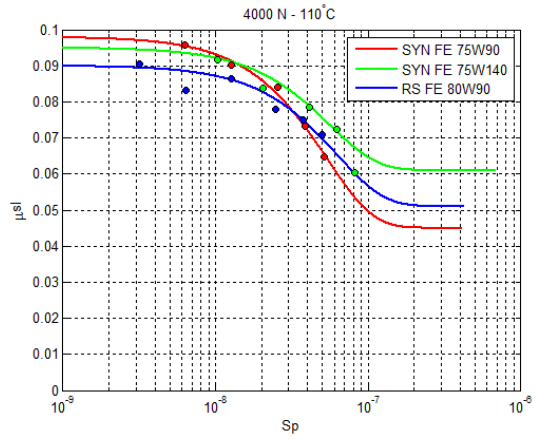

(e) 4000 N/110 °C

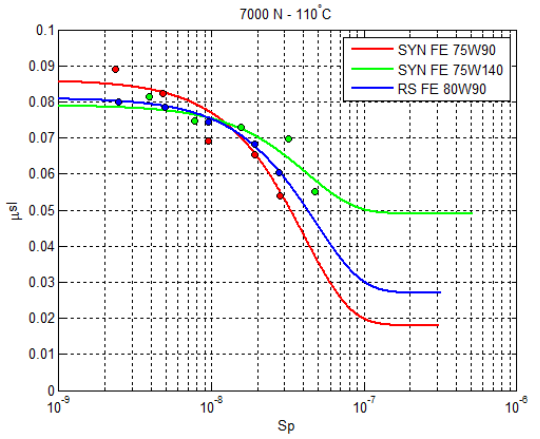

(f) 7000 N/110 °C

Figure 7.11.: Evolution of the sliding coefficient of friction [μ_{sl}^{exp} / -] with the Stribeck parameter calculated for the three tested oils in every tested conditions

Table 7.5.: Values of the coefficients μ_{bl} and μ_{EHL} for each tested oil in any testing conditions

	75W90 (PAO)		75W140 (PAO)		80W90 (MIN)	
	μ_{bl}	μ_{EHL}	μ_{bl}	μ_{EHL}	μ_{bl}	μ_{EHL}
4000 N/70 °C	0,086	0,038	0,098	0,050	0,089	0,055
4000 N/90 °C	0,090	0,054	0,088	0,052	0,088	0,062
4000 N/110 °C	0,098	0,045	0,095	0,061	0,090	0,051
7000 N/70 °C	0,075	0,046	0,075	0,041	0,068	0,031
7000 N/90 °C	0,079	0,042	0,074	0,050	0,085	0,033
7000 N/110 °C	0,086	0,018	0,079	0,049	0,081	0,027

$$\mu_{sl} = \phi_{bl} \cdot \mu_{bl} + (1 - \phi_{bl}) \cdot \mu_{EHL} \tag{7.2}$$

Apparently both the boundary and full film coefficients of friction depend on the oil formulation, as both the PAOs (75W90 and 75W140) present similar values, while the mineral oil (80W90) has different values of both coefficients with a 7000 N load and a 4000 N load.

Comparing tests made with different load conditions and the same temperature, it is possible to observe that in almost all cases, both the coefficients μ_{bl} and μ_{EHL} decrease with an increase in load. In fact, the degree of decrease of μ_{bl} is higher in the 75W90 and 75W140 oils, while the degree of decrease of μ_{EHL} is higher in the 80W90 oil. This may imply the influence of the oil's composition and nature on both parameters, and also additive activation due to load and temperature effects.

In the opposite case, when comparing tests with different temperatures and the same load for each oil, in almost all cases a similarity in the values of μ_{bl} is verified. So it is possible to conclude that under equal load conditions, the value of μ_{bl} is mainly influenced by each oil's composition and not its thermal properties. In some cases, the similarity in the values of μ_{EHL} is also verified, but is not as frequent as the similarity between values of μ_{bl} for the same load and different temperatures.

It is also important to notice that for the tested conditions, the values of μ_{bl} and μ_{EHL} are very different of the values proposed by SKF to use in the model (0,15 and 0,02 respectively), and the difference can be seen when comparing the originally predicted sliding friction coefficient with the value obtained using the new values of μ_{bl} and μ_{EHL}, as it is shown in Figure F.1, Figure F.2 and Figure F.3 in Appendix F. Figure 7.12 shows the optimization of the model for the 75W90 oil for every test performed. In Figure 7.13 is represented the predicted evolution of the friction torque, as well as the experimental friction torque, in the bearings for each oil and test using the calibrated values of μ_{bl} and μ_{EHL} in the SKF friction torque model.

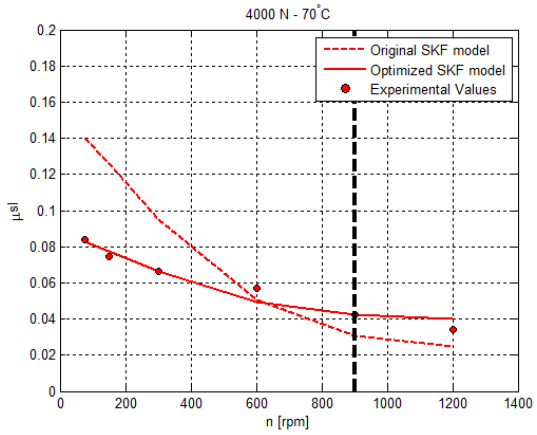

(a) 4000 N/70°C

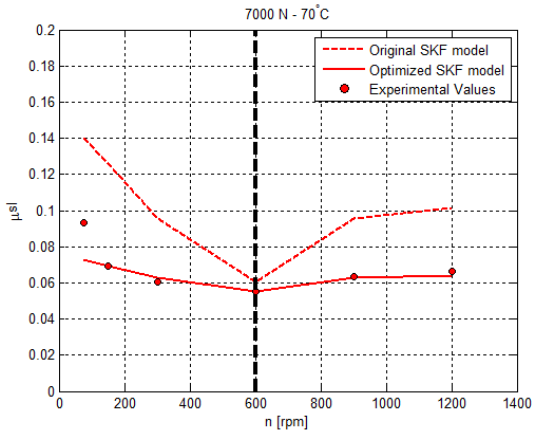

(b) 7000 N/70°C

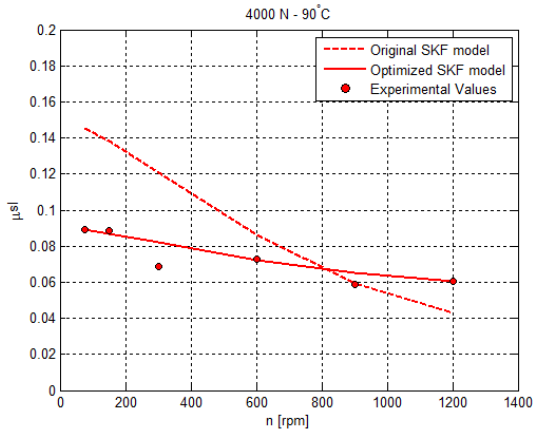

(c) 4000 N/90°C

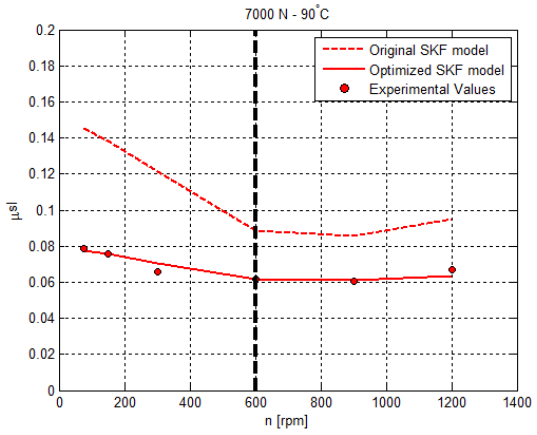

(d) 7000 N/90°C

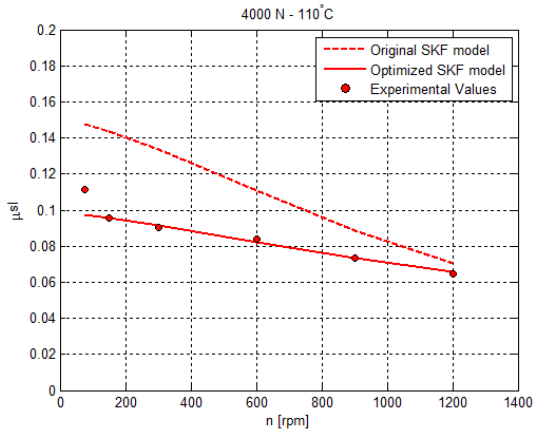

(e) 4000 N/110°C

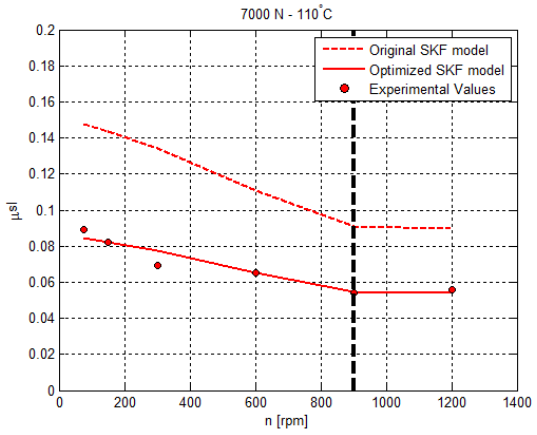

(f) 7000 N/110°C

Figure 7.12.: Comparison between the SKF original model and the calibrated model for the 75W90 oil in all tested conditions

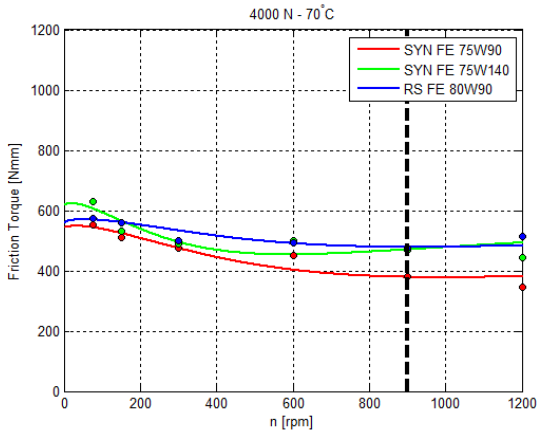

(a) 4000 N/70 °C

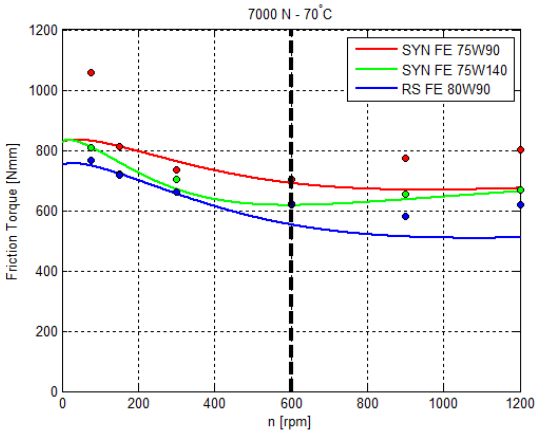

(b) 7000 N/70 °C

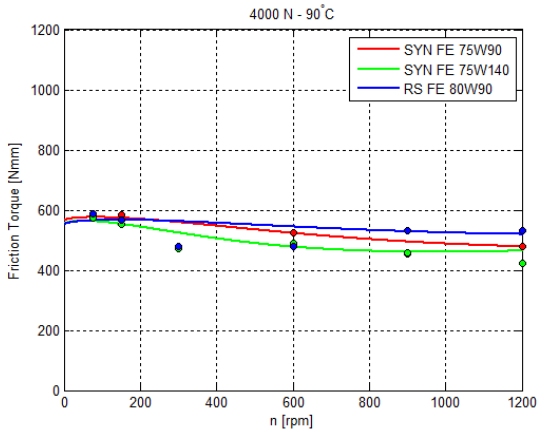

(c) 4000 N/90 °C

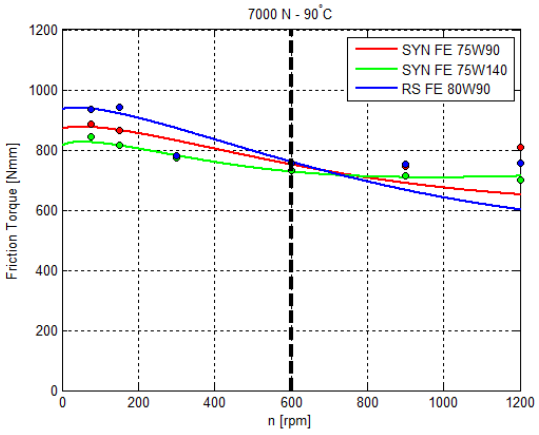

(d) 7000 N/90 °C

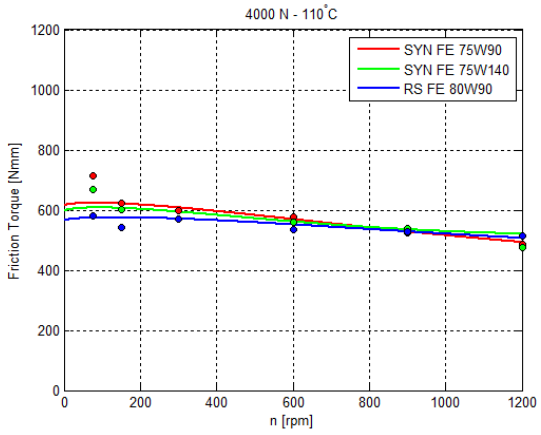

(e) 4000 N/110 °C

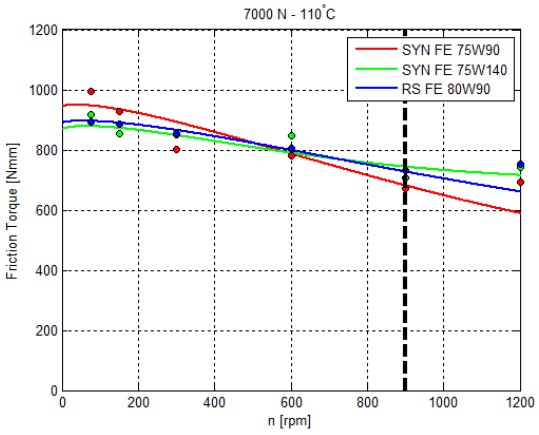

(f) 7000 N/110 °C

Figure 7.13.: Evolution of the total friction torque [M_t^{exp} / Nmm] obtained using the SKF calibrated model for each oil in every tested condition

7.9. Free Temperature Measurements

To simulate the behaviour of the lubricants at real cold start-up conditions, a battery of tests where the temperature was not set to a pre-determined value was performed and called free temperature measurements.

Measurements were made with a 7000 N load at the first three rotational speeds tested with constant temperature (75, 150 and 300 rpm) since at 600 rpm a slight increase in temperature was already observed in the three oils when the operating temperature was 70 °C.

Under free temperature measurements, the first thing noticeable is that for the three oils, the stabilization temperatures for each rotational speed are very similar (temperature differences inferior to 1 °C comparing the three oils - Table 7.6).

Comparing the values of the measured friction torque, it is observed that at these rotational speeds, the 75W140 and 80W90 oil have lower values than the 75W90 oil, mainly due to the difference in the calculated specific film thickness (Figure 7.14e). Consequently, the sliding coefficient of friction is obviously higher in the 75W90 oil than in the other two oils.

Other observation possible to be made is the fact that the value of the specific film thickness doesn't suffer significant changes when changing the rotational speed from 150 rpm to 300 rpm, so the three oils have the tendency to maintain their value of the specific film thickness as the temperature increases with the rotational speed.

In free temperature tests, it doesn't make sense to obtain the Stribeck curves since by definition it shows the evolution of the coefficient of friction in steady state conditions (constant temperature). Calculating the modified Hersey parameter for each rotational speed, it is verified that with the increase in temperature for the three oils, the Stribeck parameter increases when increasing the rotational speed as shown in Table 7.7.

Table 7.6.: Stabilization temperatures at the first three rotational speeds for the three tested oils

	75W90 (PAO)	75W140 (PAO)	80W90 (MIN)
75 rpm	31,5 °C	31,8 °C	31,6 °C
150 rpm	37,8 °C	37,5 °C	38,1 °C
300 rpm	50,8 °C	50,5 °C	50,0 °C

Table 7.7.: Modified Hersey Parameter obtained at the first three rotational speeds for the three tested oils at free temperature measurements

	75W90 (PAO)	75W140 (PAO)	80W90 (MIN)
75 rpm	$3,70 \times 10^{-8}$	$7,08 \times 10^{-8}$	$5,21 \times 10^{-8}$
150 rpm	$5,41 \times 10^{-8}$	$1,05 \times 10^{-7}$	$7,24 \times 10^{-8}$
300 rpm	$6,09 \times 10^{-8}$	$1,16 \times 10^{-7}$	$7,86 \times 10^{-8}$

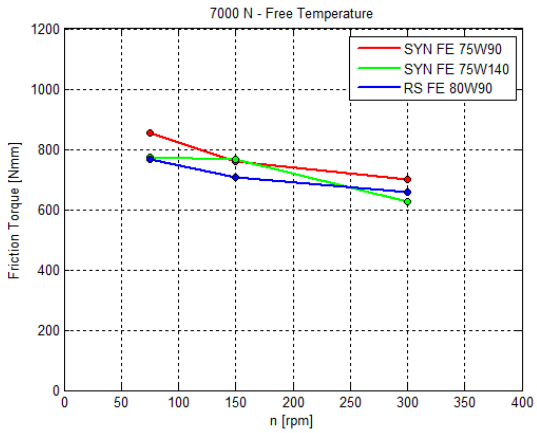

(a) Total Friction Torque

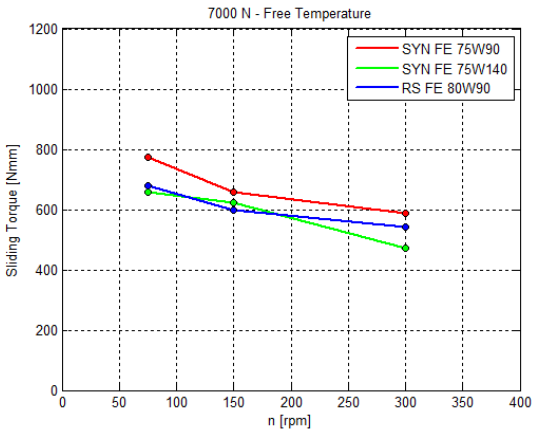

(b) Sliding Friction Torque

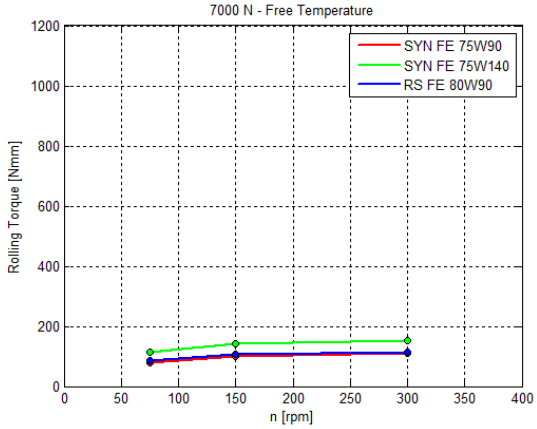

(c) Rolling Friction Torque

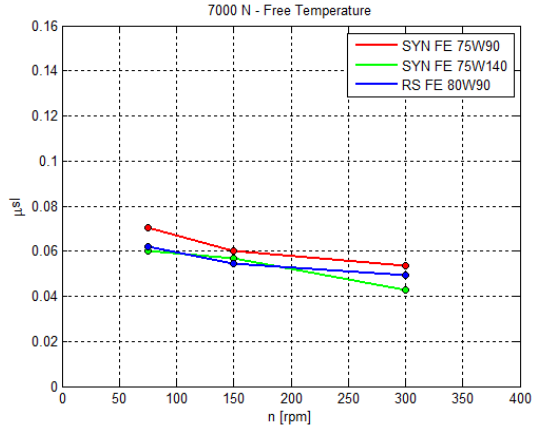

(d) Sliding coefficient of friction

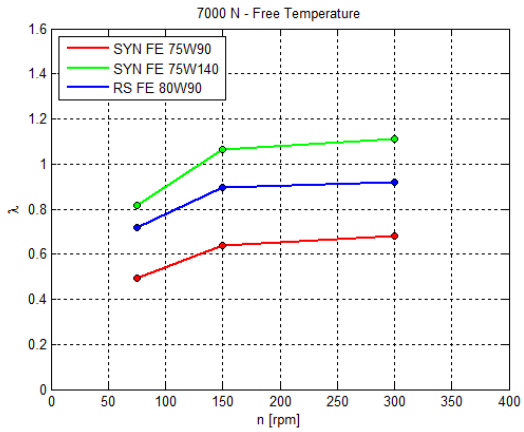

(e) Specific Film Thickness

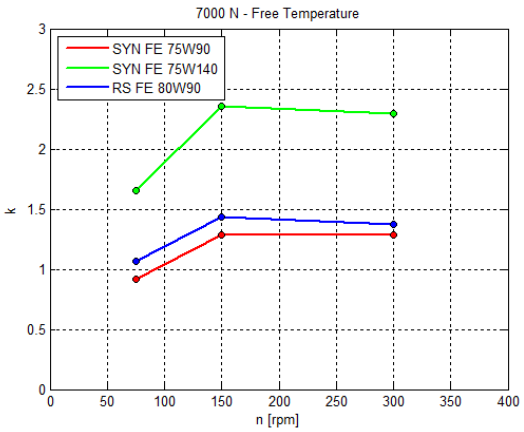

(f) Viscosity Ratio

Figure 7.14.: Total friction torque (a), sliding torque (b), rolling torque (c), sliding coefficient of friction (d), specific film thickness (e) and viscosity ratio (f) calculated for the three oils under free temperature measurement conditions

8. Conclusions and Future Work

8.1. Conclusions

8.1.1. Conclusions based on experimental evidence

- The preliminary oil analysis confirmed the values on the data sheets provided by the manufacturers, verified that the three oils present a newtonian behaviour at the tested shear rates and showed no signs of significant contamination of the oils;

- Ball-on-disc tests confirmed the expected order of the oils in terms of film thickness;

- Ball-on-disc tests provided information on the values of the traction coefficient for each oil under several testing conditions. It was concluded that the values of the traction coefficient under full-film conditions are high, given that the oils are labeled as "fuel-economy" oils;

- In all friction torque measurement tests at constant temperature, it is verified that all of them perform under boundary and mixed lubrication regimes;

- Increasing the rotational speed and maintaining constant temperature and load conditions, it is verified that the friction torque decreases with the increase in rotational speed. Also, as expected, the friction torque increases when increasing the load or the temperature;

- With a 4000 N load, the measured friction torque is very similar in the three tested oils at lower rotational speeds. For rotational speeds higher than 600 rpm, the oil's properties (viscosity at the working temperature and specific film thickness) and nature (being mineral or synthetic combined with the additive composition) define the evolution of torque loss with the increase in rotational speed;

- With a 7000 N load, the 75W140 oil generally presents the lowest values of measured friction torque due to its higher viscosity. The 75W90 oil has lower values of friction torque than the 80W90 oil at 90 °C and 110 °C, suggesting that the 80W90 oil suffers larger increases in friction torque with the increase in temperature.

8.1.2. Conclusions based on numerical results

- As expected, the 75W140 oil has the highest values of specific film thickness in any test performed;
- Generally, the 75W90 oil has lower values of measured friction torque even though the specific film thickness is always lower than the 80W90 oil;
- Sliding coefficient of friction calculations confirm that the 75W140 oil generally has the better behaviour at the tested conditions due to its higher viscosity. Comparing the 75W90 with the 80W90 oil, it is verified that when operating in the same lubrication regime, the 75W90 oil generally presents lower values of the sliding coefficient of friction due to the base oil properties;
- The model proposed by Fernandes *et al.* used to calibrate the values of μ_{bl} and μ_{EHL} increased greatly the accuracy of the SKF model;
- The calculated values of μ_{bl} and μ_{EHL} generally decrease when increasing the load, and have similar values for a constant load and different temperatures;
- Synthetic oils have similar values of μ_{bl} and μ_{EHL} in the same tested conditions.

8.2. Future Work

Further studies regarding this theme include:

- Repeating the rolling bearing tests in order to confirm the accuracy of the friction torque measurements;
- Performing longer tests (wear tests) at a constant temperature to analyse the degradation of the oils, changes in the mass of the bearings and bearing failures;
- Measuring the friction torque with different types of bearings (tapered-roller bearings) at the same conditions performed in the work of this thesis;
- Performing free temperature tests at higher input speeds.

Overall, the aim of this thesis was to verify the effect of different axle gear oils in terms of viscosity and formulation in the power loss of cylindrical thrust roller bearings.

In the end, it was possible to analyse the most efficient oil for different loads, temperatures and rotational speeds and discuss whether the rheological properties of the oils or their composition are more influent in each operating condition.

Bibliography

[1] K. Holmberg, P. Andersson, and A. Erdemir, "Global energy consumption due to friction in passenger cars," *Tribology International*, vol. 47, pp. 221–234, 2012.

[2] F. Joachim, J. Börner, and N. Kurz, "How to minimize power losses in transmissions, axles and steering systems," *Gear Technology*, pp. 58–66, 2012.

[3] H. Heisler, *Advanced Vehicle Technology*. Butterworth-Heinemann, 2002.

[4] H. Naunheimer, B. Bertsche, J. Ryborz, and W. Novak, *Automotive Transmissions*. Springer, 2011.

[5] T. Garrett, K. Newton, and W. Steeds, *The Motor Vehicle*. Butterworth-Heinemann, 2001.

[6] J. Erjaveck, *Manual Transmissions*. Thomson - Delmar Learning, 2004.

[7] D. Spindler and G. Von Petery, "Angular contact ball bearings for a rear axle differential," tech. rep., SOCIETY OF AUTOMOTIVE ENGINEERS. Warrendale (PA US), 2003. SAE Technical paper series.

[8] P. Willermet and L. Dixon, "Fuel economy- contribution of the rear axle lubricant," tech. rep., SOCIETY OF AUTOMOTIVE ENGINEERS. Warrendale (PA US), 1977. SAE Technical paper series.

[9] G. E. Totten, *Handbook of Lubrication and Tribology - Volume I - Application and Maintenance*. CRC Press, 2006.

[10] B. M. O'Connor, L. F. Schiemann, and R. I. Johnson, "Axle efficiency - response to synthetic lubricant components," tech. rep., SOCIETY OF AUTOMOTIVE ENGINEERS. Warrendale (PA US), 1982. SAE Technical paper series.

[11] D. A. Law and C. N. Rowe, "The design of fuel efficient automotive hypoid gear lubricants," *Journal of Synthetic Lubrication*, vol. 11, pp. 3–15, 1993.

[12] R. F. Watts and G. I. Willette, "Newtonian multigrade gear lubricants: formulation and performance testing," tech. rep., SOCIETY OF AUTOMOTIVE ENGINEERS. Warrendale (PA US), 1982. SAE Technical paper series.

[13] V. Bala, G. Brandt, and D. K. Walters, "Fuel economy of multigrade gear lubricants," *Industrial Lubrication and Tribology*, vol. 52, pp. 165–173, 2000.

[14] M. Devlin, J. Senn, M. Sturtz, and V. Bala, "Improved understanding of axle oil rheology effects on torque transfer efficiency and axle oil operating temperature," tech. rep., SOCIETY OF AUTOMOTIVE ENGINEERS. Warrendale (PA US), 2003. SAE Technical paper series.

[15] B. J. Hamrock, S. R. Schmid, and B. O. Jacobson, *Fundamentals of Fluid Film Lubrication.* CRC Press, 2004.

[16] T. Mang and W. Dresel, eds., *Lubricants and Lubrication.* Wiley and Sons, 2007.

[17] G. W. Stachoviak and A. W. Batchelor, *Engineering Tribology.* Butterworth-Heinemann, 2001.

[18] E. W. Dean and G. H. B. Davis, "Viscosity variation of oils and temperature," *Chemical and Metallurgical Engineering*, vol. 36, pp. 618–619, 1929.

[19] ASTM International, West Conshohocken, PA, *ASTM Standard D2270: Standard Practice for Calculating Viscosity Index from Kinematic Viscosity at 40 and* 100°*C*, 1993.

[20] E. E. Klaus and B. Y. C. So, "Viscosity-pressure correlations of liquids," *Tribology Transactions*, vol. 23, pp. 409–421, 1980.

[21] P. W. Gold, A. Schmidt, H. Dicke, J. Loos, and C. Assmann, "Viscosity-pressure-temperature behaviour of mineral and synthetic oils," *Journal of Synthetic Lubrication*, vol. 18, pp. 51–79, 2001.

[22] B. J. Hamrock and D. Dowson, *Ball Bearing Lubrication.* John Wiley and Sons, 1981.

[23] P. K. Gupta, H. S. Cheng, D. Zhu, N. H. Forster, and J. B. Schrand, "Viscoelastic effects in mil-l-7808-type lubricant, part i: Analytical formulation," *Tribology Transactions*, vol. 35 (2), pp. 269–274, 1992.

[24] J. A. Brandão, M. Meheux, F. Ville, J. Seabra, and M. J. Castro, "Traction curves and rheological parameters of fully formulated gear oils," *Proceedings of the Institution of Mechanical Engineers, Part J: Journal of Engineering Tribology*, vol. 225, pp. 577–593, 2011.

[25] J. A. Brandão, *Gear tooth flank damage prediction using high-cycle fatigue and wear models.* PhD thesis, Faculdade de Engenharia da Universidade do Porto, 2013.

[26] A. N. Grubin, *Fundamentals of the Hydrodynamic Theory of Lubrication of Heavily Loaded Cylindrical Surfaces.* Central Scientific Institute for Technology and Mechanical Engineering, Moscow, 1949.

[27] D. Dowson and G. R. Higginson, *Elastohydrodynamic Lubrication.* Pergamon Press Ltd., 1966.

[28] A. W. Crook, "Elastohydrodynamic lubrication of rollers," *Nature*, vol. 190, p. 1182, 1961.

[29] A. Cameron and R. Gohar, "Optical measurement of oil film thickness under elastohydrodynamic lubrication," *Nature*, vol. 200, pp. 458–459, 1963.

[30] A. Harnoy, *Bearing Design in Machinery: Engineering Tribology and Lubrication.* CRC Press, 2002.

[31] R. Gohar, *Elastohydrodynamics.* Imperial College Press, 2001.

[32] T. E. Tallian, "On competing failure modes in rolling contact," *ASLE Transactions*, vol. 10 (4), pp. 418–439, 1967.

[33] J. Seabra, A. Campos, and A. Sottomayor, *Lubrificação Elastohidrodinâmica.* 2002.

[34] M. D. Hersey, *Theory and Research in Lubrication.* John Wiley and Sons, 1966.

[35] B.-R. Höhn, K. Michaelis, and M. Hinterstoiβer, "Optimization of gearbox efficiency," *goriva i maziva*, vol. 48 (4), pp. 441–480, 2009.

[36] *SKF General Catalogue.* SKF, 2003.

[37] C. Fernandes, *Power Loss in Rolling Bearings and Gears Lubricated with Wind Turbine Gear Oils.* PhD thesis, Faculdade de Engenharia da Universidade do Porto, 2015.

[38] C. Fernandes, P. Marques, R. Martins, and J. Seabra, "Gearbox power loss. part i: Losses in rolling bearings," *Tribology International*, vol. 88, pp. 298–308, in press.

[39] International Organization for Standardization, *ISO 281: Rolling bearings - Dynamic load ratings and rating life*, 2007.

[40] T. Cousseau, B. Graça, A. Campos, and J. Seabra, "Experimental measuring procedure for the friction torque in rolling bearings," *Lubrication Science*, vol. 22, pp. 133–147, 2010.

[41] A. S. Kolekar, A. V. Olver, A. E. Sworski, and F. E. Lockwood, "The efficiency of a hypoid axle - a thermally coupled lubrication model," *Tribology International*, vol. 59, pp. 203–209, March 2013.

[42] H. Matsuyama, H. Dodoro, K. Ogino, H. Ohshima, and K. Toda, "Development of super-low friction torque tapered roller bearing for improved fuel efficiency," tech. rep., SOCIETY OF AUTOMOTIVE ENGINEERS. Warrendale (PA US), 2004. SAE Technical paper series.

Part IV.

Appendix

A. Lubricants

A.1. Introduction

The main function of a lubricant is to control the friction and wear between two surfaces in order to facilitate the relative motion between them. Theoretically speaking, any substance that managed to perform this function could be considered as a lubricant, however, there are other requirements that need to be fulfilled.

Technological development in mechanical components needs to be closely followed by an improvement in lubricant properties in order to maintain proper functioning of a given system. Besides controlling friction and wear in a contact, a lubricant is required to work at high temperatures, evacuate the heat generated in the contact, minimize corrosion and being able to mix with other substances, i.e., the additives that improve the lubricant's characteristics.

Another crucial parameter is the lubricant's resistance to degradation, because the performance of the lubricant in the initial stage of application needs to be maintaned during its lifetime, otherwise it may cause damage and corrosion to the components being lubricated.

Besides the demands related to the performance of the lubricant and the system where its applied, there are also social and economical factors that influence the choice of a certain lubricant, such as its impact in the environment (toxicity, biodegradability), and the costs associated with the application (mainly when large quantities of lubricant are used).

In summary, lubricants must meet a compromise when used, because they must be viscous enough to maintain the lubricant film necessary at certain operating conditions while being fluid enough to be able to remove heat and avoid power losses due to viscous drag. Adding this to the lubricant's ability to maintain its quality during the expected lifetime and avoid corrosive behaviour, it becomes clear how hard it is to select a proper lubricant for a given application.

The information of this chapter is based on literature about the topic in analysis [15] [16] [17].

A.2. Types of Lubricants

In the following paragraphs it will be described the four major types of lubricants in the market: liquid lubricants, greases, solid lubricants and gaseous lubricants. Liquid

lubricants will be described in finer detail as they are the type of lubricants which will be used in the experimental work that will be described in further chapters.

A.2.1. Liquid Lubricants (Oils)

Oils are the most commonly used type of lubricant, and their typical composition is 95% base and 5% additives. They can be classified according to its origin as vegetable oils, animal oils, mineral oils or synthetic oils.

Vegetable and Animal Oils

These oils were the first to be used for lubrication purposes, before the development of the industry and crude exploration. In comparison with mineral oils, vegetable and animal oils have some advantages such as an higher viscosity index, a lower evaporation rate and quicker biodegradability. However these oils also have low resistance to high temperatures and oxidize easily. Therefore, with the increasing demands on lubricating properties, being the ability to withstand higher temperatures a crucial one, these oils were progressively replaced with mineral and synthetic oils.

Nevertheless, these oils are still used and are even being given more importance due to its environmental impact. In northern european countries these oils are heavily used in industry, and they are also used in applications where the risk of contamination must be minimal, e.g., the food and the pharmaceutical industries.

Mineral Oils

Mineral oils are the most commonly used oils and they are typically applied in situations where the temperature is considered moderate (e.g., gears, bearings, engines, turbines, etc.). These oils have its origins in crude oil from different exploration sites all over the world. For this reason, there are considerable differences in the physical properties of the oils depending on the location in which the raw material (crude) was extracted from. A mineral oil is characterized by the source of the crude and the refining process used to make the oil.

Due to the large amount of sources of crude oil, the classification of mineral oils will be based upon the predominant molecular structure present in the oil (which is directly related with the location of the extraction). Mineral oils are mainly constituted by hydrocarbons, and the difference is centered in the chemical forms of the hydrocarbons. Therefore it is possible to divide mineral oils into three main groups: paraffinic basis, naphthenic basis and aromatic basis.

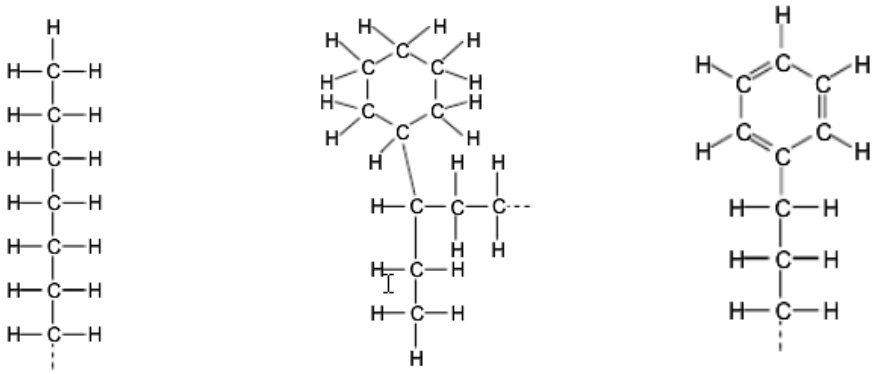

(a) Paraffinic Basis (b) Naphthenic Basis (c) Aromatic Basis

Figure A.1.: Types of Basis

Paraffinic Basis

Paraffinic basis are the most commonly found in lubricant oils, because they can operate over a wide range of temperatures. Its molecular structure consists of long hydrocarbon chains. Their most important properties include:

- low density
- low freezing point
- excellent resistance to degradation
- high viscosity index (near 100)
- wide range of fire and flash points

This type of basis are not agressive towards elastomers used in sealing expansion joints. However, the high molecular weight of certain chains can cause the crystallization of the oil at room temperature. They also contain some wax.

Naphthenic Basis

Naphthenic basis are mainly used in applications in which temperature variations are very small, and its molecular structure consists of hydrocarbon rings, so they are often referred to as "cycloparaffinic". Their most important properties include:

- high density
- high freezing point
- little resistance to degradation

- low viscosity index (near 50)
- wide range of fire and flash points

Other properties of this type of oils include good miscibility, high volatility, low pour point and they are agressive towards elastomers used in sealing expansion joints. They contain little wax.

Aromatic Basis

The aromatic basis represents a small portion of mineral oils and are often considered undesirable. Its molecular structure consists of hydrocarbon rings, but with some double links between carbon atoms (naphthenic basis' hydrocarbons only have a single link between carbon atoms).

There are also mineral oils that are a mixture of paraffinic and naphthenic basis, and are widely used because they have a low cost and combine different properties from both basis such as:

- broad range of viscosities
- low volatility
- high resistance to degradation
- allow protection against corrosion

Synthetic Oils

Synthetic oils are artificially made oils, developed to manufacture lubricants with better properties than mineral oils, and therefore used in cases where mineral oils are unsuitable. Mineral oils have some defects, such as oxidation and viscosity loss at high temperatures, combustion in the presence of some oxidizing agents and solidification at low temperatures. These defects are prohibitive in some applications, more specifically in gas turbine engines where there is a need to withstand very high temperatures and ocasionally very low temperatures. Other cases where synthetic oils are preferred include:

- vacuum pumps and jet engines (low pressure lubricant)
- food and pharmaceutical industry (low toxicity lubricant)

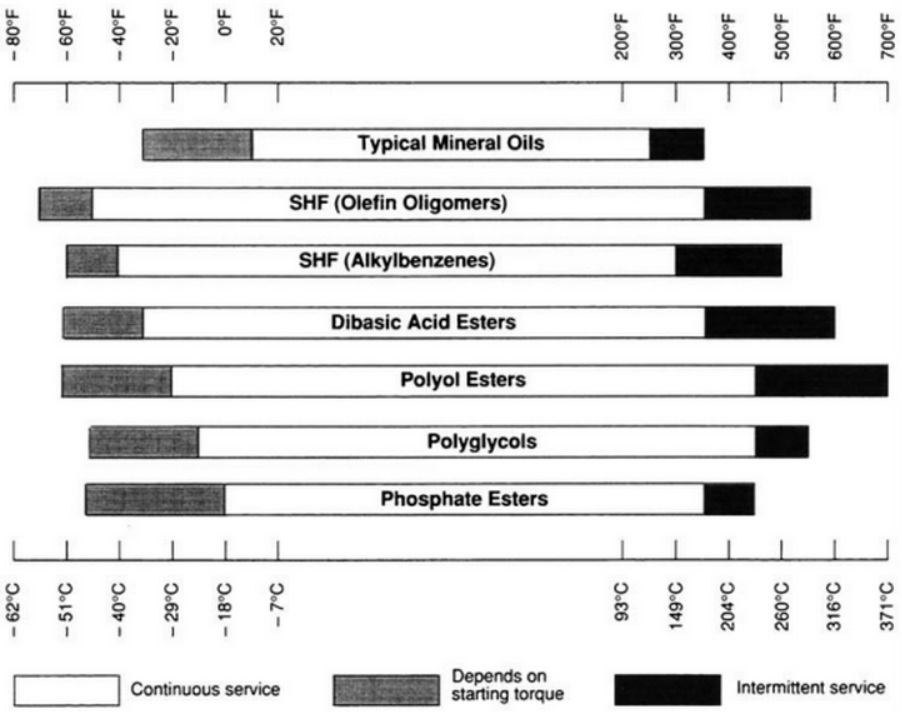

Figure A.2.: Working temperatures of mineral oils and some synthetic oils

- high performance gas turbines (thermically stable and not inflamable lubricant)

Synthetic oils are obtained from hydrocarbons or its chemical elements, and can have as its basis petroleum derived products, vegetable oils and others. In the majority of cases, synthetic oils are obtained from petroleum derived products and other components are added to obtain the desired properties. The process required to make a synthetic oil, generally traduces in it being more expensive than a mineral oil, but it will have better properties and therefore, a bigger life capability which may justify the cost. Synthetic oils can be divided in several groups, but only four will be highlighted in this text as being considered the most important:

Synthetic Hydrocarbons

Synthetic hydrocarbons are mainly constituted with carbon and hydrogen compounds, and include the Poly-alpha-olefins (PAOs) and the benzenes. Some of its most important characteristics are obtained due to the ability to control the molecular weight in a specific range, and therefore control properties that depend on molecular weight. Some of the characteristics of synthetic hydrocarbons include:

- high viscosity index (they can work at a broad range of temperatures)
- good thermal stability

- compatibility with seals (may be a disadvantage if swelling is required)
- miscible with mineral oils
- excellent behaviour at low temperatures

PAO based lubricants are the most common synthetic hydrocarbons, and are vastly used in automotive and industrial applications because they have a lower coefficient of friction and a higher resistance to oxidation than mineral oils. This translates in higher energetic efficiency and longer drain intervals. Other applications for these oils include the food and pharmaceutical industries.

Polyglycols

The polyglycols are the most widely used synthetic oils, as they are available in a wide range of viscosities. Its main characteristic is the low coefficient of friction, which makes it attractive to use in gears with high values of specific sliding (worm-gears). Other characteristics of polyglycols are:

- good response to additives
- high flash point
- high viscosity index
- low pour point
- generally compatible with seals (depending on the temperature)
- high volatility under extreme thermal and oxidative environments
- poor protection against corrosion
- solvent action on nonresistant paints
- not miscible with mineral oils

The applications in which polyglycols are used are distinguished depending on the polyglycol being water-soluble or not.

Water-soluble polyglycols are utilized in hydraulic brake fluids, metalworking lubricants, fire-resistant hydraulic fluids and water-diluted lubricants for rubber bearings and joints. Water-insoluble polyglycols are used as heat transfer fluids and as high temperature gear and bearing lubricants.

Esters

Esters are a type of synthetic oils which are produced by reactions of alcohols with acids. There is a great variety of esters, and as such, physical and chemical characteristics are particular to each is ester. General characteristics of esters include:

- high thermal resistance and excellent behaviour at low temperatures
- biodegradability
- low coefficient of friction (depending on the ester)

The most commonly used esters are diesters, whose use is limited to type I jet engines oils (older), automotive engine oils and air compressor lubricants, and polyol esters which are used in type II jet engine oils, air compressor oils and refrigeration lubricants.

Silicones

Silicones are synthetic oils with a polymeric structure, in which the carbon atoms in its structure are replaced with silicon ones. Their main characteristics are:

- high viscosity index (300 or more)
- low pour point and good low temperature fluidity
- chemically inert and non-toxic
- fire resistant and water repellent
- low surface tension (they spread on metallic surfaces)
- poor response to additives that minimize friction

Some of its applications include being the base fluid in greases appliable for a broad range of temperatures, and being utilized in hydraulic fluids for brakes, liquid springs and torsional dampers.

Semi-Synthetic Oils

Semi-Synthetic oils are basically a mixture of a mineral oil with a synthetic oil. These oils may not confer properties as good as fully synthetic oils, but they have the advantage of being cheaper and suitable for the required application where the use of a synthetic oil would provide similar benefits.

A.2.2. Greases

According to the American Society for Testing and Materials (ASTM), a grease is defined as "A solid to semifluidproduct of dispersion of a thickening agent in a liquid lubricant. Other ingredients imparting special properties may be included".

The consistency of a grease is described as colloidal or a gel, therefore they are used in situations where it is inviable (technically and economically) to maintain a continuous feed of oil, and protection against corrosion and contaminants is required. Greases are, for example, used in caterpillar track assemblies and agricultural machinery because they have contacts which are impossible to access. The major inconvenient associated with greases is the inability to cool and clean the mechanism as a continuous flow of oil would.

The vast majority of greases includes soap (Aluminum, Barium, Calcium, Lithium, Sodium and Strontium) as its thickener. Other thickeners include organic clays, polyureas and inorganic compounds.

A.2.3. Solid Lubricants

A solid lubricant is a film of solid material, constituted by organic or inorganic compounds, which is used between the surfaces where lubrication is required. This type of lubricants is used when the surfaces in contact must be completely separated, and at the same time friction between the surfaces must be reduced. Solid lubricants can be distinguished as inorganic or organic.

Inorganic Solid Lubricants

- Gelatinous Solids (graphite, molybdenium disulphide)
- Soft Solid Mixtures (lead, calcium oxide, talc, silver iodide, lead monoxide)
- Coatings produced by chemical reaction with the surface (chlorides, oxides, phosphates, oxalates, sulfides)

Organic Solid Lubricants

- Soaps, Waxes and Fats (metallic soaps of calcium, sodium and lithium, bee wax, fat acids)
- Polymeric Films (PTFE - polymeric films have high resistance to environmental agressive effects)

A.2.4. Gaseous Lubricants

Gaseous lubricants' analysis is in many ways similar to liquid lubricants' analysis as the principles of hydrodinamic lubrication can be applied to both. The biggest difference between gaseous and liquid lubricants is that gaseosus lubricants' viscosity increases by increasing the temperature, and the opposite occurs with liquid lubricants. Gaseous lubricants' viscosity is generally much lower than liquid lubricants' viscosity, and the compressibility is much higher. This means that load capacity and film thickness are lower when using a gaseous lubricant. Viscosity variation with temperature and pressure is much lower in gaseous lubricants than in liquid ones.

A.3. Additives

Additives are chemicals which are added to lubricant oils in order to increase their lubricating properties, add new properties that the oil didn't originally have and improve the durability. The use of additives has been employed since the 1920s and nowadays every lubricant oil contains at least one additive (additive percentage in an oil may go up to 30%). The most common additives available for use are:

A.3.1. Additives to improve the viscosity index

These additives basically increase the oil's viscosity at high temperatures and/or decrease the oil's viscosity at low temperatures. The most common ocorrence is a significant increase of viscosity at high temperatures and a minimal increase of viscosity at low temperatures (for a low viscosity oil).

Additives of this type include butane polymers, methacrylic acid esters and fatty alcohols, and are mainly applied in engine oils, gearbox fluids and hydraulic systems.

A.3.2. Anti Wear (AW) and Extreme Pressure (EP) additives

These additives are used to decrease friction and wear in extreme lubricating conditions, and can be separated as:

- Adsorption additives - they are used to decrease the friction coefficient in limit lubricating conditions, and therefore prevent the slip-stick phenomena. These additives are usually fatty oils and are used in automatic gearboxes.

- Anti Wear additives - they increase wear-preventing properties of lubricants by forming a protective film from reaction with the surfaces in contact. Fatty oils, organic compounds and zinc compounds are commonly used as additives for oils present in automotive engines, pillow blocks and industrial gears.

- Extreme Pressure additives - these additives prevent the adhesion of the surfaces in contact with relative sliding when subjected to extreme loads or velocities, by chemically reacting with the surfaces and forming a protective coating at high pressures. This coating prevents the ocorrence of galling phenoms and surface deterioration. These additives are constituted by sulphurous, phosphorous or chloride compounds and are used in oils for gears that can have contact pressure between teeth of over 700 MPa.

A.3.3. Antioxidants

Antioxidants' function is to avoid or retard the reaction of the lubricants with the oxygen, as oxidation promotes the increase in the oils' viscosity and acidity, making them corrosive towards some metals. Commonly used additives of this type include sulphur and phosphorus compounds.

A.3.4. Detergents

Also known as dispersants, their main function is to control the contamination in the oil. This control is essential in engine oils which are regularly exposed to combustion products, oil-water emulsions and acids, and it will slow down the processes of corrosion and wear in the engine, and prevent the formation of viscous deposits in the engine. These additives can be distinguished as mild dispersants (simple hydrocarbons and ashless compounds) and over-based dispersants (calcium, zinc and barium salts of sulphonic, phenol or salicylic acids).

A.3.5. Corrosion inhibitors

Corrosion inhibitors prevent corrosion phenoms in pillow blocks and can be considered as an antioxidant additive.

A.3.6. Rust inhibitors

These additives react with metallic surfaces and create a coating that stops water from reaching the metallic surface. Despite being appliable to any type of lubricating oil, one must be aware that these additives may cause corrosion in non-ferrous surfaces and originate water emulsions, which are prejudicial effects. Some of these additives include acid esters, phosphorous and metallic soaps.

A.3.7. Foam inhibitors

These additives are used in very small quantities (0,05% to 0,5%) and they avoid the formation of foam in the oil when subjected to turbulence in high speed machinery. The most used additive of this type is a silicone polymer.

A.3.8. Pour Point depressants

These additives are applied to lower the pour point in paraffinic oils (naphthenic oils don't require them since the pour point is already low). They are generally polymers with high molecular weight.

B. Physical Properties of Lubricants

In the previous chapter it was observed that when describing a particular lubricant, each one had a particular assembly of properties that made him suitable or not for a certain application. In this chapter the basic properties of a lubricant will be described.

B.1. Viscosity

The viscosity of a fluid is defined as the resistance offered by the fluid to the sliding of its molecules over each other. It is a very important parameter in lubrication since each oil as a specific viscosity, which varies with the temperature, pressure and shear rate, and it is directly related to the film thickness.

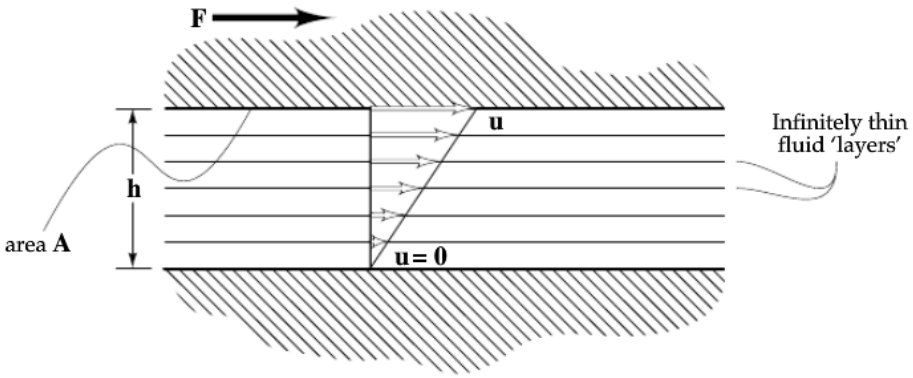

Figure B.1.: Laminar flux of a fluid between two surfaces

It is easily observed in Figure B.1 that the velocity is different in any point along the vertical line given by h. Assuming y as the vertical axis, it can be said that for an height $y + dy$ the corresponding velocity is $u + du$. So, the shear stress τ is given by:

$$\tau = \sigma_{xy} = \eta \cdot \frac{du}{dy} \tag{B.1}$$

The parameter η in the equation is a proportionality constant characteristic of each fluid and represents the dynamic viscosity. The existance of this constant which represents the relation between shear stress and shear rate (gradient of velocity) is experimentally verified for newtonian fluids (water, oils at laminar flux). For non-newtonian fluids, this proportional relation doesn't exist. The SI unit that represents dynamic viscosity is [Pa·s].

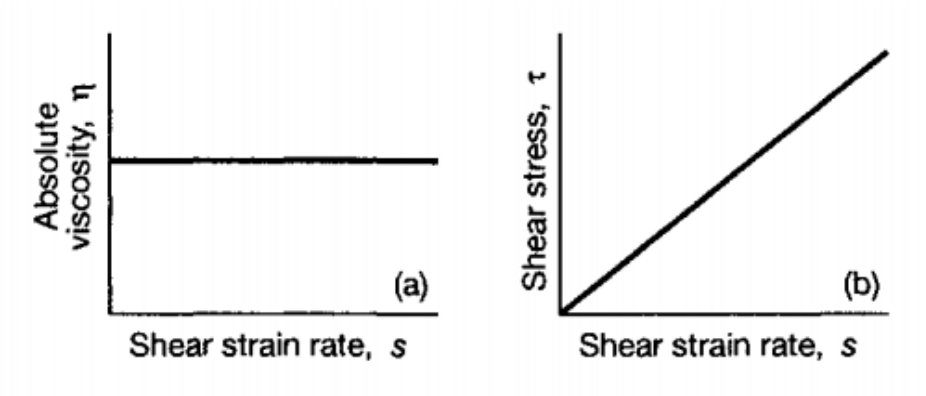

Figure B.2.: Variation of dynamic viscosity (a) and shear stress (b) with the shear rate for a newtonian fluid

Dynamic viscosity is applied mainly in calculations which are used in elastohydrodinamic lubrication of bearings and gears. However, for the characterization of a lubricant it is preferred to use the kinematic viscosity, which represents a relation between the dynamic viscosity and the density (ρ) of a fluid. Also, it is easier to determine experimentally kinematic viscosity with very good precision. The relationship between kinematic viscosity ν and dynamic viscosity η is given by:

$$\nu = \frac{\eta}{\rho} \tag{B.2}$$

Kinematic viscosity is represented in SI units as [m^2/s] but the most commonly used unit for describing a lubricant's viscosity is the centistoke [cSt] which is equal to [mm^2/s].

To measure the viscosity of a fluid experimentally, two major types of viscometers can be used: absolute viscometers and empirical viscometers. The difference between them is in if the viscosity can be determined directly from an equation (absolute viscometers) or not (empirical viscometers).

Table B.1.: Different types of viscometers

Viscometers	
Absolute	Empirical
Capillary	Engler (Europe)
Couette's	Saybolt (USA)
Disc and Conic	Redwood (UK)

B.1.1. Viscosity variation with the temperature

In fluids, the viscosity depends a lot on the temperature, and the degree of change in viscosity is different for every fluid. If the work temperature is increased, the viscosity of mineral and synthetic oils will decrease (sometimes dramatically). To measure the degree of change in viscosity with the temperature, the viscosity index (VI) is used.

Viscosity Index

The viscosity index was developed by Dean and Davis [18] in 1929 to characterize the viscosity variation with temperature in different oils. The method used to develop this concept, was to measure the kinematic viscosity of every oil known at that time at 210 °F (approximately 100 °C).

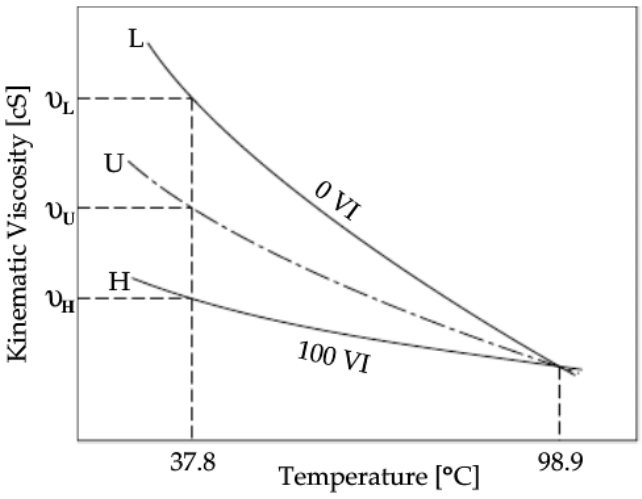

Figure B.3.: Viscosity Index definition

Comparing all the oils with the same viscosity at 210 °F they chose as reference the

oils with the highest and lowest viscosities at 100 °F (approximately 40 °C). To the oil with highest viscosity variation was attributed $VI = 0$ (viscosity at 40 °C - L), and to the oil with the lowest viscosity variation was attributed $VI = 100$ (viscosity at 40 °C - H). For intermediate oils, knowing the viscosity at 40 °C (U), it's possible to calculate the viscosity index with the formula:

$$VI = 100 \cdot \left(\frac{L - U}{L - H} \right) \tag{B.3}$$

Viscosity indexes close to 0 represent typically naphthenic oils (bigger variations of viscosity), while viscosity indexes near 100 are characteristic of paraffinic oils (smaller variations of viscosity). It is important to mention that Equation B.3 is, according to the ASTM D2270 Standard [19], only valid for oils with a viscosity index between 0 and 100. For oils with a viscosity index greater than 100 it is used:

$$VI = \frac{10^N - 1}{0,00715} + 100 \tag{B.4}$$

$$N = \frac{log(H) - log(U)}{log(Y)} \tag{B.5}$$

Where Y is the kinematic viscosity of the oil whose viscosity index will be calculated at 100 °C. The values of L and H are given in the ASTM D2270 Standard for a wide range of viscosities.

However, the viscosity index is not enough to characterize the behaviour of an oil's viscosity with the temperature as it is dependant on the reference oils used (two oils with the same viscosity index will most likely have different viscosity variations with the temperature). Therefore the concept of thermoviscosity needs to be introduced.

Thermoviscosity

Thermoviscosity represents the variation of the viscosity of an oil with the temperature. There are various equations that can express this variation and in this chapter three will be represented:

- Cameron's Equation:

$$\nu_1 = \nu_0 \cdot e^{(-\beta \Delta \theta)} \tag{B.6}$$

  - ν_1 - kinematic viscosity at a tested temperature θ_1
  - ν_0 - kinematic viscosity at a reference temperature θ_0

- β - thermoviscosity's coefficient
- $\Delta\theta$ - lubricant's temperature variation $(\theta_1 - \theta_0)$

Despite being simple, Equation B.6 is only valid for small temperature variations.

- ASTM D341 Standard:

$$log(log(\nu + a)) = n - m \cdot log(T) \tag{B.7}$$

  - ν - kinematic viscosity [cSt]
  - T - temperature [K]
  - n, m, a - lubricant constants

Assuming $a = 0,7$ it is possible to calculate the parameters m and n knowing the viscosities at two different temperatures (usually 40 °C and 100 °C).

- Vogel's Law:

$$\nu = K \cdot e^{(\frac{b}{\theta + c})} \tag{B.8}$$

  - ν - kinematic viscosity at a temperature θ
  - θ - temperature [°C]
  - K, b, c - lubricant constants

Knowing the viscosities for three given temperatures, it is possible to calculate the parameters K, b, and c for an oil.

Using the ASTM D341 Standard or Vogel's Law, it is possible to obtain with great precision the values of the thermoviscosity's coefficient for any given temperature of an oil, with the knowledge that this coefficient is defined as the first derivative in order to the temperature of a viscosity. Translating this to an equation it is possible to obtain:

$$\frac{d\nu}{d\theta} = \beta \cdot \nu \iff \frac{1}{\nu} \cdot \left(\frac{d\nu}{d\theta}\right) = \beta \tag{B.9}$$

Applying this equality it is possible to obtain the thermoviscosity's coefficient for any temperature using Equation B.7 or Equation B.8.

B.1.2. Viscosity variation with pressure

The viscosity of the majority of lubricants increases with pressure. In fact, if the working pressure is considerably bigger than the atmospheric pressure, the viscosity is more altered by this parameter than temperature or shear stress. This concept is important in contacts between gears or bearings where pressure can achieve values of $10^9 Pa$. The variation of viscosity with the pressure is exponential and it is given by Barus' Law for moderate pressures (close to atmospheric):

- Barus' Law:

$$\eta_s = \eta_0 \cdot e^{(\alpha p)} \tag{B.10}$$

  - η_s - dynamic viscosity at the intended pressure p [Pa·s]
  - η_0 - dynamic viscosity at $p = 0$ [Pa·s]
  - α - piezoviscosity's coefficient [Pa^{-1}]

The piezoviscosity's coefficient is a parameter that depends on the lubricant and the temperature. Various equations have been developed to determine this coefficient (Klaus and So equation [20], Gold's equation [21]). However, only Gold's equation will be presented due to its accuracy and simplicity:

- Gold's Equation:

$$\alpha = s \cdot \nu^t \cdot 10^{-9} \tag{B.11}$$

  - α - piezoviscosity's coefficient [Pa^{-1}]
  - ν - kinematic viscosity at a given temperature [cSt]
  - s, t - constants depending on the type of lubricant

Table B.2.: s and t constants for each lubricant type

Type of Oil		Mineral	PAO	Ester
0,2 GPa	s	9,904	7,382	6,605
	t	0,1390	0,1335	0,1360
0,6 GPa	s	8,097	7,008	5,897
	t	0,1534	0,0984	0,1173

As mentioned before, Barus' equation only works for pressures close to the atmospheric pressure. For pressure values above 0,5 GPa or high temperatures, this equation becomes unsuitable for some calculations. Despite being adequate to calculate the film

thickness using Reynolds' equation, its use is improper when calculating shear stress and the friccion coefficient inside a contact.

To evaluate the viscosity of a lubricant taking into account the effects of both temperature and pressure, there is an equation proposed by Roelands which is of great utility in computational applications.

- Roelands' Equation:

$$\eta_R = \eta_0 \cdot e^{(\alpha^* \cdot p)} \tag{B.12}$$

  - η_R - dynamic viscosity at the intended pressure p and lubricant temperature [Pa·s]
  - η_0 - dynamic viscosity at atmpospheric pressure $p = 0$ [Pa·s]
  - α^* - Roelands' piezoviscosity's coefficient [Pa^{-1}]

Where:

$$\alpha^* \cdot p = [ln(\eta_0) + 9,67]\left(\left(\frac{T - 138}{T_0 - 138}\right)^{-S_0} \cdot (1 + 5,1 \cdot 10^{-9} p)^Z - 1\right) \tag{B.13}$$

In Equation B.13 T represents the film temperature [K], T_0 is the reference temperature [K], p is the film pressure [Pa] and S_0 and Z are Roelands' constants (for each oil) for temperature and pressure respectively. These constants are independent of temperature and pressure (are only dependent of the lubricant).

B.1.3. Viscosity variation with the shear rate

Fluids can be classified as Newtonian fluids if the viscosity remains constant with the shear rate, or Non-Newtonian fluids if the viscosity changes with the shear rate. Oils usually present the behaviour of a Newtonian fluid, but when subjected to shear rates usually higher than 10^6 s^{-1} they start to behave like a Non-Newtonian fluid.

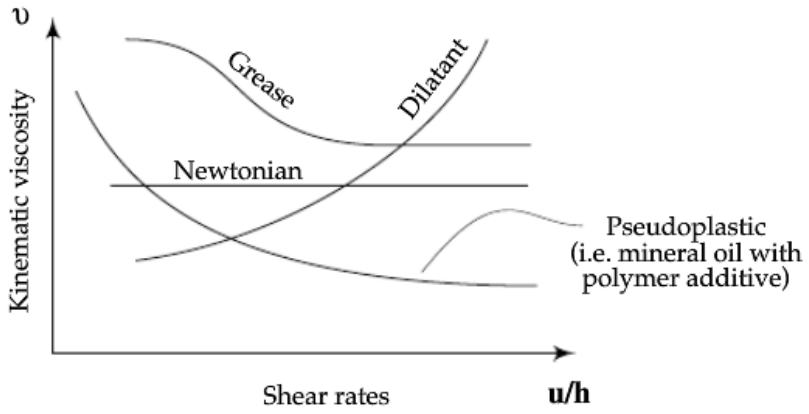

Figure B.4.: Viscosity variation with the shear rate for Newtonian and Non-Newtonian fluids

For Non-Newtonian fluids it is necessary to develop models that explain their behaviour with temperature, pressure and shear rate, as the relation between shear stress and shear rate is not linear.

B.2. Density

Density is defined as the quocient between the mass of a body over its volume. Despite the density of a fluid changing with the temperature, the change is so small that is considered insignificant. However, with pressure the density may suffer significant alterations, specially if we consider that elastohydrodinamic films can be subjected to extremely high pressures.

A concept that is linked with density is the concept of specific gravity, which represents the ratio between the lubricant's and water's density.

B.3. Thermal Properties

It's important to know the thermal properties of a lubricant, in order to find the amount of heat it will be able to dissipate in operating conditions and the temperature the contact surfaces will be able to withstand. These properties are of great importance in bearing design.

The most important thermal properties of a lubricant are:

- Specific Heat [J/kg·K] - it's the ratio of the amount of heat required to raise the temperature of a unit mass of a substance by one unit of temperature to the

amount of heat required to raise the temperature of the same mass of a reference material(water) by the same amount.

- Thermal Conductivity [W/m·K] - it's the heat energy transferred per unit of time and surface area due to a unitary temperature gradient. It measures the ability of a material to allow the flow of heat from the warmer surface to the colder surface.
- Thermal Diffusivity [m^2/s] - it's the ratio between the thermal conductivity, and the product of specific heat with the density. It transmits the ability of a substance to provoke a change in temperature.

C. Oil Data Sheets

TRANSMISSION SYN FE 75W-90

HIGH PERFORMANCE SYNTHETIC OIL FOR GEARS

APPLICATIONS

- High performance synthetic oil developed for synchronised or non-synchronised manual gearboxes, axles and reduction gears.

PROPERTIES

- Very high viscosity index
- increased extreme pressure and antiwear properties for an optimized lubrication of hypoid and non hypoid axles
- excellent antifoam, anticorrosion, antitrust properties
- excellent thermal stability
- very low loss in viscosity through shear
- driving comfort
- excellent stability in service
- compatible with most types of synchronizers for an optimized lubrication of manual gearboxes

CHARACTERISTICS

TRANSMISSION SYN FE	Unités	Grade SAE **75W-90**
Volumetric mass at 15°C	kg/m^3	866
Viscosity àt 40°C / àt 100°C	mm²/s	101 / 15
Viscosity Index	-	157
Dynamic viscosity at - 40°C	mPa.s	66 000
Pour point	°C	-51
Flash point	°C	190

Les valeurs des caractéristiques figurant dans ce tableau sont des valeurs typiques données à titre indicatif

SPÉCIFICATIONS

DAF (first fill)
MB-Approval 235.8
MAN 341 type E3, M3, Z2
SCANIA STO 1:0
VOLVO 97312
ZF TE-ML 02B, 05B, 12B, 16F, 17B, 19C, 21 B
SAE J2360 *(n°PRI GL 0432)*

Satisfies performance requirements of :
API GL-4
API GL-5
API MT-1
MIL-PRF-2105E

TOTAL LUBRIFIANTS
562 Avenue du Parc de l'île
92029 NANTERRE Cedex
FRANCE

TRANSMISSION SYN FE 75W-90
Updated : 05/2014
Référence étiquette : MPR/11/06

TRANSELF SYN FE 75W-140

Fully synthetic lubricant for heavily loaded gearboxes and axles.

APPLICATIONS

- For lubricating mechanical gearboxes and axles differentials in the most heavily loaded conditions.
- TRANSELF SYN FE 75W-90 is particularly recommended when looking for greater ease of gear-shifting in cold weather as well as satisfactory gearbox operation when hot.

APPROVALS

Specifications	API GL-5
Meets the requirements of	SCANIA : STO 1.0 (gearboxes, high mileage) RENAULT : approval on OT1 Axle (Trafic 1st generation): n° 7711229320

PERFORMANCES AND CUSTOMER BENEFITS

Super multigrade

Extended drain interval

Fuel saving

- Extreme-pressure and anti-wear properties enabling gearboxes or axles to function under the most severe conditions.
- High resistance to degradation, ensuring stable performance after prolonged use at high temperature.
- Outstanding anti-rust and anticorrosion properties even in the presence of water.
- Very high viscosity index and low pour point ensuring perfect lubrication at all temperatures.
- Good shear stability.
- Inert to seals even at high temperatures..
- Very high anti-foaming power thus guaranteeing a resistant lubricating film even at high speeds.
- Very good filterability allowing the lubrication of devices (gearboxes or axles) fitted with oil filters..

PHYSICAL AND CHEMICAL CHARACTERISTICS

TRANSELF SYN FE 75W-140		Method	Value
Density at 15°C	--	ASTM D1298	885
Kinematic Viscosity at 40°C	mm^2/s	ASTM D445	183
Kinematic Viscosity at 100°C	mm^2/s	ASTM D445	26.3
Viscosity Index	-	ASTM D2270	178
Pour Point	°C	ASTM D97	-36

The features mentioned above are average values obtained with some variability in production and do not constitute a specification.

TOTAL LUBRIFIANTS
562 avenue du Parc de l'Ile
92029 Nanterre
FRANCE

TRANSMISSION RS FE 80W-90

SEMI-SYNTHETIC OIL FOR GEARBOXES AND AXLES


APPLICATIONS

- Semi-synthetic oil with a high viscosity index for the lubrication of gears under severe conditions of use.
- Designed to meet the challenge of the T.D.L. (Total Drive Line) concept: high performance lubrication of hypoid axles as well as synchronized gearboxes, to simplify maintenance without any compromise on components durability.
- Is recommended for use on manual gearboxes, rear axles, or any gear assembly requiring API GL-4, API GL-5, API MT-1 or SAE J2360 levels of performance
- Allows extended service intervals up to 160 000 km on ZF axles and gearboxes (without Intarder), and more generally on all commercial vehicles hypoid axles.
- Suitable for use on Scania gearboxes

PROPERTIES

- Very good low temperature fluidity due to a high viscosity index, generating benefits during cold starts and limiting drag losses and fuel consumption.
- Very high extreme-pressure performance for optimal protection of gears and bearings against scoring and scuffing.
- Excellent antiwear, anticorrosion and antirust properties for the durability of components including gearbox synchronizers.
- Semi synthetic formulation, very resistant to oxidation and allowing extended drain intervals (up to 160 000 kms) compared to standard mineral.

CHARACTERISTICS

TRANSMISSION RS FE	Units	Grade SAE **80W-90**
Volumetric mass at 15°C	kg/m^3	886
Viscosity at 40°C	mm²/s	115
Viscosity at 100°C	mm²/s	14,1
Viscosity Index	-	123
Pour point	°C	- 33

The typical characteristics mentioned represent mean values.

SPECIFICATIONS

MAN 341 TYPE E2, Z2
MAN 342 TYPE M2
ZF TE-ML 02B, 05A, 16B, 17B, 19B, 21A

Meets the performance requirements of the following international specifications :
API GL-4
API GL-5
API MT-1
MIL-PRF-2105E / SAE J2360

TOTAL LUBRIFIANTS
16, rue de la République
92800 PUTEAUX

D. Analytical Ferrography

D.1. 75W90

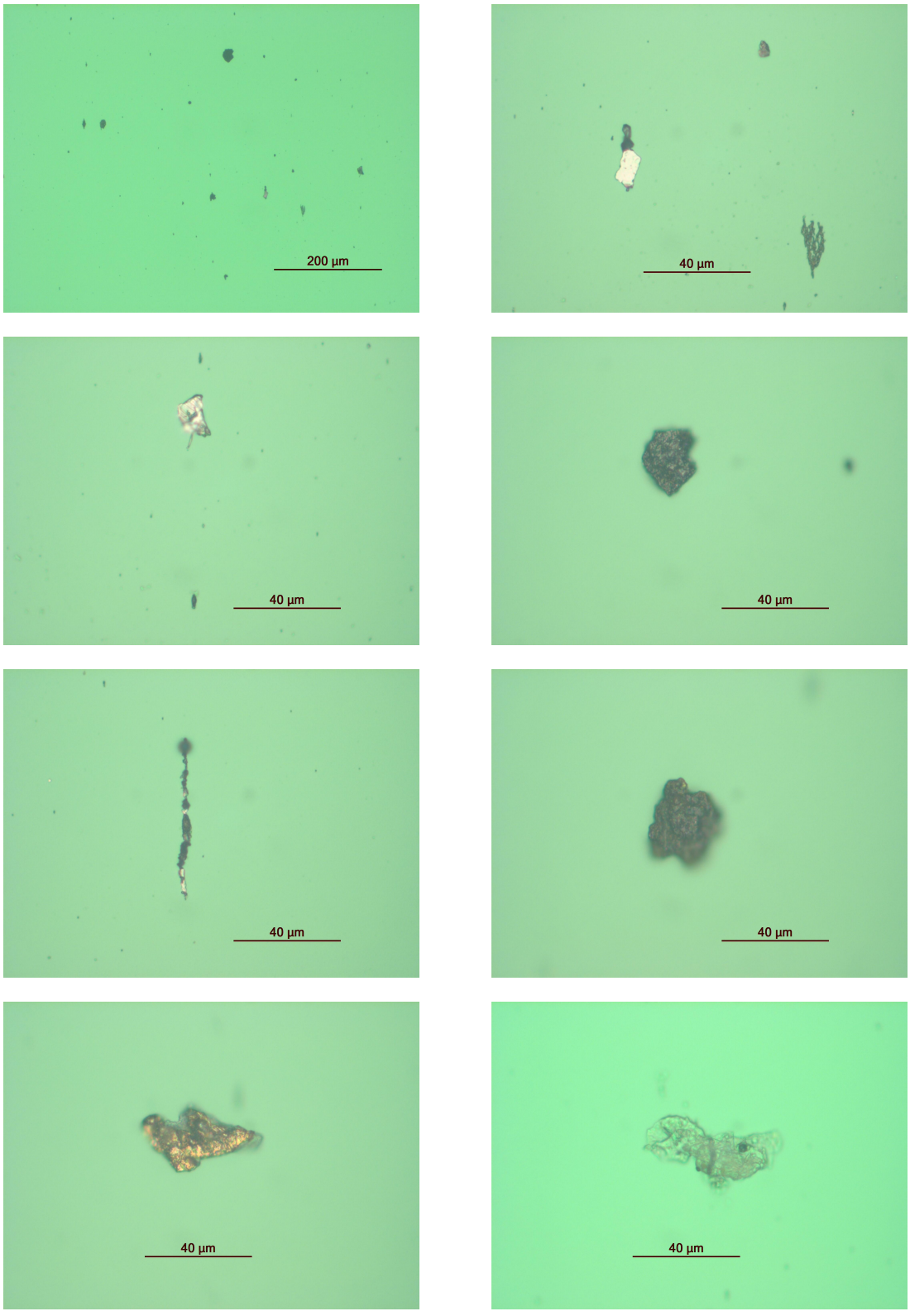

Figure D.1.: Analytical ferrography of a sample of 75W90 oil before being used

D.2. 75W140

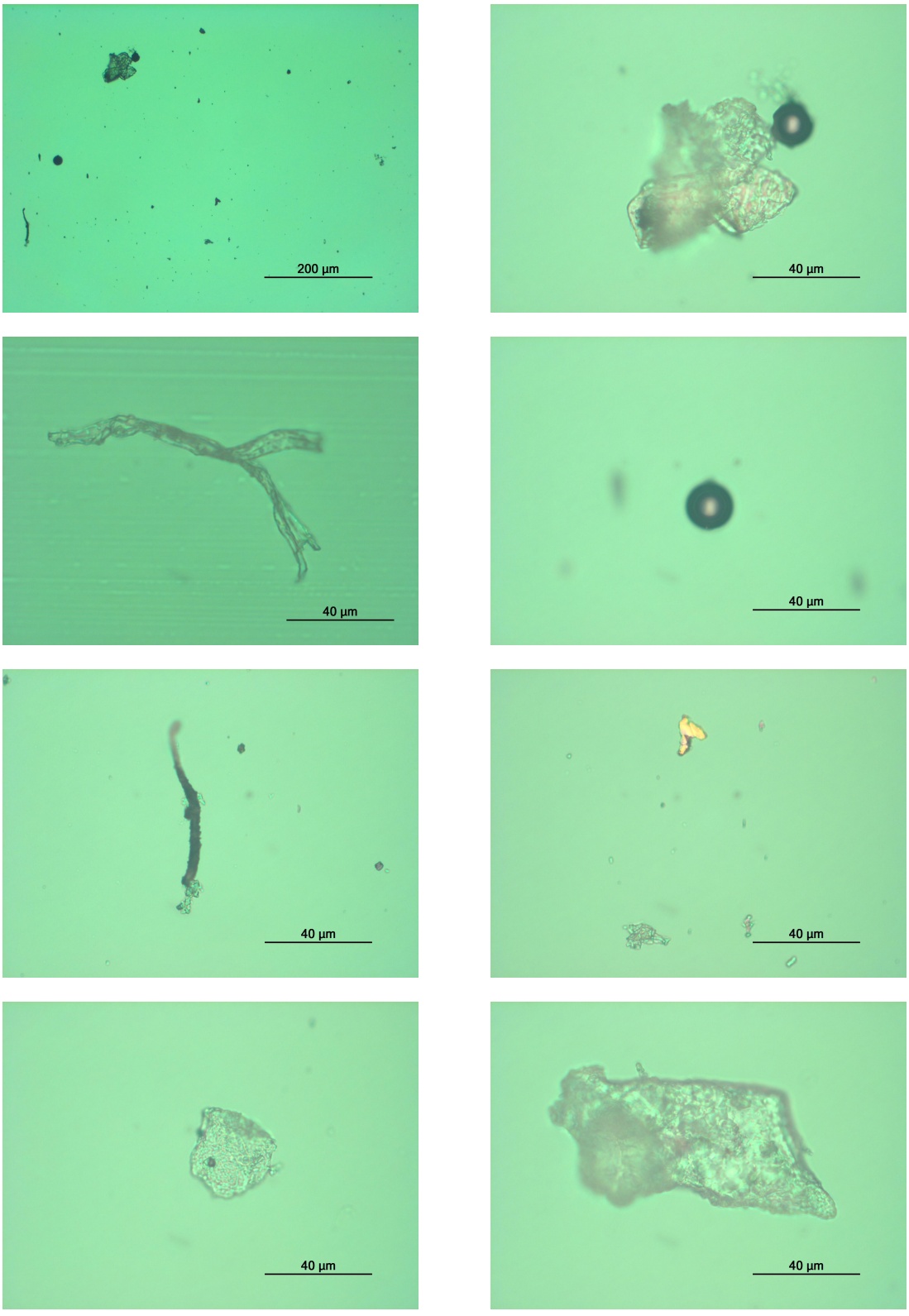

Figure D.2.: Analytical ferrography of a sample of 75W140 oil before being used

D.3. 80W90

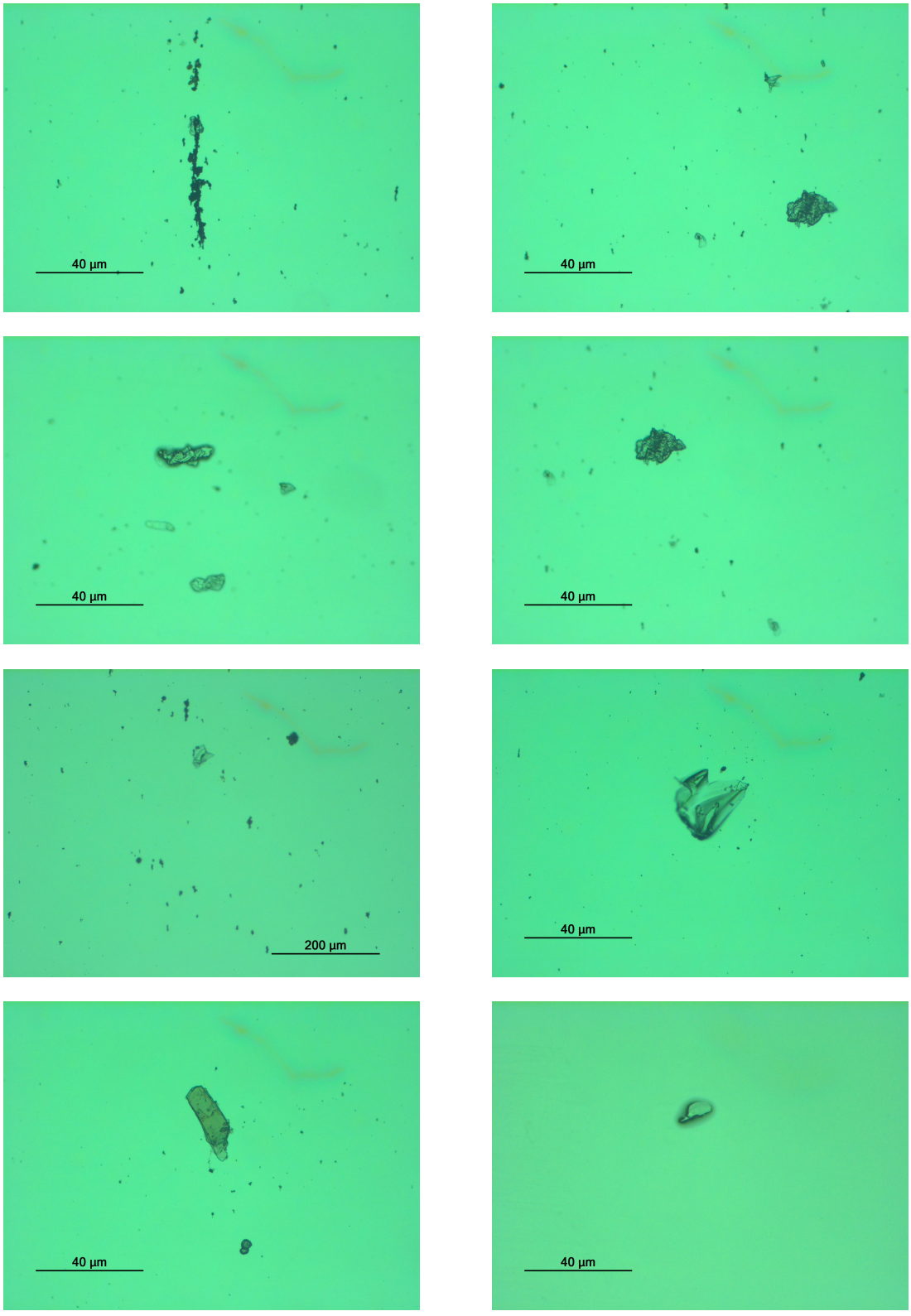

Figure D.3.: Analytical ferrography of a sample of 80W90 oil before being used

E. Appendix to the SKF Model

E.1. Rolling Friction Torque Calculation

$R_1 = 2,25 \cdot 10^{-6}$ (constant given for cylindrical roller thrust bearings)

$K_{rs} = 3,00 \cdot 10^{-8}$ (starvation constant for low level oil bath)

$K_z = 4,4$ (constant given for cylindrical roller thrust bearings)

$$\phi_{ish} = \frac{1}{1 + 1,84 \cdot 10^{-9} \cdot (n \cdot d_m)^{1,28} \cdot \nu^{0,64}}$$

$$\phi_{rs} = \frac{1}{e^{\left[K_{rs} \cdot \nu \cdot n \cdot (d+D) \cdot \sqrt{\frac{K_Z}{2(D-d)}}\right]}}$$

$$G_{rr} = R_1 \cdot d_m^{2,38} \cdot F_a^{0,31}$$

$$M_{rr} = \phi_{ish} \cdot \phi_{rs} \cdot G_{rr} \cdot (\nu \cdot n)^{0,6}$$

E.2. Sliding Friction Torque Calculation

$S_1 = 0,154$ (constant given for cylindrical roller thrust bearings)

$$G_{sl} = S_1 \cdot d_m^{0,62} \cdot F_a$$

$$\phi_{bl} = \frac{1}{e^{[2,6 \cdot 10^{-8} \cdot (n \cdot \nu)^{1,4} \cdot d_m]}}$$

$$M_{sl} = M_{exp} - M_{rr}$$

E.3. Seals Friction Torque

$$M_{seal} = K_{S1} \cdot d_s^{\beta} + K_{S2}$$

This equation would only be only applied if the bearing had seals. K_{S1}, β and K_{S2} are constants that depend on the type and size of seals and bearings.

E.4. Drag Losses

Due to the small size of the bearings that are used in the experimental procedure, drag losses can be disregarded as they present values almost null when compared with the friction torque measured on the four-ball machine. For cylindrical thrust roller bearings, drag losses can be expressed as:

$$M_{drag} = 4 \cdot V_M \cdot K_{roll} \cdot C_w \cdot B \cdot d_m^4 \cdot n^2 + 1,093 \cdot 10^{-7} \cdot n^2 \cdot d_m^3 \cdot \left(\frac{n \cdot d_m^2 \cdot f_t}{\nu}\right)^{-1,379} \cdot R_s$$

$$K_{roll} = \left(\frac{K_L \cdot K_Z \cdot (D+d)}{D-d}\right) \cdot 10^{-12}$$

$$C_w = 2,789 \cdot 10^{-10} \cdot l_D^3 - 2,786 \cdot 10^{-4} \cdot l_D^2 + 0,0195 \cdot l_D + 0,6439$$

$$l_D = 5 \cdot \left(\frac{K_L \cdot B}{d_m}\right)$$

$$f_t = \sin(0,5 \cdot t), (0 \leq t \leq \pi) / f_t = 1, (\pi < t < 2 \cdot \pi)$$

$$R_s = 0,36 \cdot d_m^2 \cdot (t - \sin(t)) \cdot f_A$$

$$t = 2 \cdot \arccos\left(\frac{0,6 \cdot d_m - H}{0,6 \cdot d_m}\right)$$

$$f_A = 0,05 \cdot \left(\frac{K_Z \cdot (D+d)}{D-d}\right)$$

$K_L = 0,43$ (constant given for cylindrical roller thrust bearings)

$K_Z = 4,4$ (constant given for cylindrical roller thrust bearings)

E.5. Sliding Friction Coefficient Calculation

$$\mu_{sl} = \frac{M_{sl}}{G_{sl}}$$

$$\mu_{sl} = \phi_{bl} \cdot \mu_{bl} + (1 - \phi_{bl}) \cdot \mu_{EHL}$$

E.6. Viscosity Ratio Calculation

Table E.1.: Rated viscosity of the lubricant obtained knowing the bearing's mean diameter

Rotational Speed [rpm]	ν_1 [cSt]
75	187,5
150	100
300	59,4
600	34,3
900	21,4
1200	17,7

$$k = \frac{\nu}{\nu_1}$$

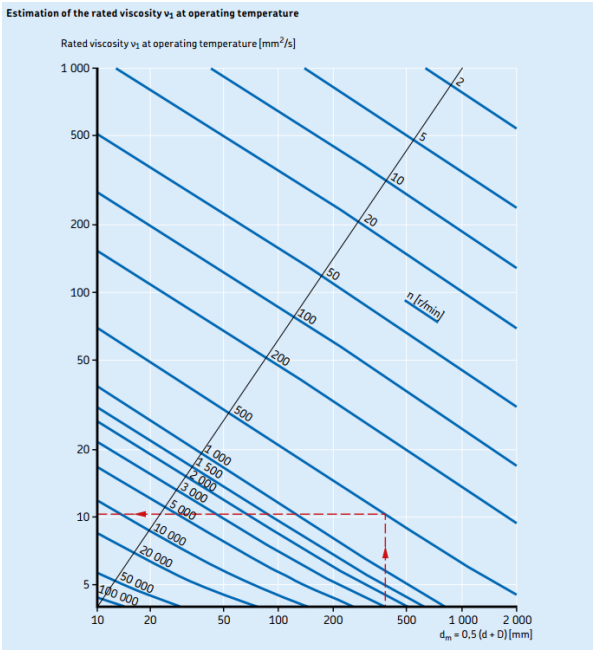

Figure E.1.: SKF abaqus to determine the rated viscosity ν_1

F. Friction Torque Measurements and Calculations

Table F.1.: Load: 4000 N / Temperature: 70°C / Oil: 75W90

Rotational Speeds [rpm]	75	150	300	600	900	1200
Temperature [°C]	70,33	70,04	69,96	69,84	70,35	72,99
Viscosity [cSt]	37,83	38,18	38,27	38,41	37,82	34,88
M_{exp} [Nmm]	552,41	509,65	477,09	451,62	381,31	343,88
M_{sl} [Nmm]	525,11	468,19	414,63	358,22	265,17	213,99
M_{rr} [Nmm]	27,30	41,46	62,46	93,40	116,14	129,89
μ_{sl}^{exp}	0,084	0,075	0,066	0,057	0,042	0,034
μ_{sl}^{SKF}	0,083	0,077	0,066	0,050	0,042	0,040
error	$9,98 \cdot 10^{-4}$	$2,70 \cdot 10^{-3}$	$1,14 \cdot 10^{-7}$	$7,52 \cdot 10^{-3}$	$3,36 \cdot 10^{-7}$	$5,95 \cdot 10^{-3}$
λ	0,148	0,244	0,403	0,663	0,882	0,999
k	0,204	0,382	0,644	1,115	1,784	1,966
μ_{bl}				0,086		
μ_{EHL}				0,038		

Table F.2.: Load: 4000 N / Temperature: 70°C / Oil: 75W140

Rotational Speeds [rpm]	75	150	300	600	900	1200
Temperature [°C]	69,75	69,60	68,92	68,97	69,85	82,65
Viscosity [cSt]	64,73	65,05	66,55	66,44	64,52	43,34
M_{exp} [Nmm]	629,04	533,25	490,32	501,40	468,71	445,50
M_{sl} [Nmm]	591,44	476,41	404,08	374,10	313,14	299,39
M_{rr} [Nmm]	37,60	56,83	86,24	127,30	155,57	146,11
μ_{sl}^{exp}	0,094	0,076	0,064	0,060	0,050	0,048
μ_{sl}^{SKF}	0,091	0,081	0,064	0,052	0,050	0,050
error	$3,66 \cdot 10^{-3}$	$4,95 \cdot 10^{-3}$	$8,28 \cdot 10^{-7}$	$7,82 \cdot 10^{-3}$	$4,71 \cdot 10^{-9}$	$2,47 \cdot 10^{-3}$
λ	0,231	0,381	0,628	1,028	1,362	1,225
k	0,342	0,642	1,081	1,872	2,996	2,489
μ_{bl}				0,098		
μ_{EHL}				0,050		

Table F.3.: Load: 4000 N / Temperature: 70°C / Oil: 80W90

Rotational Speeds [rpm]	75	150	300	600	900	1200
Temperature [°C]	69,90	69,93	69,88	70,32	71,10	83,43
Viscosity [cSt]	36,67	36,63	36,69	36,14	35,19	23,77
M_{exp} [Nmm]	573,06	558,60	499,89	492,17	476,41	514,69
M_{sl} [Nmm]	546,27	518,14	438,95	401,99	364,86	409,79
M_{rr} [Nmm]	26,80	40,45	60,94	90,18	111,55	104,91
μ_{sl}^{exp}	0,087	0,083	0,070	0,064	0,058	0,065
μ_{sl}^{SKF}	0,086	0,083	0,075	0,064	0,059	0,060
error	$9,34 \cdot 10^{-4}$	$3,91 \cdot 10^{-5}$	$5,18 \cdot 10^{-3}$	$2,26 \cdot 10^{-7}$	$6,04 \cdot 10^{-4}$	$5,32 \cdot 10^{-3}$
λ	0,182	0,300	0,495	0,813	1,082	0,938
k	0,195	0,365	0,615	1,066	1,705	1,357
μ_{bl}				0,089		
μ_{EHL}				0,055		

Table F.4.: Load: 7000 N / Temperature: 70°C / Oil: 75W90

Rotational Speeds [rpm]	75	150	300	600	900	1200
Temperature [°C]	70,30	70,21	70,15	74,96	113,83	135,55
Viscosity [cSt]	37,88	37,98	38,05	32,90	12,71	8,51
M_{exp} [Nmm]	1058,00	811,33	736,64	704,72	772,42	800,08
M_{sl} [Nmm]	1025,51	762,16	662,59	603,09	698,53	731,03
M_{rr} [Nmm]	32,50	49,17	74,05	101,63	73,89	69,05
μ_{sl}^{exp}	0,093	0,070	0,060	0,055	0,064	0,067
μ_{sl}^{SKF}	0,073	0,070	0,063	0,055	0,063	0,064
error	$2,08 \cdot 10^{-2}$	$5,67 \cdot 10^{-7}$	$2,36 \cdot 10^{-3}$	$2,78 \cdot 10^{-7}$	$9,48 \cdot 10^{-4}$	$2,52 \cdot 10^{-3}$
λ	0,141	0,232	0,383	0,555	0,333	0,295
k	0,204	0,382	0,644	0,958	0,591	0,484
μ_{bl}				0,075		
μ_{EHL}				0,046		

Table F.5.: Load: 7000 N / Temperature: 70°C / Oil: 75W140

Rotational Speeds [rpm]	75	150	300	600	900	1200
Temperature [°C]	70,22	70,09	70,22	70,48	91,14	127,52
Viscosity [cSt]	63,72	64,00	63,73	63,19	34,19	14,92
M_{exp} [Nmm]	808,04	721,79	702,66	620,69	652,90	668,61
M_{sl} [Nmm]	763,73	654,84	602,63	473,48	522,28	572,92
M_{rr} [Nmm]	44,31	66,95	100,04	147,21	130,63	95,70
μ_{sl}^{exp}	0,070	0,060	0,055	0,043	0,048	0,052
μ_{sl}^{SKF}	0,070	0,063	0,052	0,043	0,045	0,053
error	$2,24 \cdot 10^{-7}$	$3,34 \cdot 10^{-3}$	$2,71 \cdot 10^{-3}$	$6,23 \cdot 10^{-8}$	$2,46 \cdot 10^{-3}$	$1,12 \cdot 10^{-3}$
λ	0,219	0,362	0,597	0,977	0,793	0,473
k	0,342	0,642	1,081	1,872	1,645	0,833
μ_{bl}				0,075		
μ_{EHL}				0,041		

Table F.6.: Load: 7000 N / Temperature: 70°C / Oil: 80W90

Rotational Speeds [rpm]	75	150	300	600	900	1200
Temperature [°C]	70,34	69,82	70,05	70,19	88,28	113,58
Viscosity [cSt]	36,12	36,77	36,48	36,30	20,66	11,04
M_{exp} [Nmm]	768,04	719,12	660,65	622,03	581,36	681,49
M_{sl} [Nmm]	736,46	670,90	588,41	514,48	483,38	538,09
M_{rr} [Nmm]	31,59	48,23	72,23	107,55	97,98	80,40
μ_{sl}^{exp}	0,067	0,061	0,054	0,047	0,044	0,049
μ_{sl}^{SKF}	0,066	0,062	0,054	0,041	0,044	0,050
error	$1,25 \cdot 10^{-3}$	$7,23 \cdot 10^{-4}$	$2,45 \cdot 10^{-7}$	$5,79 \cdot 10^{-3}$	$3,73 \cdot 10^{-7}$	$1,34 \cdot 10^{-3}$
λ	0,173	0,285	0,471	0,773	0,645	0,479
k	0,195	0,365	0,615	1,066	0,972	0,644
μ_{bl}				0,068		
μ_{EHL}				0,031		

Table F.7.: Load: 4000 N / Temperature: 90°C / Oil: 75W90

Rotational Speeds [rpm]	75	150	300	600	900	1200
Temperature [°C]	90,13	89,78	89,43	89,29	89,10	89,82
Viscosity [cSt]	21,73	21,93	22,12	22,20	22,31	21,90
M_{exp} [Nmm]	577,61	584,51	477,42	524,71	455,34	478,36
M_{sl} [Nmm]	558,01	554,70	432,21	456,70	369,24	378,20
M_{rr} [Nmm]	19,60	29,81	45,21	68,01	86,10	100,16
μ_{sl}^{exp}	0,089	0,088	0,069	0,073	0,059	0,060
μ_{sl}^{SKF}	0,089	0,087	0,082	0,073	0,065	0,060
error	$2,50 \cdot 10^{-7}$	$1,49 \cdot 10^{-3}$	$1,32 \cdot 10^{-2}$	$3,56 \cdot 10^{-4}$	$6,06 \cdot 10^{-3}$	$1,98 \cdot 10^{-7}$
λ	0,092	0,152	0,252	0,415	0,554	0,679
k	0,116	0,218	0,367	0,636	1,018	1,229
μ_{bl}				0,090		
μ_{EHL}				0,054		

Table F.8.: Load: 4000 N / Temperature: 90°C / Oil: 75W140

Rotational Speeds [rpm]	75	150	300	600	900	1200
Temperature [°C]	89,92	89,69	89,56	89,22	89,21	90,11
Viscosity [cSt]	35,32	35,55	35,67	36,01	36,02	35,14
M_{exp} [Nmm]	574,08	553,36	470,36	489,66	458,59	421,26
M_{sl} [Nmm]	547,88	513,62	410,42	399,62	345,56	290,88
M_{rr} [Nmm]	26,21	39,74	59,94	90,00	113,03	130,38
μ_{sl}^{exp}	0,087	0,082	0,065	0,064	0,055	0,046
μ_{sl}^{SKF}	0,086	0,082	0,074	0,061	0,055	0,053
error	$1,67 \cdot 10^{-3}$	$3,35 \cdot 10^{-5}$	$8,43 \cdot 10^{-3}$	$2,43 \cdot 10^{-3}$	$5,42 \cdot 10^{-8}$	$6,43 \cdot 10^{-3}$
λ	0,140	0,231	0,381	0,626	0,835	1,020
k	0,188	0,353	0,594	1,028	1,645	1,987
μ_{bl}				0,088		
μ_{EHL}				0,052		

Table F.9.: Load: 4000 N / Temperature: 90°C / Oil: 80W90

Rotational Speeds [rpm]	75	150	300	600	900	1200
Temperature [°C]	90,71	90,36	89,99	90,01	89,96	90,92
Viscosity [cSt]	19,31	19,50	19,70	19,69	19,77	19,20
M_{exp} [Nmm]	588,73	566,69	477,92	480,68	529,85	530,13
M_{sl} [Nmm]	570,46	538,90	435,72	417,28	449,55	437,19
M_{rr} [Nmm]	18,27	27,79	42,20	63,40	80,31	92,94
μ_{sl}^{exp}	0,091	0,086	0,070	0,067	0,072	0,070
μ_{sl}^{SKF}	0,087	0,086	0,083	0,077	0,072	0,068
error	$3,82 \cdot 10^{-3}$	$6,11 \cdot 10^{-8}$	$1,35 \cdot 10^{-2}$	$1,03 \cdot 10^{-2}$	$5,33 \cdot 10^{-9}$	$1,34 \cdot 10^{-3}$
λ	0,108	0,178	0,295	0,485	0,648	0,794
k	0,105	0,197	0,332	0,574	0,919	1,110
μ_{bl}				0,088		
μ_{EHL}				0,062		

Table F.10.: Load: 7000 N / Temperature: 90°C / Oil: 75W90

Rotational Speeds [rpm]	75	150	300	600	900	1200
Temperature [°C]	89,96	90,04	89,78	90,63	106,20	128,57
Viscosity [cSt]	21,83	21,78	21,93	21,46	14,91	9,60
M_{exp} [Nmm]	885,26	863,34	775,73	754,45	745,99	807,37
M_{sl} [Nmm]	861,89	828,03	722,24	675,14	664,86	733,26
M_{rr} [Nmm]	23,38	35,32	53,49	79,31	81,13	74,11
μ_{sl}^{exp}	0,079	0,076	0,066	0,062	0,061	0,067
μ_{sl}^{SKF}	0,077	0,076	0,071	0,062	0,061	0,063
error	$1,10 \cdot 10^{-3}$	$2,46 \cdot 10^{-7}$	$4,86 \cdot 10^{-3}$	$7,07 \cdot 10^{-7}$	$2,11 \cdot 10^{-4}$	$3,45 \cdot 10^{-3}$
λ	0,088	0,145	0,239	0,394	0,383	0,324
k	0,116	0,218	0,367	0,636	0,696	0,541
μ_{bl}				0,079		
μ_{EHL}				0,042		

Table F.11.: Load: 7000 N / Temperature: 90°C / Oil: 75W140

Rotational Speeds [rpm]	75	150	300	600	900	1200
Temperature [°C]	89,33	89,10	89,36	88,96	97,39	122,03
Viscosity [cSt]	35,90	36,13	35,87	36,27	29,05	16,63
M_{exp} [Nmm]	842,30	816,35	773,49	730,99	713,34	701,29
M_{sl} [Nmm]	810,83	768,63	701,96	623,50	594,24	599,39
M_{rr} [Nmm]	31,47	47,72	71,52	107,49	119,10	101,90
μ_{sl}^{exp}	0,074	0,070	0,064	0,057	0,054	0,054
μ_{sl}^{SKF}	0,073	0,070	0,065	0,056	0,054	0,057
error	$1,28 \cdot 10^{-3}$	$3,14 \cdot 10^{-7}$	$7,10 \cdot 10^{-4}$	$5,82 \cdot 10^{-4}$	$2,41 \cdot 10^{-7}$	$2,67 \cdot 10^{-3}$
λ	0,133	0,219	0,362	0,595	0,676	0,491
k	0,188	0,353	0,594	1,028	1,355	0,872
μ_{bl}				0,074		
μ_{EHL}				0,050		

Table F.12.: Load: 7000 N / Temperature: 90°C / Oil: 80W90

Rotational Speeds [rpm]	75	150	300	600	900	1200
Temperature [°C]	89,83	89,31	89,16	89,75	104,11	131,55
Viscosity [cSt]	19,79	20,07	20,16	19,83	13,70	7,70
M_{exp} [Nmm]	933,76	941,84	779,25	757,70	753,86	755,25
M_{sl} [Nmm]	911,72	908,20	728,35	681,97	676,64	690,10
M_{rr} [Nmm]	22,04	33,63	50,89	75,73	77,22	65,16
μ_{sl}^{exp}	0,083	0,083	0,066	0,062	0,062	0,063
μ_{sl}^{SKF}	0,083	0,081	0,074	0,062	0,061	0,068
error	$2,51 \cdot 10^{-10}$	$2,25 \cdot 10^{-3}$	$8,01 \cdot 10^{-3}$	$1,00 \cdot 10^{-9}$	$3,65 \cdot 10^{-4}$	$4,66 \cdot 10^{-3}$
λ	0,102	0,169	0,280	0,461	0,455	0,344
k	0,105	0,197	0,332	0,574	0,641	0,435
μ_{bl}				0,085		
μ_{EHL}				0,033		

Table F.13.: Load: 4000 N / Temperature: 110°C / Oil: 75W90

Rotational Speeds [rpm]	75	150	300	600	900	1200
Temperature [°C]	109,99	109,26	109,36	108,82	108,47	108,76
Viscosity [cSt]	13,75	13,97	13,94	14,10	14,20	14,12
M_{exp} [Nmm]	714,82	623,19	599,64	578,76	524,85	484,47
M_{sl} [Nmm]	699,91	600,42	565,27	526,65	458,56	406,55
M_{rr} [Nmm]	14,91	22,77	34,37	52,11	66,29	77,92
μ_{sl}^{exp}	0,112	0,096	0,090	0,084	0,073	0,065
μ_{sl}^{SKF}	0,097	0,096	0,092	0,082	0,073	0,066
error	$1,42 \cdot 10^{-2}$	$2,96 \cdot 10^{-7}$	$1,57 \cdot 10^{-3}$	$1,70 \cdot 10^{-3}$	$4,58 \cdot 10^{-7}$	$7,71 \cdot 10^{-4}$
λ	0,062	0,103	0,170	0,281	0,376	0,462
k	0,073	0,138	0,232	0,401	0,642	0,775
μ_{bl}				0,098		
μ_{EHL}				0,045		

Table F.14.: Load: 4000 N / Temperature: 110°C / Oil: 75W140

Rotational Speeds [rpm]	75	150	300	600	900	1200
Temperature [°C]	109,95	110,10	110,46	109,98	109,90	110,79
Viscosity [cSt]	21,53	21,46	21,29	21,52	21,55	21,13
M_{exp} [Nmm]	668,80	603,29	568,75	558,67	537,12	476,45
M_{sl} [Nmm]	649,31	573,86	524,56	491,88	452,70	378,32
M_{rr} [Nmm]	19,49	29,43	44,19	66,79	84,42	98,13
μ_{sl}^{exp}	0,104	0,092	0,084	0,079	0,072	0,060
μ_{sl}^{SKF}	0,093	0,092	0,087	0,078	0,072	0,067
error	$1,02 \cdot 10^{-2}$	$5,49 \cdot 10^{-7}$	$3,61 \cdot 10^{-3}$	$2,98 \cdot 10^{-5}$	$7,20 \cdot 10^{-4}$	$6,76 \cdot 10^{-3}$
λ	0,092	0,152	0,252	0,415	0,554	0,680
k	0,115	0,215	0,362	0,627	1,004	1,212
μ_{bl}				0,095		
μ_{EHL}				0,061		

Table F.15.: Load: 4000 N / Temperature: 110°C / Oil: 80W90

Rotational Speeds [rpm]	75	150	300	600	900	1200
Temperature [°C]	110,23	110,17	110,46	111,17	111,19	110,70
Viscosity [cSt]	11,89	11,91	11,83	11,64	11,64	11,77
M_{exp} [Nmm]	580,57	542,98	571,87	535,48	529,00	514,14
M_{sl} [Nmm]	566,91	522,28	540,70	488,94	470,01	444,00
M_{rr} [Nmm]	13,66	20,70	31,17	46,54	58,99	70,14
μ_{sl}^{exp}	0,090	0,083	0,086	0,078	0,075	0,071
μ_{sl}^{SKF}	0,090	0,089	0,086	0,081	0,075	0,070
error	$8,72 \cdot 10^{-4}$	$5,30 \cdot 10^{-3}$	$8,81 \cdot 10^{-7}$	$2,88 \cdot 10^{-3}$	$3,31 \cdot 10^{-4}$	$8,39 \cdot 10^{-4}$
λ	0,071	0,117	0,193	0,318	0,426	0,523
k	0,064	0,120	0,201	0,349	0,558	0,674
μ_{bl}				0,090		
μ_{EHL}				0,051		

Table F.16.: Load: 7000 N / Temperature: 110°C / Oil: 75W90

Rotational Speeds [rpm]	75	150	300	600	900	1200
Temperature [°C]	109,96	109,04	109,67	108,86	109,96	123,61
Viscosity [cSt]	13,76	14,03	13,85	14,09	13,76	10,51
M_{exp} [Nmm]	993,06	928,95	800,03	779,54	670,60	692,55
M_{sl} [Nmm]	975,32	901,79	759,31	717,59	593,21	614,36
M_{rr} [Nmm]	17,74	27,16	40,72	61,95	77,39	78,19
μ_{sl}^{exp}	0,089	0,082	0,069	0,065	0,054	0,056
μ_{sl}^{SKF}	0,084	0,082	0,077	0,065	0,055	0,054
error	$4,62 \cdot 10^{-3}$	$3,40 \cdot 10^{-7}$	$8,03 \cdot 10^{-3}$	$2,06 \cdot 10^{-7}$	$8,70 \cdot 10^{-4}$	$1,69 \cdot 10^{-3}$
λ	0,059	0,098	0,162	0,267	0,357	0,350
k	0,073	0,138	0,232	0,401	0,642	0,593
μ_{bl}				0,086		
μ_{EHL}				0,018		

Table F.17.: Load: 7000 N / Temperature: 110°C / Oil: 75W140

Rotational Speeds [rpm]	75	150	300	600	900	1200
Temperature [°C]	110,22	110,38	110,01	109,26	109,25	121,85
Viscosity [cSt]	21,40	21,32	21,50	21,87	21,88	16,69
M_{exp} [Nmm]	916,21	855,48	852,63	846,42	706,12	742,65
M_{sl} [Nmm]	893,11	820,61	799,75	766,23	604,88	640,57
M_{rr} [Nmm]	23,10	34,87	52,88	80,19	101,24	102,08
μ_{sl}^{exp}	0,081	0,075	0,073	0,070	0,055	0,058
μ_{sl}^{SKF}	0,078	0,077	0,073	0,065	0,059	0,058
error	$3,00 \cdot 10^{-3}$	$2,00 \cdot 10^{-3}$	$5,47 \cdot 10^{-9}$	$5,00 \cdot 10^{-3}$	$3,52 \cdot 10^{-3}$	$5,55 \cdot 10^{-7}$
λ	0,088	0,145	0,239	0,394	0,527	0,523
k	0,115	0,125	0,362	0,627	1,004	0,941
μ_{bl}				0,079		
μ_{EHL}				0,049		

Table F.18.: Load: 7000 N / Temperature: 110°C / Oil: 80W90

Rotational Speeds [rpm]	75	150	300	600	900	1200
Temperature [°C]	109,35	109,12	110,31	110,11	111,76	131,31
Viscosity [cSt]	12,13	12,19	11,87	11,93	11,49	7,74
M_{exp} [Nmm]	892,99	885,59	853,43	803,76	732,25	752,15
M_{sl} [Nmm]	876,55	860,62	812,28	747,61	662,60	686,80
M_{rr} [Nmm]	16,45	24,97	37,15	56,15	69,65	65,35
μ_{sl}^{exp}	0,080	0,079	0,074	0,068	0,060	0,063
μ_{sl}^{SKF}	0,080	0,079	0,075	0,067	0,060	0,063
error	$9,05 \cdot 10^{-5}$	$2,29 \cdot 10^{-7}$	$8,24 \cdot 10^{-4}$	$7,16 \cdot 10^{-4}$	$3,61 \cdot 10^{-7}$	$5,73 \cdot 10^{-5}$
λ	0,067	0,111	0,183	0,303	0,405	0,344
k	0,064	0,120	0,201	0,349	0,558	0,436
μ_{bl}				0,081		
μ_{EHL}				0,027		

Table F.19.: Load: 7000 N / Temperature: FREE / Oil: 75W90

Rotational Speeds [rpm]	75	150	300
Temperature [°C]	31,36	37,57	50,22
Viscosity [cSt]	172,49	128,95	76,00
M_{exp} [Nmm]	853,39	759,33	699,64
M_{sl} [Nmm]	773,53	658,44	588,90
M_{rr} [Nmm]	79,86	100,89	110,74
μ_{sl}^{exp}	0,071	0,060	0,054
μ_{sl}^{SKF}		not applicable	
error		not applicable	
λ	0,495	0,641	0,680
k	0,918	1,288	1,281
μ_{bl}		not applicable	
μ_{EHL}		not applicable	

Table F.20.: Load: 7000 N / Temperature: FREE / Oil: 75W140

Rotational Speeds [rpm]	75	150	300
Temperature [°C]	31,67	37,30	49,66
Viscosity [cSt]	310,85	235,61	136,24
M_{exp} [Nmm]	772,17	776,69	625,63
M_{sl} [Nmm]	659,64	624,21	471,46
M_{rr} [Nmm]	112,53	142,48	154,17
μ_{sl}^{exp}	0,060	0,057	0,043
μ_{sl}^{SKF}		not applicable	
error		not applicable	
λ	0,814	1,066	1,110
k	1,655	2,356	2,291
μ_{bl}		not applicable	
μ_{EHL}		not applicable	

Table F.21.: Load: 7000 N / Temperature: FREE / Oil: 80W90

Rotational Speeds [rpm]	75	150	300
Temperature [°C]	31,47	37,72	49,48
Viscosity [cSt]	200,55	143,28	81,59
M_{exp} [Nmm]	766,70	705,80	658,84
M_{sl} [Nmm]	679,47	598,56	543,49
M_{rr} [Nmm]	87,23	107,24	115,35
μ_{sl}^{exp}	0,062	0,055	0,050
μ_{sl}^{SKF}		not applicable	
error		not applicable	
λ	0,718	0,896	0,920
k	1,068	1,434	1,373
μ_{bl}		not applicable	
μ_{EHL}		not applicable	

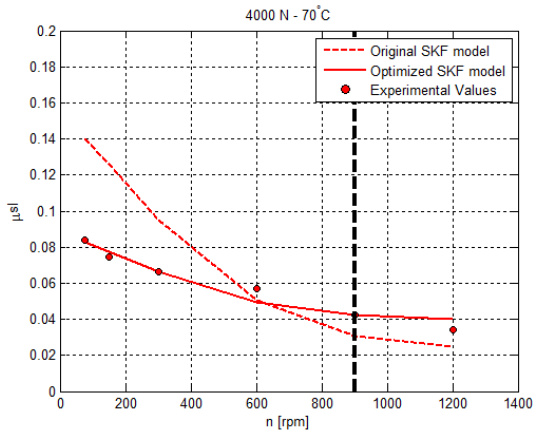

(a) 4000 N/70°C

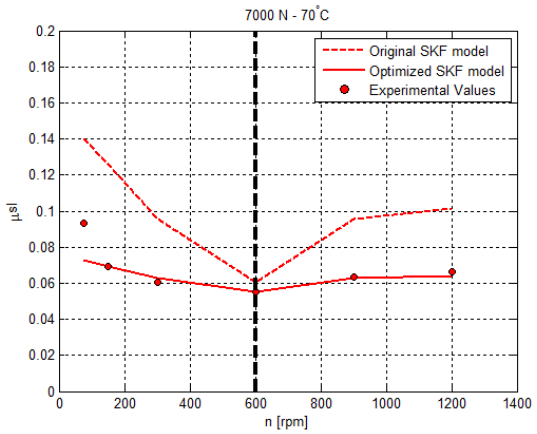

(b) 7000 N/70°C

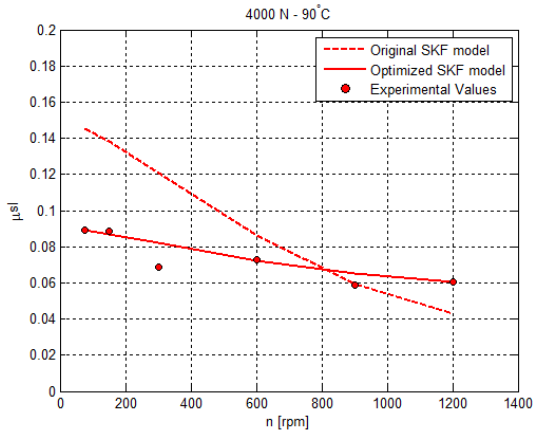

(c) 4000 N/90°C

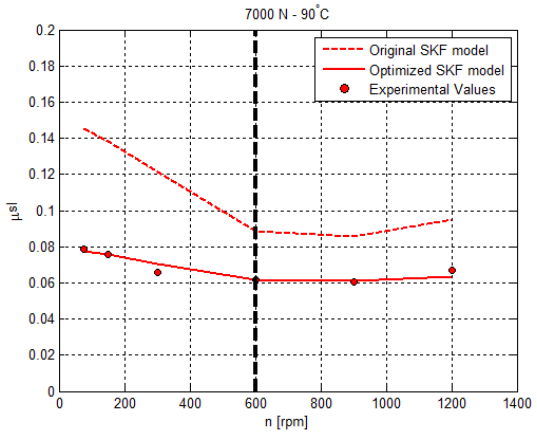

(d) 7000 N/90°C

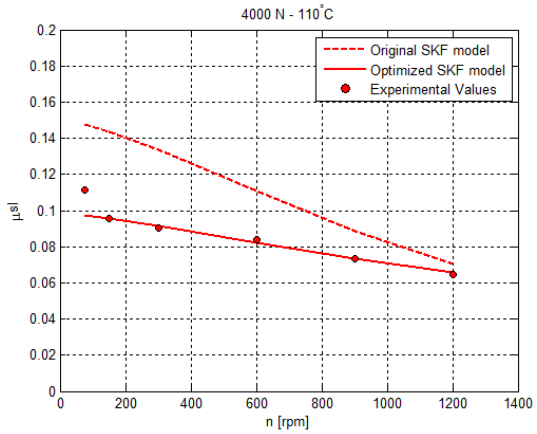

(e) 4000 N/110°C

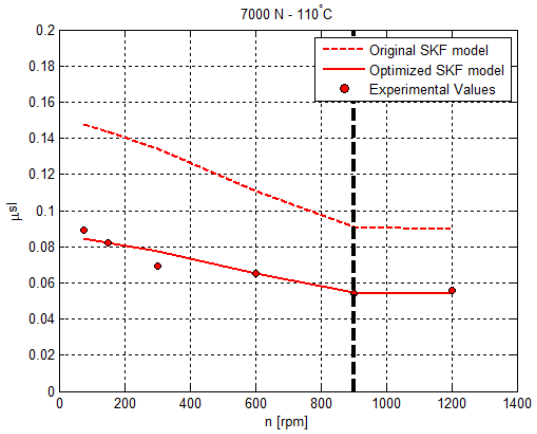

(f) 7000 N/110°C

Figure F.1.: Comparison between the SKF original model and the calibrated model for the 75W90 oil in all tested conditions

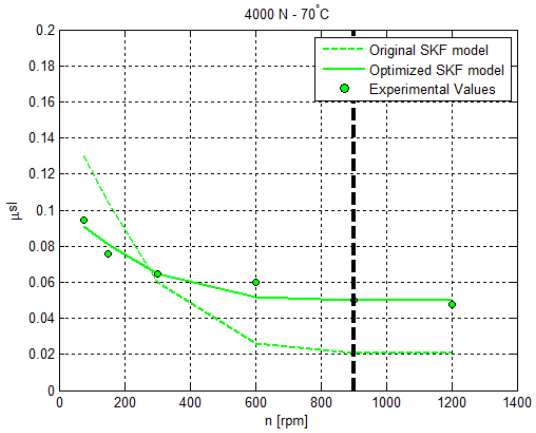

(a) 4000 N/70°C

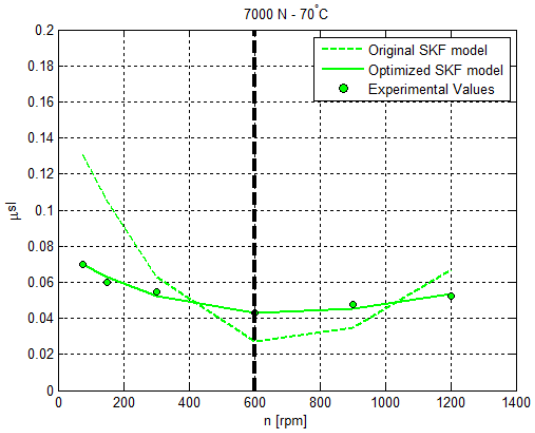

(b) 7000 N/70°C

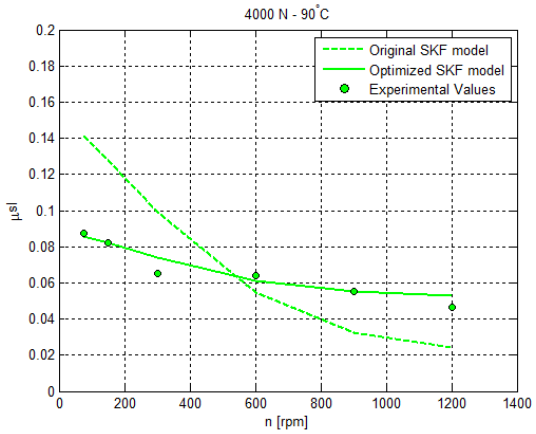

(c) 4000 N/90°C

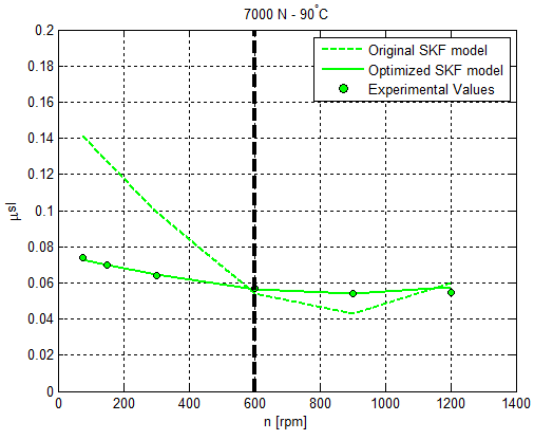

(d) 7000 N/90°C

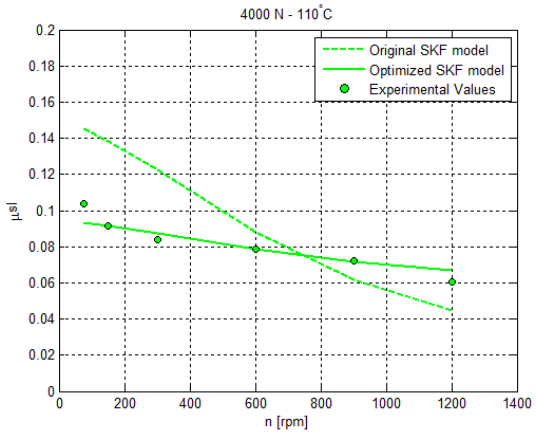

(e) 4000 N/110°C

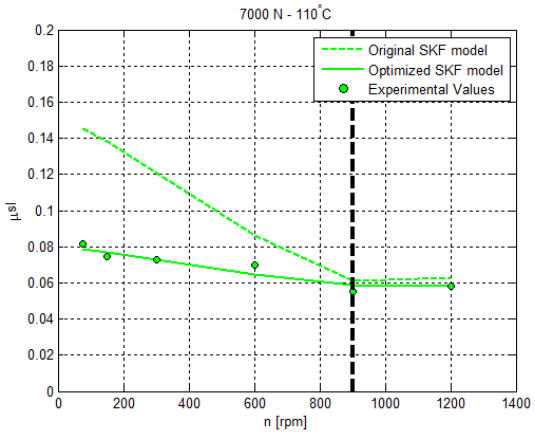

(f) 7000 N/110°C

Figure F.2.: Comparison between the SKF original model and the calibrated model for the 75W140 oil in all tested conditions

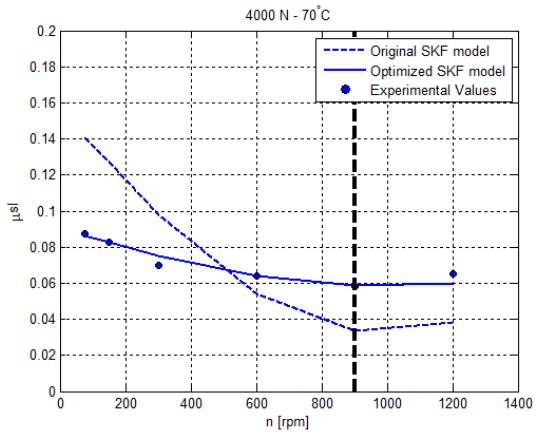

(a) 4000 N/70°C

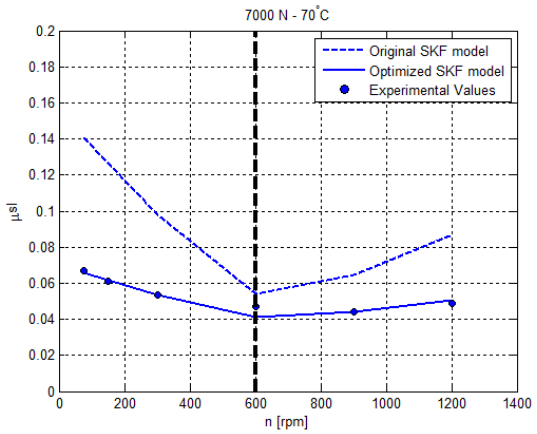

(b) 7000 N/70°C

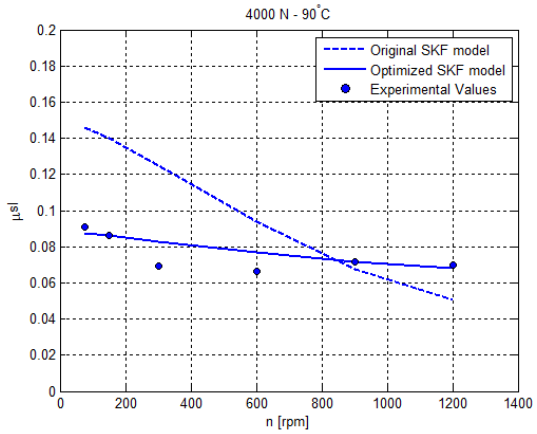

(c) 4000 N/90°C

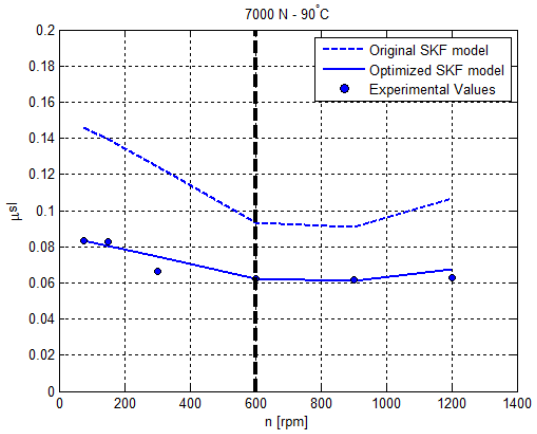

(d) 7000 N/90°C

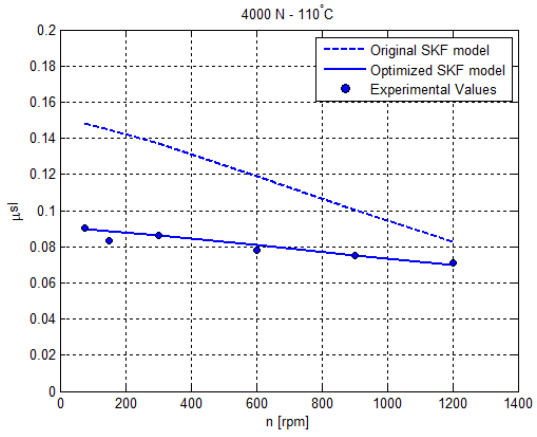

(e) 4000 N/110°C

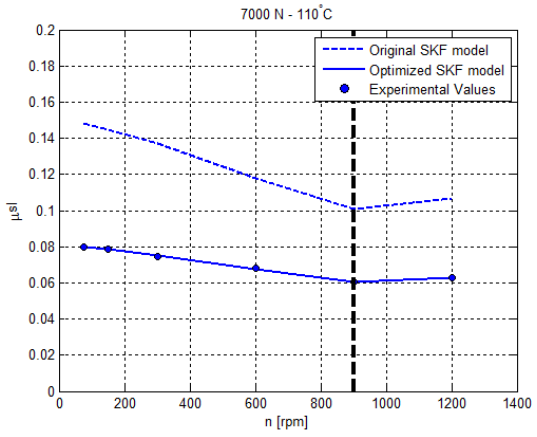

(f) 7000 N/110°C

Figure F.3.: Comparison between the SKF original model and the calibrated model for the 80W90 oil in all tested conditions